Tang et al. *Advances in Difference Equations* (2015) 2015:322
DOI 10.1186/s13662-015-0661-x

Advances in Difference Equations
a SpringerOpen Journal

RESEARCH Open Access

Global dynamics of a state-dependent feedback control system

Sanyi Tang[1*], Wenhong Pang[1], Robert A Cheke[2] and Jianhong Wu[3]

*Correspondence:
sytang@snnu.edu.cn
[1]School of Mathematics and Information Science, Shaanxi Normal University, Xi'an, 710062, P.R. China
Full list of author information is available at the end of the article

Abstract

The main purpose is to develop novel analytical techniques and provide a comprehensive qualitative analysis of global dynamics for a state-dependent feedback control system arising from biological applications including integrated pest management. The model considered consists of a planar system of differential equations with state-dependent impulsive control. We characterize the impulsive and phase sets, using the phase portraits of the planar system and the Lambert W function to define the Poincaré map for impulsive point series defined in the phase set. The existence, local and global stability of an order-1 limit cycle and obtain sharp sufficient conditions for the global stability of the boundary order-1 limit cycle have been provided. We further examine the flip bifurcation related to the existence of an order-2 limit cycle. We show that the existence of an order-2 limit cycle implies the existence of an order-1 limit cycle. We derive sufficient conditions under which any trajectory initiating from a phase set will be free from impulsive effects after finite state-dependent feedback control actions, and we also prove that order-k ($k \geq 3$) limit cycles do not exist, providing a solution to an open problem in the integrated pest management community. We then investigate multiple attractors and their basins of attraction, as well as the interior structure of a horseshoe-like attractor. We also discuss implications of the global dynamics for integrated pest management strategy. The analytical techniques and qualitative methods developed in the present paper could be widely used in many fields concerning state-dependent feedback control.

MSC: 34A37; 34C23; 92B05; 93B52

Keywords: planar impulsive semi-dynamical system; integrated pest management; Poincaré map; impulsive set; phase set; global stability

1 Introduction

This study concerns the global dynamics of semi-dynamical systems with state-dependent feedback arising from modeling integrated pest management (IPM) [1–4]. The challenge for the study of the system's global dynamics is due to the state-dependent impulsive control.

Impulsive semi-dynamical systems arise from many important applications in the life sciences including population dynamics (biological resource and pest management programs, and chemostat cultures) [1–10], virus dynamics (HIV) [11–17], medicine and pharmacokinetics (diabetes mellitus and tumor control) [18–22], epidemiology (vaccination strategies, the control of epidemics and plant epidemiology) [23–32], and neuroscience

[33–40]. In some applications such as spraying pesticides and releasing natural enemies for pest control and impulse vaccinations and drug administrations for disease treatment [1–5, 8, 41, 42], the impulsive control is implemented at fixed moments to reflect how human actions are taken at fixed periods. In some applications, however, impulsive differential equations with state-dependent feedback control have to be used to model density-dependent control strategies [1, 3, 4, 19, 31, 43]. In particular, in an integrated pest management (IPM) strategy, actions are taken only when the density of pests reaches an economic threshold [44, 45]. Feedback control strategies have also been applied in different fields in quite different ways [46–49].

There has also been substantial theoretical development for impulsive semi-dynamical systems [50–55]. Techniques including the Lyapunov method have been developed to study the stability and boundedness of solutions for impulsive differential equations with fixed moments, with applications in many important areas [1–5, 8]. Despite a few interesting studies on more complicated dynamics such as limit cycles [56–58], invariant and limiting sets [59–64], LaSalle's invariance principle [65] and the Poincaré-Bendixson theorem [58, 60], much remains to be done for the qualitative theory, and especially the global dynamics, of impulsive semi-dynamical systems. This is particularly so for impulsive differential equations with state-dependent feedback control.

Some prototype models with biological motivation are needed to guide the development of a general qualitative theory of semi-dynamical systems with state-dependent control. A good example in the series of models motivated by integrated pest management (IPM) [1–4], where the classical Lotka-Volterra model with state-dependent feedback control is used and some novel techniques for the existence and stability of an order-1 limit cycle, non-existence of limit cycles with order no less than 3, the coexistence of multiple attractors and their basins of attraction are developed. The modeling framework and the developed analytical techniques have been used in a number of recent studies. For example, Huang *et al.* [19] proposed mathematical models depicting impulsive injection of insulin for type 1 and type 2 diabetes mellitus, and considered the existence and local stability of an order-1 limit cycle. Based on biomass concentration-dependent impulsive perturbations, the studies [6, 66] proposed and analyzed chemostat models with state-dependent feedback control, again focusing on the existence and stability of an order-1 limit cycle. These studies also found that the models have no limit cycles with order no less than 3. The work [30, 67] also considered the existence and stability of limit cycles with different orders, in relation to the biological issue of maintaining the density of an infected plant population below a certain threshold level. See also similar work on population dynamics [10, 58, 68–73] and epidemiology [31]. These studies, however, focused on the existence and local stability of an order-1 limit cycle for specific cases.

Here, we develop novel analytical techniques in order to understand the global dynamics of a very general class of impulsive models with state-dependent feedback control, commonly used in a number of biological applications including IPM. In particular, we address the following issues and explore their biological implications:

- the precise information as regards the domains of impulsive sets and the phase sets, and the domains for the Poincaré map of impulsive point series;
- the global stability of order-1 limit cycles (including boundary order-1 limit cycles);
- the existence of order-2 limit cycles and non-existence of limit cycles with order no less than 3, an open problem listed in [1];

- the necessary condition for the existence of order-2 limit cycles, and the relation between the existence of order-2 limit cycles and order-1 limit cycles;
- the precise information on parameter space for the finite state-dependent feedback control actions, crucial for designing threshold control strategies;
- the description of smaller attractors, their basins of attraction and how they are related to phase sets and interior structures of horseshoe-like attractors.

2 The model with state-dependent feedback control

A threshold policy can be defined in broad terms as follows: control (grazing, harvesting, pesticide application, treatment *etc.*) is suppressed when a specific species abundance is below a previously chosen threshold density; above the threshold, control is applied. Its application can be seen in wide areas. For an IPM strategy, a long-term management strategy that uses a combination of biological, cultural, and chemical tactics to reduce pests to tolerable levels, actions must be taken once a critical density of pests (economic threshold, ET) is observed in the field so that the economic injury level (EIL) is not exceeded [44, 45, 74], as shown in Figure 1. Note that EIL and ET are important components of a cost effective IPM program and are useful for decision-making in the applications of pesticides [44, 45]. For chemostat setting, when the lactic acid concentration in the bioreactor reaches the critical level, the appropriate control measures (extraction, dilutedness, *etc.*) should be used such that the concentration of the substrate and the lactic acid change instantaneously [6]. Similarly, once the concentration of the tumor cells reaches the therapeutic threshold level in tumor tissue, a combination of photodynamic therapy and sonodynamic therapy should be used [75–80]. Moreover, including $CD4^+$ T cell counts and/or viral load level, state-dependent guided antiretroviral therapy has been widely used in HIV [81–84], hepatitis B virus, and hepatitis C virus treatment [16, 85–88].

Let x and y be the densities of the pest and its natural enemy populations. The integrated control interventions are implemented once the x grows and reaches the threshold level. Denoting the threshold level as V_L, the state-dependent impulsive differential equations

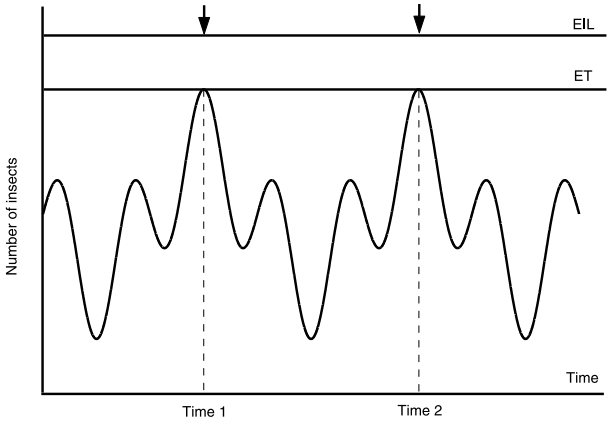

Figure 1 Illustration of IPM program. Economic Injury Level (EIL) = lowest population density that will cause economic damage. Economic Threshold (ET) = population density at which control measures should be determined to prevent an increasing pest population from reaching the EIL. The arrow indicates the point where pest levels exceeded the ET and an IPM strategy would be applied.

are

$$\begin{cases} \left.\begin{aligned} &\frac{dx(t)}{dt} = rx(t)[1 - x(t)/k] - ax(t) - px(t)y(t), \\ &\frac{dy(t)}{dt} = \frac{cx(t)y(t)}{1+\omega x(t)} - qx(t)y(t) - \delta y(t), \end{aligned}\right\} & x < V_L, \\ \left.\begin{aligned} &x(t^+) = (1-\theta)x(t), \\ &y(t^+) = y(t) + \tau, \end{aligned}\right\} & x = V_L, \end{cases} \tag{2.1}$$

where $x(t^+)$ and $y(t^+)$ denote the numbers of pests and natural enemies after a control strategy applied at time t, and $x(0^+)$ and $y(0^+)$ denote the initial densities of pest and natural enemy populations. Throughout this paper we assume that the initial density of the pest population is always less than V_L, *i.e.* $x(0^+) = x_0 < V_L$, $y(0^+) = y_0 > 0$. Otherwise, the initial values are taken after an integrated control strategy application.

For the model without control strategy in (2.1), r represents the intrinsic growth rate of the pest population, k represents the carrying capacity. The pest population dies at a rate ax and is predated by the predator population at a rate pxy. The predator response expands at a rate $\frac{cxy}{1+\omega x}$, which is a saturating function of the amount of pest present. The prey population also inhibits the predator response at a rate qxy, which is the so-called anti-predator behavior, and in the absence of the pest declines at a rate δy. Note that all parameters shown in model (2.1) are non-negative constants.

Many experiments show that the predator and prey populations can reverse their roles, whereby adult prey attack vulnerable young predators [89–92], the so called anti-predator behavior. If the variables x and y in model (2.1) describe the prey and predator populations, then the term qxy represents the effects of the prey population on the predator population, *i.e.* the prey can kill their predators. Simple predator-prey models with anti-predator behavior have been studied [90, 93].

In model (2.1) $0 \leq \theta < 1$ is the proportion by which the pest density is reduced by killing or trapping once the number of pests reaches V_L, while τ is the constant number of natural enemies released at this time t. Different releasing methods including a proportion for the release rate rather than a constant number can be used in model (2.1) [3, 5, 8]. In order to control the pest we assume, throughout the paper, that $\tau \geq \frac{b}{p}$ if $\theta = 0$ (from a biological point of view, sufficient of the natural enemies must be released to prevent the pest population exceeding V_L, *i.e.*, by maintaining $\frac{dx(t)}{dt} < 0$ (for some time) and $\theta > 0$ if $\tau = 0$. Such a strategy ensures that $x(t)$ is a decreasing function of time once the pest population reaches the V_L.

It is interesting to note that this model can be commonly used in depicting (i) the anti-predator behavior of the interaction between pest and its natural enemies, as shown above; (ii) the interaction between the virus population (such as HIV) and its immune cells [94]; (iii) the cytotoxic T lymphocyte response to the growth of an immunogenic tumor [95]; and (iv) the interaction between a toxic phytoplankton population and a zooplankton population [96, 97].

We use this widely used model (2.1) to illustrate systematic methods for investigating global dynamics, and address the basic problems related to models with state-dependent feedback control (*i.e.* state-dependent impulsive effects). Of most interest, are questions of how the instant killing rate θ, releasing constant τ and threshold parameter V_L affect the dynamics of model (2.1)? To address this question completely, we choose those three parameters as bifurcation parameters and fix all others aiming to comprehensively inves-

tigate the qualitative behavior of model (2.1), of particular interest in the dynamics listed in the Introduction.

Note that this work will focus on model (2.1) with state-dependent feedback control, aiming to maintain the density of x below the previous given threshold level. Thus, it is reasonable to assume that the population x could grow exponentially before reaching the threshold level as the threshold value is relatively small compared with the carrying capacity, *i.e.* we can let $k \to +\infty$, then model (2.1) becomes

$$\begin{cases} \left.\begin{aligned} \frac{dx(t)}{dt} &= bx(t) - px(t)y(t), \\ \frac{dy(t)}{dt} &= \frac{cx(t)y(t)}{1+\omega x(t)} - qx(t)y(t) - \delta y(t), \end{aligned}\right\} & x < V_L, \\ \left.\begin{aligned} x(t^+) &= (1-\theta)x(t), \\ y(t^+) &= y(t) + \tau, \end{aligned}\right\} & x = V_L, \end{cases} \tag{2.2}$$

with $b = r - a$.

Some special cases of model (2.2) have been investigated [1, 4, 58]. For example, let $\omega = 0$ and $q = 0$, then model (2.2) becomes

$$\begin{cases} \left.\begin{aligned} \frac{dx(t)}{dt} &= bx(t) - px(t)y(t), \\ \frac{dy(t)}{dt} &= cx(t)y(t) - \delta y(t), \end{aligned}\right\} & x < V_L, \\ \left.\begin{aligned} x(t^+) &= (1-\theta)x(t), \\ y(t^+) &= y(t) + \tau, \end{aligned}\right\} & x = V_L, \end{cases} \tag{2.3}$$

which has been investigated by Tang and Cheke [1], and we will see that all results related to model (2.3) can be easily obtained based on the results for model (2.2).

3 The ODE model and its main properties

The ODE model considered in this work becomes

$$\begin{cases} \frac{dx(t)}{dt} = bx(t) - px(t)y(t) \doteq P(x,y), \\ \frac{dy(t)}{dt} = \frac{cx(t)y(t)}{1+\omega x(t)} - qx(t)y(t) - \delta y(t) \doteq Q(x,y). \end{cases} \tag{3.1}$$

It is easy to see that for model (3.1) there exists a trivial equilibrium $(0,0)$ and the interior equilibrium (x^*, y^*) satisfies $y^* = \frac{b}{p}$ and x^* is the root of the following equation:

$$q\omega x^2 + (-c + q + \delta\omega)x + \delta = 0,$$

which indicates that

$$x^*_{1,2} = \frac{c - q - \delta\omega \pm \sqrt{(c-q-\delta\omega)^2 - 4q\omega\delta}}{2q\omega}.$$

Therefore, there are two interior equilibria, denoted by

$$E_1 = \left(x_1^*, y_e^*\right) = \left(\frac{c - q - \delta\omega + \sqrt{(c-q-\delta\omega)^2 - 4q\omega\delta}}{2q\omega}, \frac{b}{p}\right) \tag{3.2}$$

and

$$E_2 = \left(x_2^*, y_e^*\right) = \left(\frac{c - q - \delta\omega - \sqrt{(c-q-\delta\omega)^2 - 4q\omega\delta}}{2q\omega}, \frac{b}{p}\right) \tag{3.3}$$

provided that $c-q-\delta\omega>0$ and $\Delta=(c-q-\delta\omega)^2-4q\omega\delta>0$. Therefore, if

$$c-q-\delta\omega>2\sqrt{q\omega\delta}, \tag{3.4}$$

then there are two interior equilibria E_1 and E_2. Moreover, the two roots collide together if $c-q-\delta\omega=2\sqrt{q\omega\delta}$. Throughout this work we assume that the condition (3.4) holds true. It is easy to show that E_1 is a saddle point and E_2 is a center.

It follows from model (3.1) that we have

$$\frac{dy}{dx}=\frac{y}{x}\frac{\frac{cx}{1+\omega x}-qx-\delta}{b-py}, \tag{3.5}$$

which implies that model (3.1) possesses the first integral

$$H(x,y)=\int_{x^*}^{x}\left(\frac{c}{1+\omega z}-\frac{\delta}{z}-q\right)dz-\int_{y^*}^{y}\left(\frac{b}{z}-p\right)dz.$$

That is, we have

$$H(x,y)=b\ln(y)-py-\frac{c}{\omega}\ln(1+\omega x)+\delta\ln(x)+qx=h, \tag{3.6}$$

where h is a constant. In order to solve the equation $H(x,y)=h$ with respect to y, the Lambert W function and its properties [98] are necessary throughout the paper, for details see the Appendix.

Thus, according to the definition of the Lambert W function and solving $H(x,y)=h$ with respect to y yields two roots

$$y_L=-\frac{b}{p}W\left[-\frac{p}{b}\exp\left(\frac{c\ln(1+\omega x)-\delta\omega\ln(x)-q\omega x+h\omega}{b\omega}\right)\right]$$

and

$$y_U=-\frac{b}{p}W\left[-1,-\frac{p}{b}\exp\left(\frac{c\ln(1+\omega x)-\delta\omega\ln(x)-q\omega x+h\omega}{b\omega}\right)\right].$$

Again, according to the domains of the Lambert W function we require

$$-\frac{p}{b}\exp\left(\frac{c\ln(1+\omega x)-\delta\omega\ln(x)-q\omega x+h\omega}{b\omega}\right)\geq -e^{-1}$$

to ensure that y_L and y_U are well defined. So we first consider the following equation:

$$\frac{c\ln(1+\omega x)-\delta\omega\ln(x)-q\omega x+h\omega}{b\omega}=\ln\left[\frac{be^{-1}}{p}\right]$$

i.e.

$$c\ln(1+\omega x)-\delta\omega\ln(x)=q\omega x-h\omega+b\omega\ln\left[\frac{be^{-1}}{p}\right].$$

Denote

$$F_1(x) = c\ln(1+\omega x) - \delta\omega\ln(x)$$

and

$$F_2(x) = q\omega x - h\omega + b\omega\ln\left[\frac{be^{-1}}{p}\right].$$

By simple calculation we have

$$F_1'(x) = \frac{c\omega}{1+\omega x} - \frac{\delta\omega}{x}, \qquad F_1''(x) = -\frac{c\omega^2}{(1+\omega x)^2} + \frac{\delta\omega}{x^2}$$

and solving $F_1'(x) = 0$ with respect to x yields the extreme point, denoted by $x_m = \frac{\delta}{c-\delta\omega}$, and $x_m > 0$ holds true due to $c - q - \delta\omega > 0$. $F_2'(x) = q\omega$. Solving $F_1''(x) = 0$ yields two inflection points, denoted by x_I^1 and x_I^2, and

$$x_I^1 = \frac{\delta\omega + \sqrt{c\delta\omega}}{\omega(c-\delta\omega)}, \qquad x_I^2 = \frac{\delta\omega - \sqrt{c\delta\omega}}{\omega(c-\delta\omega)}$$

with $x_I^2 < x_m < x_I^1$.

Moreover, it is easy to see that $\lim_{x\to 0^+} F_1(x) = +\infty$, and solving $F_1'(x) = F_2'(x)$ with respect to x yields two roots (as shown in Figure 2), which are exactly the abscissas of two interior equilibria E_1 and E_2, *i.e.*

$$x_{1,2}^* = \frac{c - q - \delta\omega \pm \sqrt{(c-q-\delta\omega)^2 - 4q\omega\delta}}{2q\omega}.$$

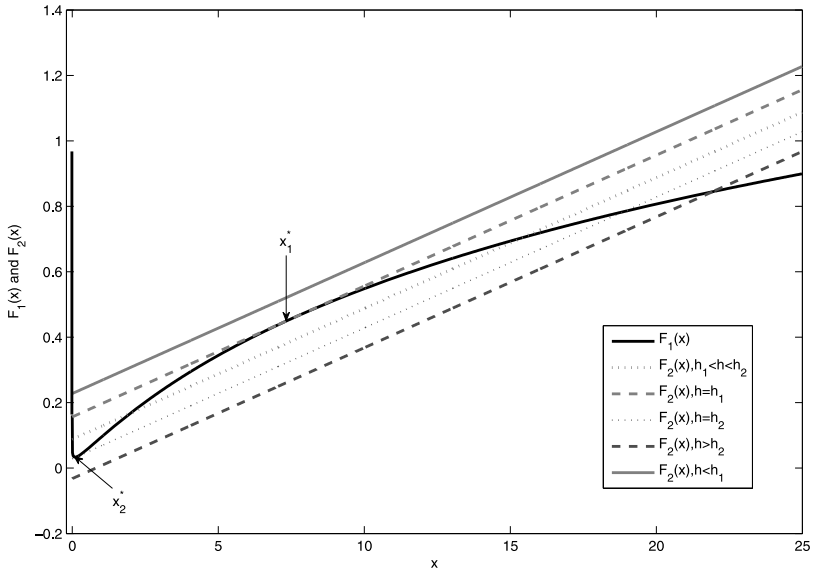

Figure 2 The roots of $F_1(x) = F_2(x)$ with respect to different h values, where parameter values are fixed as follows: $b = 0.3$, $p = 1$, $c = 0.52$, $\omega = 0.2$, $q = 0.2$, $\delta = 0.05$, $h_1 = -1.4429$, and $h_2 = -0.8027$.

Denote

$$\begin{aligned} h_1 &= b\ln\left(y_1^*\right) - py_1^* - \frac{c}{\omega}\ln\left(1+\omega x_1^*\right) + \delta\ln\left(x_1^*\right) + qx_1^* \\ &= b\ln(b/p) - b - \frac{c}{\omega}\ln\left(1+\omega x_1^*\right) + \delta\ln\left(x_1^*\right) + qx_1^* \\ &= b\ln\left(be^{-1}/p\right) - \frac{c}{\omega}\ln\left(1+\omega x_1^*\right) + \delta\ln\left(x_1^*\right) + qx_1^* \end{aligned}$$

and

$$\begin{aligned} h_2 &= b\ln\left(y_2^*\right) - py_2^* - \frac{c}{\omega}\ln\left(1+\omega x_2^*\right) + \delta\ln\left(x_2^*\right) + qx_2^* \\ &= b\ln\left(be^{-1}/p\right) - \frac{c}{\omega}\ln\left(1+\omega x_2^*\right) + \delta\ln\left(x_2^*\right) + qx_2^*. \end{aligned}$$

The family of closed orbits is

$$\Gamma_h = \left\{(x,y)|H(x,y) = h, h_1 < h < h_2\right\}, \tag{3.7}$$

moreover, Γ_h converts to the equilibrium point E_2 as $h \to h_2$, and Γ_h becomes the homoclinic cycle as $h \to h_1$.

Therefore, the two curves $F_1(x)$ and $F_2(x)$ are tangent at $x = x_1^*$ or $x = x_2^*$, *i.e.* $h = h_1$ or $h = h_2$. If we choose h as a bifurcation parameter, then the domains of two branches of y_L and y_U can be determined as follows:

- If $h_1 < h < h_2$, then there are three intersect points between two functions $F_1(x)$ and $F_2(x)$, denoted by $x_{\min}$, x_{mid}, and $x_{\max}$, as shown in Figure 2. For this case, the two branches of y_L and y_U are well defined for all $x \in [x_{\min}, x_{\mathrm{mid}}] \cup [x_{\max}, +\infty)$ with $y_L \le \frac{b}{p} \le y_U$, as shown in Figure 3.

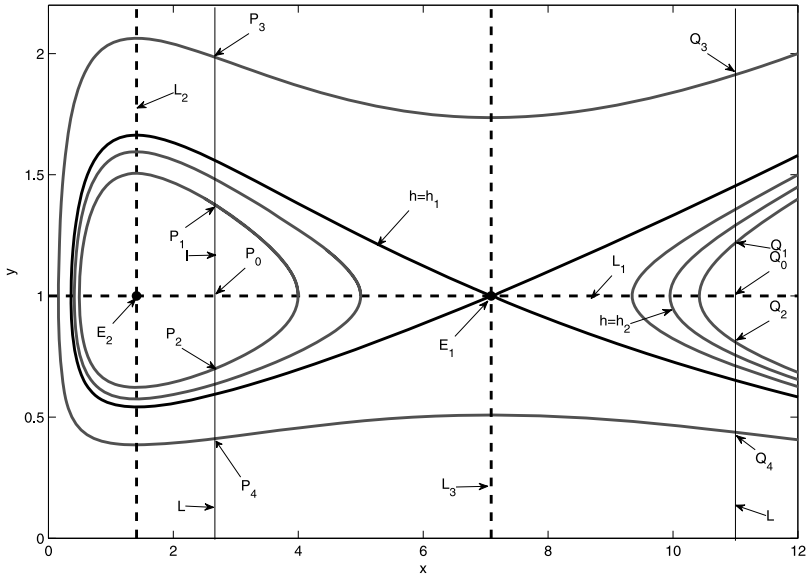

Figure 3 Two branches of y_L and y_U with respect to different h values and the diagram for Theorem 3.1.

- If $h \le h_1$ or $h \ge h_2$, then there exists a unique intersect point between two functions $F_1(x)$ and $F_2(x)$, denoted by $x_{\min}$. For this case, the two branches of y_L and y_U with $y_L \le \frac{b}{p} \le y_U$ are well defined for all $x \in [x_{\min}, +\infty)$, as shown in Figure 3.

Similarly, for any solution $x = x(t), y = y(t)$ of system (3.1) initiating from (x_0, y_0) satisfies the relation

$$\int_{x_0}^{x} \left(\frac{c}{1+\omega z} - \frac{\delta}{z} - q \right) dz = \int_{y_0}^{y} \left(\frac{b}{z} - p \right) dz. \tag{3.8}$$

That is, we have

$$\frac{c}{\omega} \ln\left(\frac{1+\omega x(t)}{1+\omega x_0} \right) - \delta \ln\left(\frac{x(t)}{x_0} \right) - q\big[x(t) - x_0\big] = b \ln\left(\frac{y(t)}{y_0} \right) - p\big[y(t) - y_0\big], \tag{3.9}$$

$$b \ln(y) - py - \frac{c}{\omega} \ln(1+\omega x) + \delta \ln(x) + qx = h_0 \tag{3.10}$$

with $h_0 = b \ln(y_0) - py_0 - \frac{c}{\omega} \ln(1+\omega x_0) + \delta \ln(x_0) + qx_0$.

In particular, if $\omega = q = 0$, then the model becomes the classical Lotka-Volterra model, and the unique interior $(\delta/c, b/p)$ is a center. The first integral is as follows:

$$b \ln\left(\frac{y}{y_0} \right) - p[y - y_0] = c[x - x_0] - \delta \ln\left(\frac{x}{x_0} \right), \tag{3.11}$$

i.e. we have

$$b \ln(y) - py + \delta \ln(x) - cx = b \ln(y_0) - py_0 + \delta \ln(x_0) - cx_0.$$

The following theorem is useful for discussing the existence of multiple attractors of models with state-dependent feedback control proposed in this work.

Theorem 3.1 *Let straight line L_1 through point (x_1^*, y_e^*) be parallel to the x axis, as shown in Figure* 3. *Take any point P_0 (or Q_0) in L, draw the line L through P_0 (or Q_0), perpendicular to L_1. Choose a point P_1 (or Q_1) in L such that $|P_0P_1| = \ell > 0$ (or $|Q_0Q_1| = \ell > 0$), and then there exists a unique trajectory of system* (3.1) *through point P_1 (or Q_1) and it intersects another point P_2 (or Q_2) in L. Then we must have $|P_0P_1| = \ell \ge |P_0P_2|$ (or $|Q_0Q_1| = \ell \ge |Q_0Q_2|$), where $|\cdot|$ denotes the length of the line segment. Similar results can be had for the trajectory through point P_3 (or Q_3), as shown in Figure* 3.

Proof Note that there are three different trajectories shown in Figure 3, so in the following the closed orbits are chosen to illustrate Theorem 3.1, and the other two cases can be proved similarly. Therefore, taking any closed orbit as shown in Figure 4(A) which contains the center point E_2, and the closed orbit divided into two branches by the line $y = b/p$: the upper branch (denoted by U_b) and the lower branch (denoted by L_b). Let $\xi = x - x_2^*$, $\eta = y - b/p$, *i.e.*, $x = \xi + x_2^* > 0$, $y = \eta + b/p > 0$, then model (3.1) becomes

$$\begin{cases} \frac{d\xi(t)}{dt} = \frac{dx(t)}{dt} = -p\eta(\xi + x_2^*) \triangleq \phi(\xi, \eta), \\ \frac{d\eta(t)}{dt} = \frac{dy(t)}{dt} = \frac{\xi(\eta + b/p)[-q\omega\xi + (c - q - \delta\omega) - 2q\omega x_2^*]}{1+\omega(\xi + x_2^*)} \triangleq \psi(\xi, \eta), \end{cases} \tag{3.12}$$

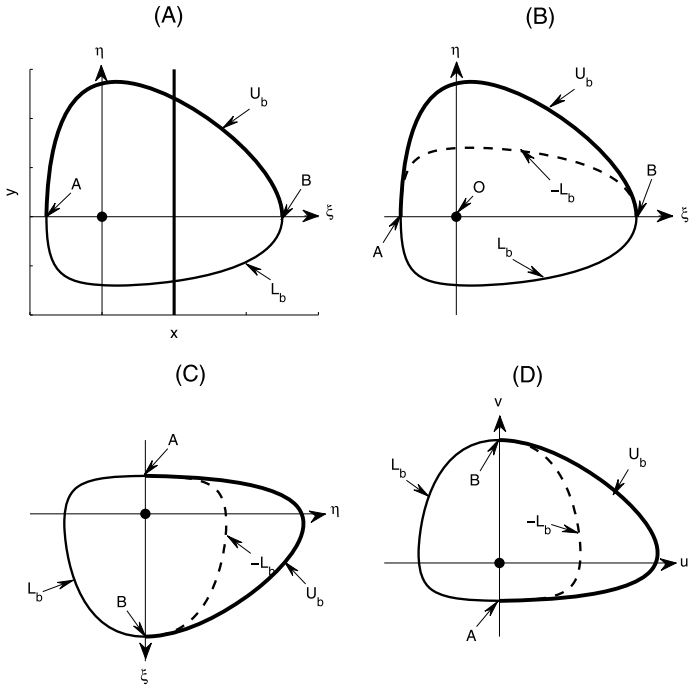

Figure 4 Illustration of transformations used in proof of Theorem 3.1.

which implies that

$$\frac{d\eta}{d\xi} = \frac{-\xi(\eta + b/p)[-q\omega\xi + (c - q - \delta\omega) - 2q\omega x_2^*]}{p\eta(\xi + x_2^*)(1 + \omega(\xi + x_2^*))} \triangleq F(\xi, \eta). \tag{3.13}$$

Meanwhile, the $-L_b$ shown in Figure 4(B) satisfies the following scalar differential equation:

$$\frac{d\eta}{d\xi} = \frac{-\psi(\xi, -\eta)}{\phi(\xi, -\eta)} = \frac{-\xi(-\eta + b/p)[-q\omega\xi + (c - q - \delta\omega) - 2q\omega x_2^*]}{p\eta(\xi + x_2^*)(1 + \omega(\xi + x_2^*))} \triangleq f(\xi, \eta). \tag{3.14}$$

Note that $\eta > 0$, $\xi + x_2^* > 0$, and $(c - q - \delta\omega) - 2q\omega x_2^* = \sqrt{(c - q - \delta\omega)^2 - 4q\omega\delta}$, and it is easy to know that $F(\xi, \eta) > f(\xi, \eta)$ for $\xi < 0$, $F(\xi, \eta) < f(\xi, \eta)$ for $0 < \xi < x_1^* - x_2^* = \sqrt{(c - q - \delta\omega)^2 - 4q\omega\delta}/(q\omega)$. Further, we have $F(\xi, \eta) \to \infty$ and $f(\xi, \eta) \to \infty$ as $\eta \to 0$.

Therefore, if we can show that the curve U_b lies above the curve $-L_b$ at the right hand side of point A and left hand of point B for all $0 < \eta \ll 1$ (as shown in Figure 4(B)), then, according to the comparison theorem of ODE, the whole curve U_b must lie above the whole curve $-L_b$ and the results follow. In the following we only prove the curve U_b lies above the curve $-L_b$ at the right hand side of point A. To do this, we rotate Figure 4(B) 90 degrees clockwise about the origin, as shown in Figure 4(C), and then denote $u = \eta$ and $v = -\xi$, which yields Figure 4(D). Consequently, (3.13) and (3.14) become

$$\begin{aligned} \frac{dv}{du} &= -\frac{1}{F(\xi, \eta)} = -\frac{1}{F(-v, u)} \\ &= \frac{pu(-v + x_2^*)(1 + \omega(-v + x_2^*))}{-v(u + b/p)[q\omega v + (c - q - \delta\omega) - 2q\omega x_2^*]} \triangleq g(u, v) \end{aligned} \tag{3.15}$$

and

$$\frac{dv}{du} = -\frac{1}{f(\xi,\eta)} = -\frac{1}{f(-v,u)} = \frac{pu(-v+x_2^*)(1+\omega(-v+x_2^*))}{-v(-u+b/p)[q\omega v+(c-q-\delta\omega)-2q\omega x_2^*]} \triangleq G(u,v). \tag{3.16}$$

Similarly, at the point A we have $v<0$ and $0<u\ll 1$, and then $0<-u+b/p<u+b/p$. Therefore, we have $g(u,v)<G(u,v)$ for $0<u\ll 1$ and $v<0$, and $g(u,v)=G(u,v)$ for $u=0$ and $v<0$. So if we choose the initial point A with $(u_0,v_0)=(0,v_0)$, then according to the second comparison theorem of ODE the results are true. □

Corollary 3.1 *If $\omega=0$ and $q=0$, then model* (3.1) *reduces to the classical Lotka-Volterra model, and we conclude that the results shown in Proposition* 2.1 *of reference* [1] *are true.*

4 Impulsive set, phase set, and Poincaré map

In order to employ the ideas of the Poincaré map or its successor function to address the existence and stability of order-k limit cycles, we must know the exact conditions under which the solution of model (2.2) initiating from $(x_0^+,y_0^+)\in\mathcal{N}$ is free from impulsive effects, *i.e.* the more exact phase set $\mathcal{N}$ should be provided. Moreover, for the impulsive set $\mathcal{M}$, $0\le y\le\frac{b}{p}$ is the maximum interval for the vertical coordinates of $\mathcal{M}$. Thus, we also want to know the exact interval, *i.e.* in which part of $0\le y\le\frac{b}{p}$ the solution of model (2.2) cannot reach and then the exact domains of the impulsive set can be obtained.

Based on the position of V_L for fixed θ we consider the following three cases:

$$(C_1)\quad V_L\ge x_1^*;\qquad (C_2)\quad x_2^*<V_L<x_1^*\quad\text{and}\quad (C_3)\quad V_L\le x_2^*. \tag{4.1}$$

Further, the three quantities A_{h_1}, A_h, and A_1 are useful throughout the rest of the paper, which are defined as

$$A_{h_1} = \frac{c}{\omega}\ln\left(\frac{1+\omega x_1^*}{1+\omega(1-\theta)V_L}\right)-\delta\ln\left(\frac{x_1^*}{(1-\theta)V_L}\right)-q\left[x_1^*-(1-\theta)V_L\right], \tag{4.2}$$

$$A_h = \frac{c}{\omega}\ln\left(\frac{1+\omega V_L}{1+\omega(1-\theta)V_L}\right)-\delta\ln\left(\frac{1}{1-\theta}\right)-q\theta V_L \tag{4.3}$$

and

$$A_1 = \frac{c}{\omega}\ln\left[\frac{1+\omega x_1^*}{1+\omega V_L}\right]-\delta\ln\left(\frac{x_1^*}{V_L}\right)-q\left[x_1^*-V_L\right]=A_{h_1}-A_h. \tag{4.4}$$

Based on the signs of A_{h_1}, A_h, and A_1, we can discuss of the domains of the impulsive set and the phase set of model (2.2). To show this, we let x_3^* be the horizontal component of the small intersection point (denoted by $E_3=(x_3^*,b/p)$) of the homoclinic cycle Γ_{h_1} with the line $y=b/p$ (Figure 5(A)), and x_4^* be the horizontal component of the intersection point (denoted by $E_4=(x_4^*,b/p)$) of the closed trajectory Γ_h which is contained inside the point E_2 and is tangent to the line L_4 at point T with $T=(V_L,\frac{b}{p})$, as shown in Figure 5(B). Thus, we have $x_3^*<x_4^*\le x_2^*<x_1^*$. For the third case (*i.e.* (C_3)), any solution initiating from the phase set $\mathcal{N}$ will experience infinite pulse effects, which means that the impulsive set and phase set for case (C_3) can easily be defined and obtained.

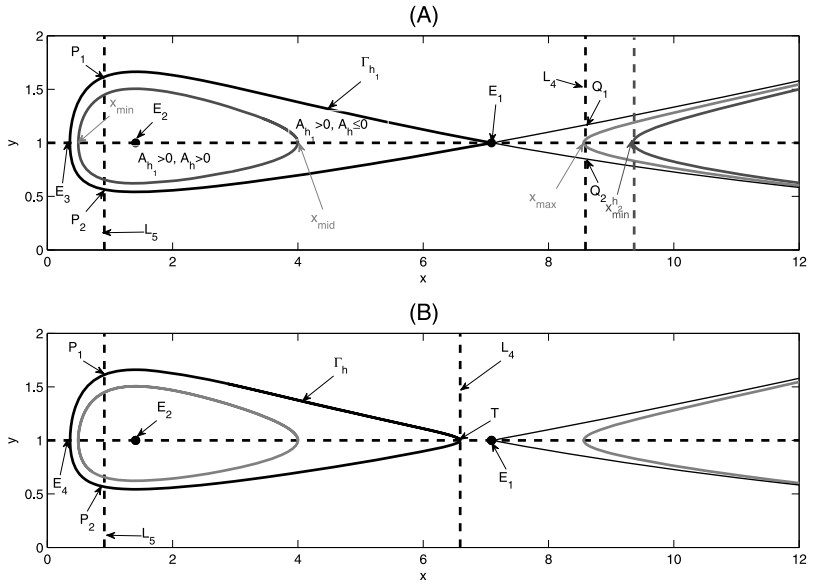

Figure 5 Illustrations of the domains of the impulsive set and the phase set for cases (C_1) and (C_2). **(A)** $V_L \geq x_1^*$ and $x_3^* \leq (1-\theta)V_L \leq x_1^*$; **(B)** $x_2^* < V_L < x_1^*$ and $x_4^* < (1-\theta)V_L$.

4.1 Impulsive set

There are two subsets $\mathcal{M}_1$ and $\mathcal{M}_2$ of the basic impulsive set $\mathcal{M}$ which are needed for providing the exact domains of the impulsive set of model (2.2), where

$$\mathcal{M}_1 = \left\{(x,y) \in R_+^2 | x = V_L, 0 \leq y \leq Y_{is}^h\right\} \tag{4.5}$$

and

$$\mathcal{M}_2 = \left\{(x,y) \in R_+^2 | x = V_L, 0 \leq y \leq Y_{is}^{h_1}\right\}, \tag{4.6}$$

where

$$Y_{is}^h = -\frac{b}{p} W\left(-e^{-1+\frac{A_h}{b}}\right), \qquad Y_{is}^{h_1} = -\frac{b}{p} W\left(-e^{-1-\frac{A_1}{b}}\right) \tag{4.7}$$

with $A_h \leq 0$ and $A_1 \geq 0$. Moreover, we have $\mathcal{M}_1 = \mathcal{M}$ once $A_h = 0$, and $\mathcal{M}_2 = \mathcal{M}$ once $A_1 = 0$.

Lemma 4.1 *For case* (C_1), *if* $(1-\theta)V_L < x_3^*$ *or* $(1-\theta)V_L > x_1^*$, *then the impulsive set is defined by* $\mathcal{M}_1$; *if* $x_3^* \leq (1-\theta)V_L \leq x_1^*$ *then the impulsive set is defined by* $\mathcal{M}_2$. *For case* (C_2), *if* $(1-\theta)V_L \leq x_4^*$, *then the impulsive set is defined as* $\mathcal{M}_1$; *if* $(1-\theta)V_L > x_4^*$, *then the impulsive set is defined by* $\mathcal{M}$. *For case* (C_3), *the impulsive set is defined by* $\mathcal{M}_1$.

Proof We first consider case (C_1). If $(1-\theta)V_L < x_3^*$, then there exists a curve Γ_1 which is tangent with line L_5 (defined as $x = (1-\theta)V_L$) at point $((1-\theta)V_L, b/p)$, where the curve Γ_1

can be determined as follows:

$$b\ln(y) - py - \frac{c}{\omega}\ln(1+\omega x) + \delta\ln(x) + qx = b\ln(b/p) - b - \frac{c}{\omega}\ln\bigl(1+\omega(1-\theta)V_L\bigr) + \delta\ln\bigl((1-\theta)V_L\bigr) + q(1-\theta)V_L. \tag{4.8}$$

For this case, the line L_4 (*i.e.* $x = V_L$) will intersect with the curve Γ_1 at two points, denoted by Q_1 and Q_2, and the vertical coordinates of both points are the two roots of the following equation:

$$b\ln(y) - py = b\ln(b/p) - b + A_h, \tag{4.9}$$

i.e. we have

$$-\frac{p}{b}ye^{-\frac{p}{b}y} = -e^{-1+\frac{A_h}{b}},$$

which can be solved by employing the Lambert W function, *i.e.* if $A_h \le 0$ then we have

$$Y_{is}^h = -\frac{b}{p}W\bigl(-e^{-1+\frac{A_h}{b}}\bigr), \qquad Y_{IS}^h = -\frac{b}{p}W\bigl(-1,-e^{-1+\frac{A_h}{b}}\bigr). \tag{4.10}$$

Thus, if $(1-\theta)V_L < x_3^*$, then the impulsive set is defined by $\mathcal{M}_1$. If so, no solution of model (2.2) initiating from the phase set can reach into the interval $(Y_{is}^h, b/p]$.

If $x_3^* \le (1-\theta)V_L \le x_1^*$, then the line L_4 intersects with the right branch of the homoclinic cycle $H(x,y) = h_1$ at two points, denoted by $Q_1 = (V_L, Y_{IS}^{h_1})$ and $Q_2 = (V_L, Y_{is}^{h_1})$ (as shown in Figure 5), where $Y_{IS}^{h_1}$ and $Y_{is}^{h_1}$ are two roots of the following equation with respect to y:

$$b\ln(y) - py = b\ln(b/p) - b - A_1.$$

Solving the above equation with respect to y yields two roots as follows:

$$Y_{is}^{h_1} = -\frac{b}{p}W\bigl(-e^{-1-\frac{A_1}{b}}\bigr), \qquad Y_{IS}^{h_1} = -\frac{b}{p}W\bigl(-1,-e^{-1-\frac{A_1}{b}}\bigr). \tag{4.11}$$

Therefore, if $x_3^* \le (1-\theta)V_L \le x_1^*$, then the impulsive set can be defined by $\mathcal{M}_2$. If so, no solution of model (2.2) initiating from the phase set can reach the interval $(Y_{is}^{h_1}, b/p]$.

If $(1-\theta)V_L > x_1^*$, then by using the same methods as subcase $(1-\theta)V_L < x_3^*$ the impulsive set is defined by $\mathcal{M}_1$. Similarly, we can prove the results for case (C_2) and case (C_3) are true. □

4.2 Phase set

The exact domains of the phase set depend on the domains of the impulsive set and whether the solution of model (2.2) initiating from $(x_0^+, y_0^+) \in \mathcal{N}$ is free from impulsive effects or not. Thus, to discuss the domains of the phase set, we define Y_D^1 and Y_D^2 related to the interval Y_D (here $Y_D = [\tau, b/p + \tau]$) as the following two intervals:

$$Y_D^1 = \bigl[\tau, Y_{is}^h + \tau\bigr], \qquad Y_D^2 = \bigl[\tau, Y_{is}^{h_1} + \tau\bigr]. \tag{4.12}$$

We first address under which conditions the solution of model (2.2) initiating from $(x_0^+, y_0^+) \in \mathcal{N}$ will be free from impulsive effects, and then provide the exact domains of the phase set for each case.

Lemma 4.2 *For case* (C_1), *if* $x_3^* \le (1-\theta)V_L \le x_1^*$, *then any solution initiating from* $(x_0^+, y_0^+) \in \mathcal{N}$ *with* $y_0^+ \in [Y_{\min}^{h_1}, Y_{\max}^{h_1}]$ *will be free from impulsive effects, where*

$$Y_{\min}^{h_1} = -\frac{b}{p} W\left(-e^{-1-\frac{A_{h_1}}{b}}\right), \qquad Y_{\max}^{h_1} = -\frac{b}{p} W\left(-1, -e^{-1-\frac{A_{h_1}}{b}}\right). \tag{4.13}$$

Moreover, $x_3^* < (1-\theta)V_L < x_1^* \Leftrightarrow A_{h_1} > 0$, *and* $A_{h_1} = 0$ *at* $(1-\theta)V_L = x_3^*$ *and* $(1-\theta)V_L = x_1^*$.

Proof Note that the curve of homoclinic cycle Γ_{h_1} can be described as follows:

$$\Gamma_{h_1}: \quad H(x,y) = b\ln(y) - py - \frac{c}{\omega}\ln(1+\omega x) + \delta\ln(x) + qx = h_1. \tag{4.14}$$

Substituting $y = b/p$ into the above equation, one can see that x_3^* satisfies the following equation:

$$F_2(x) \doteq \frac{c}{\omega}\ln\left(\frac{1+\omega x_1^*}{1+\omega x}\right) - \delta\ln\left(\frac{x_1^*}{x}\right) - q\left(x_1^* - x\right) = 0.$$

Taking the derivative of $F_2(x)$ with respect to x yields

$$F_2'(x) = -\frac{c}{1+\omega x} + q + \frac{\delta}{x}$$

and solving $F_2'(x) = 0$ yields two roots $x = x_2^*$ and $x = x_1^*$. It is easy to see that $F_2(x_1^*) = F_2'(x_1^*) = 0$. This indicates that $F_2(x) > 0$ for all $x \in (x_3^*, x_1^*) \cup (x_1^*, +\infty)$.

In this case, the line L_5 must intersect with the homoclinic cycle Γ_{h_1} at two points, denoted by $P_1 = ((1-\theta)V_L, Y_{\max}^{h_1})$ and $P_2 = ((1-\theta)V_L, Y_{\min}^{h_1})$, which are the two roots of (4.14) with respect to y for $x = (1-\theta)V_L$. In fact, substituting $x = (1-\theta)V_L$ into (4.14) and rearranging it yield

$$b\ln(y) - py = b\ln(b/p) - b - A_{h_1},$$

i.e. we have

$$-\frac{p}{b} y e^{-\frac{p}{b}y} = -e^{-1-\frac{A_{h_1}}{b}}.$$

Solving the above equation with respect to y yields two roots which are given by (4.13). Moreover, both P_1 and P_2 are well defined due to $A_{h_1} = F_2((1-\theta)V_L) \ge 0$ for all $x_3^* \le (1-\theta)V_L \le x_1^*$. Thus, any trajectory initiating from $(x_0^+, y_0^+) \in \mathcal{N}$ with $Y_{\min}^{h_1} \le y_0^+ \le Y_{\max}^{h_1}$ will be free from impulsive effects. □

Therefore, for case (C_1) (*i.e.* $V_L \ge x_1^*$), if $x_3^* \le (1-\theta)V_L \le x_1^*$, the phase set can be defined as follows:

$$\mathcal{N}_2^{h_1} = \left\{\left(x^+, y^+\right) \in R_+^2 | x^+ = (1-\theta)V_L, y^+ \in Y_D^{h_1}\right\} \tag{4.15}$$

with

$$Y_D^{h_1} = \left\{\left[0, Y_{\min}^{h_1}\right) \cup \left(Y_{\max}^{h_1}, +\infty\right]\right\} \cap Y_D^2. \tag{4.16}$$

If $(1-\theta)V_L < x_3^*$ or $(1-\theta)V_L > x_1^*$, then the phase set for model (2.2) is defined as

$$\mathcal{N}_1 = \left\{\left(x^+, y^+\right) \in R_+^2 | x^+ = (1-\theta)V_L, y^+ \in Y_D^1\right\}. \tag{4.17}$$

Moreover, any solution initiating from phase set $\mathcal{N}_1$ will experience infinite state-dependent feedback control actions.

Lemma 4.3 *For case* (C_2), *if* $x_4^* < (1-\theta)V_L$, *then any solution initiating from* $(x_0^+, y_0^+) \in \mathcal{N}$ *with* $y_0^+ \in (Y_{\min}^h, Y_{\max}^h)$ *will be free from impulsive effects, where*

$$Y_{\min}^h = -\frac{b}{p} W\left(-e^{-1-\frac{A_h}{b}}\right), \qquad Y_{\max}^h = -\frac{b}{p} W\left(-1, -e^{-1-\frac{A_h}{b}}\right). \tag{4.18}$$

Moreover, $x_4^* < (1-\theta)V_L \Leftrightarrow A_h > 0$, *and* $A_h = 0$ *at* $(1-\theta)V_L = x_4^*$.

Proof The closed orbit Γ_h for $h_1 < h < h_2$ which is contained inside the point E_2 and tangent to the line L_4 can be determined as follows:

$$\Gamma_h : \quad H(x,y) = b\ln(y) - py - \frac{c}{\omega}\ln(1+\omega x) + \delta\ln(x) + qx = h \tag{4.19}$$

with $h = b\ln(b/p) - b - \frac{c}{\omega}\ln(1+\omega V_L) + \delta\ln(V_L) + qV_L$.

Similarly, substituting $y = b/p$ into the above equation, one can see that x_4^* should be the smallest root of the following equation:

$$F_1(x) \doteq \frac{c}{\omega}\ln\left(\frac{1+\omega V_L}{1+\omega x}\right) - \delta\ln\left(\frac{V_L}{x}\right) - q(V_L - x) = 0.$$

Moreover, we have $F_1'(x_2^*) = F_1'(x_1^*) = 0$. This indicates that $F_1(x) > 0$ for all $x \in (x_4^*, V_L)$.

Further, the line L_5 must intersect with Γ_h at two points, denoted by $P_1 = ((1-\theta)V_L, Y_{\max}^h)$ and $P_2 = ((1-\theta)V_L, Y_{\min}^h)$, which are the two roots of (4.19) with respect to y for $x = (1-\theta)V_L$ and can be obtained by using the same methods as those in the proof of Lemma 4.2. Moreover, both P_1 and P_2 are well defined due to $A_h = F_1((1-\theta)V_L) \geq 0$ for all $x_4^* \leq (1-\theta)V_L$. Therefore, any trajectory initiating from $(x_0^+, y_0^+) \in \mathcal{N}$ with $Y_{\min}^h < y_0^+ < Y_{\max}^h$ will be free from impulsive effects. □

Therefore, for case (C_2) (*i.e.* $x_2^* < V_L < x_1^*$), if $x_4^* < (1-\theta)V_L$, then the phase set can be defined as follows:

$$\mathcal{N}_2^h = \left\{\left(x^+, y^+\right) \in R_+^2 | x^+ = (1-\theta)V_L, y^+ \in Y_D^h\right\} \tag{4.20}$$

with

$$Y_D^h = \left\{\left[0, Y_{\min}^h\right] \cup \left[Y_{\max}^h, +\infty\right]\right\} \cap Y_D. \tag{4.21}$$

Table 1 Exact domains of the impulsive set and phase set of model (2.2)

Cases	$(1-\theta)V_L$	Impulsive set	Phase set
(C_1)	$(1-\theta)V_L < x_3^*, (1-\theta)V_L > x_1^*$	$\mathcal{M}_1$	$\mathcal{N}_1$
	$x_3^* \le (1-\theta)V_L \le x_1^*$	$\mathcal{M}_2$	$\mathcal{N}_2^{h_1}$
(C_2)	$(1-\theta)V_L \le x_4^*$	$\mathcal{M}_1$	$\mathcal{N}_1$
	$(1-\theta)V_L > x_4^*$	$\mathcal{M}$	$\mathcal{N}_2^{h}$
(C_3)	$(1-\theta)V_L < x_2^*$	$\mathcal{M}_1$	$\mathcal{N}_1$

If $(1-\theta)V_L \le x_4^*$, then the phase set is defined by $\mathcal{N}_1$. Finally, for case (C_3), it is easy to see that the phase set for model (2.2) is defined by $\mathcal{N}_1$.

In conclusion, we list all possible cases for the domains of the impulsive set and phase set of model (2.2) in Table 1. It follows that the basic phase set $\mathcal{N}$ cannot be used to define the real phase set of model (2.2) for any case. This indicates that the exact domains of the phase set of model (2.2) should be carefully discussed. However, the domains of the impulsive set and phase set have not been discussed carefully in the previous literature [1, 4], which may result in some difficulties in employing the Poincaré map or its successor function to study the existence and stability of limit cycles of planar impulsive semi-dynamical systems.

In the following, if we consider both A_{h_1} and A_h as functions of V_L, then we have the following results.

Lemma 4.4 *$A_{h_1} = A_h$ at $V_L = x_1^*$ and $A_{h_1} > A_h$ if $V_L > x_1^*$.*

Proof It is easy to see that

$$F(V_L) \doteq A_{h_1} - A_h = \frac{c}{\omega}\ln\left[\frac{1+\omega x_1^*}{1+\omega V_L}\right] - \delta\ln\left[\frac{x_1^*}{V_L}\right] - q\left[x_1^* - V_L\right] \doteq A_1. \tag{4.22}$$

Based on the proof of Lemma 4.2 we can see that the equation $F'(V_L) = 0$ with respect to V_L has two roots $V_L = x_2^*$ and $V_L = x_1^*$. It follows from $F(x_1^*) = F'(x_1^*) = 0$ that $A_{h_1} > A_h$ for all $V_L > x_1^*$. □

The impulsive set and phase set for model (2.3). Let x_0^* be the horizontal component of the small intersection point (denoted by $E_0 = (x_0^*, b/p)$) of the closed trajectory Γ_{h_0} which is contained inside the center $(\delta/c, b/p)$ and is tangent to the line L_4 at point T with $T = (V_L, b/p)$. It follows from the first integral (3.11) that the closed cycle initiating from $(V_L, b/p)$ satisfies

$$b\ln(y) - py + \delta\ln(x) - cx = b\ln(b/p) - b + \delta\ln(V_L) - cV_L.$$

Substituting $y = b/p$ into the above equation, one can see that x_0^* satisfies

$$\delta\ln(x) - cx = \delta\ln(V_L) - cV_L,$$

solving it with respect to x we get two roots: one is V_L with $V_L \ge \frac{\delta}{c}$ and the other is given by

$$x_0^* = -\frac{\delta}{c}W\left(-\frac{cV_L}{\delta}\exp\left(-\frac{cV_L}{\delta}\right)\right).$$

Thus, by using the same methods as those in the proof of Lemma 4.3 we have the following results for model (2.3).

Lemma 4.5 *For the case $V_L > \delta/c$ in model* (2.3). *If $x_0^* < (1-\theta)V_L$, then any solution of model* (2.3) *initiating from $(x_0^+, y_0^+) \in \mathcal{N}$ with $y_0^+ \in [Y_{\min}^0, Y_{\max}^0]$ will be free from impulsive effects, where*

$$Y_{\min}^0 = -\frac{b}{p} W\left(-e^{-1-\frac{A_0}{b}}\right), \qquad Y_{\max}^0 = -\frac{b}{p} W\left(-1, -e^{-1-\frac{A_0}{b}}\right) \tag{4.23}$$

and

$$A_0 = c\theta V_L - \delta \ln\left(\frac{1}{1-\theta}\right). \tag{4.24}$$

Moreover, $x_0^* < (1-\theta)V_L \Leftrightarrow A_0 > 0$ and $A_0 = 0$ at $V_L = \frac{x_0^*}{1-\theta}$.

The impulsive set of model (2.3) can be determined as those for model (2.2), and we only need to consider two cases, *i.e.* $V_L > \delta/c$ and $V_L \le \delta/c$. For the former case, if $(1-\theta)V_L < \delta/c$ then the impulsive set is defined by $\mathcal{M}_1^0$ and

$$\mathcal{M}_1^0 = \left\{(x,y) \in R_+^2 | x = V_L, 0 \le y \le Y_{is}^0\right\} \tag{4.25}$$

with

$$Y_{is}^0 = -\frac{b}{p} W\left(-e^{-1+\frac{A_0}{b}}\right). \tag{4.26}$$

If $(1-\theta)V_L \ge \delta/c$ then the impulsive set is $\mathcal{M}$. For the latter case (*i.e.* $V_L \le \delta/c$), it is easy to see that the impulsive set is defined by $\mathcal{M}_1^0$.

Therefore, if $V_L > \delta/c$, then the phase set for the case $x_0^* < (1-\theta)V_L$ can be defined as

$$\mathcal{N}_2^{h0} = \left\{\left(x^+, y^+\right) \in R_+^2 | x^+ = (1-\theta)V_L, y^+ \in Y_D^{h0}\right\} \tag{4.27}$$

with

$$Y_D^{h0} = \left\{\left[0, Y_{\min}^0\right] \cup \left[Y_{\max}^0, +\infty\right]\right\} \cap Y_D. \tag{4.28}$$

The phase set for the case $(1-\theta)V_L \le x_0^*$ is defined by $\mathcal{N}_1^0$ and

$$\mathcal{N}_1^0 = \left\{\left(x^+, y^+\right) \in R_+^2 | x^+ = (1-\theta)V_L, y^+ \in Y_D^0\right\}, \quad \text{and} \quad Y_D^0 = \left[\tau, Y_{is}^0 + \tau\right]. \tag{4.29}$$

Finally, if $V_L \le \delta/c$, then it is easy to see that the phase set is defined by $\mathcal{N}_1^0$.

Remark 4.1 Before we provide the formula for the Poincaré map of model (2.2), we want to show how the phase sets change as the key parameters (*i.e.* θ, V_L, and τ) vary. For example, the set $\mathcal{N}_2^h$ can be defined exactly according to the relations among τ, $Y_{\min}^h$, and $Y_{\max}^h$. One simple case is as follows: if $\tau \le Y_{\min}^h$ and $Y_{\max}^h \le \tau + b/p$ then

$$\mathcal{N}_2^h = \left\{\left(x^+, y^+\right) \in R_+^2 | x^+ = (1-\theta)V_L, y^+ \in Y_D^{mM} = \left[\tau, Y_{\min}^h\right] \cup \left[Y_{\max}^h, \tau + b/p\right]\right\}. \tag{4.30}$$

Similarly, we can discuss several other cases and get the domains of Y_D^{mM} and $\mathcal{N}_2^h$, where

$$Y_D^{mM} = \begin{cases} [\tau, Y_{\min}^h] \cup [Y_{\max}^h, \tau + b/p], & \text{if } \tau \le Y_{\min}^h < Y_{\max}^h \le \tau + b/p, \\ [Y_{\max}^h, \tau + b/p], & \text{if } Y_{\min}^h < \tau \le Y_{\max}^h \le \tau + b/p, \\ [\tau, \tau + b/p], & \text{if } Y_{\min}^h < Y_{\max}^h < \tau < \tau + b/p, \\ [\tau, Y_{\min}], & \text{if } \tau \le Y_{\min}^h < \tau + b/p < Y_{\max}^h, \\ \emptyset, & \text{if } Y_{\min}^h < \tau < \tau + b/p < Y_{\max}^h. \end{cases} \tag{4.31}$$

It follows from Remark 4.1 that the relations among τ, $Y_{\min}^h$, and $Y_{\max}^h$ are crucial for the exact domains of the phase set, which will be addressed later.

4.3 Poincaré map

Theorem 4.1 *The Poincaré map for the impulsive points of model* (2.2) *defined in the phase set can be determined as*

$$(\mathrm{C}_1): \quad y_{i+1}^+ = \begin{cases} \mathcal{P}(y_i^+), & y_i^+ \in Y_D^{h_1} \quad \text{if } x_3^* \le \theta_1 V_L \le x_1^*, \\ \mathcal{P}(y_i^+), & y_i^+ \in Y_D^1 \quad \text{if } \theta_1 V_L < x_3^* \text{ or } \theta_1 V_L > x_1^*, \end{cases} \tag{4.32}$$

$$(\mathrm{C}_2): \quad y_{i+1}^+ = \begin{cases} \mathcal{P}(y_i^+), & y_i^+ \in Y_D^h \quad \text{if } x_4^* < \theta_1 V_L, \\ \mathcal{P}(y_i^+), & y_i^+ \in Y_D^1 \quad \text{if } \theta_1 V_L \le x_4^*, \end{cases} \tag{4.33}$$

$$(\mathrm{C}_3): \quad y_{i+1}^+ = \mathcal{P}(y_i^+), \quad y_i^+ \in Y_D^1. \tag{4.34}$$

Here $\theta_1 = 1 - \theta$ *and*

$$\mathcal{P}(y_i^+) \triangleq -\frac{b}{p} W\left[-\frac{p}{b} y_i^+ \exp\left(-\frac{p}{b} y_i^+ + \frac{A_h}{b} \right) \right] + \tau. \tag{4.35}$$

Proof Assuming that any solution $\Pi_{z_0^+}$ with initial condition $z_0^+ = (x_0^+, y_0^+) \in \mathcal{N}$ experiences impulses $k+1$ times (finite or infinite), we denote the corresponding coordinates $P_i = (V_L, y_i) \in \mathcal{M}$ and $P_i^+ = ((1-\theta)V_L, y_i^+) \in \mathcal{N}$, $i = 1, 2, \ldots, k$. Therefore, if both points P_i^+ and P_{i+1} lie in the same trajectory Γ (closed or non-closed) for $i = 0, 1, \ldots, k$, then the points P_i^+ and P_{i+1} satisfy the following relation:

$$\frac{c}{\omega} \ln\left(\frac{1 + \omega V_L}{1 + \omega(1-\theta)V_L} \right) - \delta \ln\left(\frac{1}{1-\theta} \right) - q\theta V_L = A_h = b \ln\left(\frac{y_{i+1}}{y_i^+} \right) - p\left[y_{i+1} - y_i^+ \right]. \tag{4.36}$$

In order to show the exact domains of the Poincaré map, we first need to know under what conditions the trajectory initiating from $P_i^+ \in \mathcal{N}$ cannot reach the point $P_{i+1} \in \mathcal{M}$. There are two cases:

Case (i): $V_L \ge x_1^*$ and $x_3^* \le (1-\theta)V_L \le x_1^*$. It follows from Lemma 4.2 that if the initial point $P_i^+ = ((1-\theta)V_L, y_i^+)$ lies in the homoclinic cycle Γ_{h_1} or its interior, then although the two points P_i^+ and P_{i+1} could satisfy (4.36), the trajectory cannot reach the line L_4 forever, which indicates that both points P_i^+ and P_{i+1} cannot lie in the same trajectory, as shown in Figure 5(A). It follows from Lemma 4.2 and Table 1 that in this case we have $A_{h_1} \ge 0$ and we require $P_i^+ \in \mathcal{N}_2^{h_1}$.

Case (ii): $x_2^* < V_L < x_1^*$ and $x_4^* < (1-\theta)V_L$. It follows from Lemma 4.3 that if the initial point $P_i^+ = ((1-\theta)V_L, y_i^+)$ lies in the interior of the closed cycle Γ_h, then the trajectory

cannot reach the line L_4, which shows that both points P_i^+ and P_{i+1} cannot lie in the same trajectory, as shown in Figure 5(B). It follows from Lemma 4.3 and Table 1 again that in this case we have $A_h > 0$ and we require $P_i^+ \in \mathcal{N}_2^h$.

Rearranging (4.36) yields

$$-\frac{p}{b}y_{i+1}\exp\left(-\frac{p}{b}y_{i+1}\right) = -\frac{p}{b}y_i^+\exp\left(-\frac{p}{b}y_i^+ + \frac{A_h}{b}\right), \quad i = 0,1,\ldots,k.$$

Solving the above equation with respect to y_{i+1}, we have

$$y_{i+1} = -\frac{b}{p}W\left[-\frac{p}{b}y_i^+\exp\left(-\frac{p}{b}y_i^+ + \frac{A_h}{b}\right)\right], \quad i = 0,1,\ldots,k \tag{4.37}$$

and

$$y_{i+1}^+ = -\frac{b}{p}W\left[-\frac{p}{b}y_i^+\exp\left(-\frac{p}{b}y_i^+ + \frac{A_h}{b}\right)\right] + \tau \triangleq \mathcal{P}\left(y_i^+\right), \quad i = 0,1,\ldots,k. \tag{4.38}$$

If $A_h \le 0$, it is easy to show that $-\frac{p}{b}y_i^+\exp(-\frac{p}{b}y_i^+ + \frac{A_h}{b}) \in [-e^{-1}, 0)$ for all $A_h \le 0$, this indicates that equation (4.38) is well defined in this case. If $A_h > 0$, we must have $-\frac{p}{b}y_i^+\exp(-\frac{p}{b}y_i^+ + \frac{A_h}{b}) \ge -e^{-1}$. It follows that we get the inequality

$$\frac{p}{b}y_i^+\exp\left(-\frac{p}{b}y_i^+\right) \le \exp\left(-1 - \frac{A_h}{b}\right),$$

which is solved to give, $y_i^+ \in (0, Y_{\min}^h] \cup [Y_{\max}^h, \infty)$, where $Y_{\min}^h$ and $Y_{\max}^h$ are given in (4.18).

Therefore, for case (C_1), if $x_3^* \le (1-\theta)V_L \le x_1^*$, then it follows from Lemma 4.4 that $A_{h_1} > A_h$ and according to the monotonicity of the Lambert W function we have $[Y_{\min}^h, Y_{\max}^h] \subset [Y_{\min}^{h_1}, Y_{\max}^{h_1}]$. So no matter what $A_{h_1} > A_h > 0$ and $A_{h_1} > 0 \ge A_h$ (as shown in Figure 5) the Poincaré map is given by the first case of (4.32) if $x_3^* \le (1-\theta)V_L \le x_1^*$. If $(1-\theta)V_L < x_3^*$ or $(1-\theta)V_L > x_1^*$, then it follows from the proofs of Lemma 4.1 and Lemma 4.2 that we must have $A_h < 0$, consequently the Poincaré map is given by the second case of (4.32).

The other two cases (C_2) and (C_3) of Theorem 4.1 can be obtained directly from the domains of the Poincaré map and the proof of Lemma 4.3. This completes the proof. □

It follows from Lemma 4.5 that we have the main results for the Poincaré map of the impulsive points of model (2.3).

Corollary 4.1 *The Poincaré map for the impulsive points of model* (2.3) *defined in the phase set can be determined as*

$$y_{i+1}^+ = \begin{cases} \mathcal{P}(y_i^+), & y_i^+ \in Y_D^{h0} \quad \text{if } V_L > \frac{\delta}{c} \text{ and } x_0^* < \theta_1 V_L, \\ \mathcal{P}(y_i^+), & y_i^+ \in Y_D^0 \quad \text{if } V_L > \frac{\delta}{c} \text{ and } \theta_1 V_L \le x_0^*, \\ \mathcal{P}(y_i^+), & y_i^+ \in Y_D^0 \quad \text{if } V_L \le \frac{\delta}{c}. \end{cases} \tag{4.39}$$

Compared with published definitions of the Poincaré map for model (2.3) [1, 4], we can see that more accurate domains have been provided in formula (4.39).

Based on the proofs of Lemmas 4.1-4.5 and Theorem 4.1 we can see that the signs of A_{h_1} and A_h play the key roles in determining the domains of the impulsive set and phase set,

Table 2 The relations among the key parameters (*i.e.* θ, V_L, and τ), the signs of A_{h_1} and A_h and the domains of the Poincaré map $\mathcal{P}(y_i^+)$

Cases	V_L	$\theta_1 V_L$	A_h and A_{h_1}	$\mathcal{P}(y_i^+)$
(C_1)	$V_L < x_{\min}^{h_2}$	$x_3^* \le \theta_1 V_L \le x_{\min}$	$A_h \le 0, A_{h_1} \ge 0$	$y_i^+ \in Y_D^{h_1}$
		$x_{\min} < \theta_1 V_L < x_{\mathbf{mid}}$	$A_h > 0, A_{h_1} \ge 0$	
		$x_{\mathbf{mid}} \le \theta_1 V_L \le x_1^*$	$A_h \le 0, A_{h_1} \ge 0$	
		$\theta_1 V_L < x_3^*$	$A_h \le 0, \times$	$y_i^+ \in Y_D^1$
		$x_1^* < \theta_1 V_L$		
	$x_{\min}^{h_2} \le V_L$	$x_3^* \le \theta_1 V_L \le x_1^*$	$A_h \le 0, A_{h_1} \ge 0$	$y_i^+ \in Y_D^{h_1}$
		$\theta_1 V_L < x_3^*$	$A_h \le 0, \times$	$y_i^+ \in Y_D^1$
		$x_1^* < \theta_1 V_L$		
(C_2)		$x_4^* < \theta_1 V_L$	$A_h > 0, \times$	$y_i^+ \in Y_D^h$
		$\theta_1 V_L \le x_4^*$	$A_h \le 0, \times$	$y_i^+ \in Y_D^1$
(C_3)			$A_h \le 0, \times$	$y_i^+ \in Y_D^1$

$\times$ means the sign of A_{h_1} is not necessary for that subcase and $\theta_1 = 1 - \theta$.

and in defining the Poincaré map $\mathcal{P}(y_i^+)$. Therefore, the relations among the key parameters (*i.e.* θ, V_L, and τ), the signs of A_{h_1} and A_h and the domains of the Poincaré map $\mathcal{P}(y_i^+)$ will be discussed briefly before we address the existence and stability of the limit cycle of model (2.2), which are also important in the rest of this work.

To do this, we take the notations shown in Figure 5, where $x_{\min}^{h_2}$ represents the intersection point of the curve $H(x,y) = h_2$ with the line $y = b/p$. Then the relations among the key parameters (*i.e.* θ, V_L, and τ), the signs of A_{h_1} and A_h and the domains of the Poincaré map $\mathcal{P}(y_i^+)$ can be summarized in Table 2.

5 Existence of order-1 limit cycles and some important relations

Investigations of the existence and stability of order-1 limit cycles of system (2.2) for the whole parameter space are quite challenging, and are similar to the study of the existence and stability of limit cycles of continuous semi-dynamical systems. Fortunately, the analytical formula of the Poincaré map defined by the impulsive points in the phase set has been obtained, which allows us to employ it to study the existence and stability of order-1 limit cycles of model (2.2).

The fixed point of the Poincaré map $\mathcal{P}(y_i^+)$ in the phase set corresponds with the existence of the order-1 limit cycles of model (2.2) and model (2.3). Without loss of generality, we first discuss the existence of a fixed point of the Poincaré map $\mathcal{P}(y_i^+)$ in the basic phase set $\mathcal{N}$, *i.e.* $y_i^+ \in Y_D$, and then we will focus on the particular domains of the Poincaré map $\mathcal{P}(y_i^+)$ in phase sets and discuss the existence of the fixed point. Denote the fixed point as y^*, then we have

$$\mathcal{P}(y^*) = -\frac{b}{p} W\left[-\frac{p}{b} y^* \exp\left(-\frac{p}{b} y^* + \frac{A_h}{b}\right)\right] + \tau = y^*. \tag{5.1}$$

Since $y^* \in Y_D = [\tau, b/p + \tau]$, we have

$$W\left[-\frac{p}{b} y^* \exp\left(-\frac{p}{b} y^* + \frac{A_h}{b}\right)\right] = -\frac{p}{b}(y^* - \tau) \ge -1.$$

Therefore, according to the definition of the Lambert W function the above yields

$$-\frac{p}{b} y^* \exp\left(-\frac{p}{b} y^* + \frac{A_h}{b}\right) = -\frac{p}{b}(y^* - \tau) \exp\left(-\frac{p}{b}(y^* - \tau)\right).$$

Note that if $\tau = 0$ and $A_h = 0$, then for any $0 \le y^* \le b/p$ the above equation holds true; if $\tau = 0$ and $A_h \neq 0$, then $y^* = 0$ is a unique fixed point of Poincaré map $\mathcal{P}(y_i^+)$. If $\tau > 0$, then solving the above equation with respect to y^* yields

$$y^* = \tau \frac{\exp(\frac{p}{b}\tau - \frac{A_h}{b})}{\exp(\frac{p}{b}\tau - \frac{A_h}{b}) - 1}. \tag{5.2}$$

The necessary condition for the existence of a fixed point of the Poincaré map $\mathcal{P}(y_i^+)$ in the phase set is $y^* \in Y_D$. Thus, it is interesting to show under what conditions the $y^* \in (\tau, b/p + \tau]$ first. To do this, we consider the following two cases: (i) $A_h \le 0$; and (ii) $A_h > 0$.

If $A_h \le 0$, then it is easy to show that $y^* > \tau$ and

$$y^* = \tau \frac{\exp(\frac{p}{b}\tau - \frac{A_h}{b})}{\exp(\frac{p}{b}\tau - \frac{A_h}{b}) - 1} \le \frac{b}{p} + \tau$$

hold true. This indicates that if $A_h \le 0$, then $y^* \in (\tau, b/p + \tau]$.

If $A_h > 0$, then we first need $\exp(\frac{p}{b}\tau - \frac{A_h}{b}) - 1 > 0$ to ensure that y^* is positive and $y^* > \tau$. Thus we must have $A_h < p\tau$. Furthermore,

$$y^* = \tau \frac{\exp(\frac{p}{b}\tau - \frac{A_h}{b})}{\exp(\frac{p}{b}\tau - \frac{A_h}{b}) - 1} \le \frac{b}{p} + \tau$$

is equivalent to

$$\exp\left(\frac{p}{b}\tau - \frac{A_h}{b}\right) - \frac{p}{b}\tau - 1 \ge 0.$$

Rearranging the above inequality yields

$$-\frac{p}{b}\left(\tau + \frac{b}{p}\right)\exp\left[-\frac{p}{b}\left(\tau + \frac{b}{p}\right)\right] \ge -\exp\left(-1 - \frac{A_h}{b}\right).$$

Solving the above inequality with respect to $\tau + \frac{b}{p}$ yields $\tau + \frac{b}{p} \le Y_{\min}^h$ (which is impossible due to $Y_{\min}^h < \frac{b}{p}$) or $\tau + \frac{b}{p} \ge Y_{\max}^h$. This indicates that if $\tau + \frac{b}{p} \ge Y_{\max}^h$, then $y^* \le \frac{b}{p} + \tau$ when $0 < A_h < p\tau$.

Based on the definition of the Poincaré map $\mathcal{P}(y_i^+)$ and its domains, the point $((1 - \theta)V_L, y^*)$ related to the fixed point y^* must lie in the domains of phase sets rather than basic phase set (*i.e.* $y^* \in Y_D$). To address this and reveal all possible dynamic behavior of model (2.2), we first need to investigate some important relations among y^*, y_2^*, $\tau + b/p$, $Y_{\min}^i$, $Y_{\max}^i$ for $i = h, h_1$ and $\tau + Y_{is}^h$, where

$$y_2^* = \frac{b + p\tau + \sqrt{b^2 + p^2\tau^2}}{2p}. \tag{5.3}$$

5.1 Some important relations

Note that the key parameters θ and V_L determine the domains of the Poincaré map $\mathcal{P}(y_i^+)$, and the third key parameter τ will play a crucial role in determining the dynamics of model (2.2). Thus, the parameter τ related to state-dependent feedback control has been chosen

to address the relations, *i.e.* we consider y^*, y_2^*, $\tau + b/p$, $Y^i_{\min}$, $Y^i_{\max}$ for $i = h, h_1$ and $\tau + Y^h_{is}$ as functions of τ. As the first step, we discuss the monotonicity of the y^*, where y^* is given by (5.2), and we have the following results.

Lemma 5.1 *If* $0 < A_h < p\tau$, *then* y^* *reaches its minimal value* (*denoted by* $y^*_{\min}$ *and* $y^*_{\min} = Y^h_{\max}$) *at* $\tau_M = Y^h_{\max} - \frac{b}{p}$.

Proof Taking the derivative of y^* with respect to τ yields

$$\frac{dy^*}{d\tau} = \frac{\exp(\frac{p}{b}\tau - \frac{A_h}{b})[b\exp(\frac{p}{b}\tau - \frac{A_h}{b}) - b - p\tau]}{b[\exp(\frac{p}{b}\tau - \frac{A_h}{b}) - 1]^2}. \tag{5.4}$$

Since $A_h < p\tau$, it is seen that $\frac{dy^*}{d\tau} = 0$ is equivalent to

$$\Im_\tau \doteq b\exp\left(\frac{p}{b}\tau - \frac{A_h}{b}\right) - b - p\tau = 0. \tag{5.5}$$

Rearranging the above equation yields

$$-\left(1 + \frac{p\tau}{b}\right)\exp\left(-1 - \frac{p\tau}{b}\right) = -\exp\left(-1 - \frac{A_h}{b}\right)$$

and it is easy to see that $A_h < p\tau$ is a necessary condition for the existence of a positive root of the above equation with respect to τ. Solving the above equation with respect to τ, one has two roots and only the larger one is positive, denoted by τ_M, where

$$\tau_M = -\frac{b}{p} - \frac{b}{p}W\left(-1, -e^{-1-\frac{A_h}{b}}\right) = Y^h_{\max} - \frac{b}{p} > \frac{A_h}{p}. \tag{5.6}$$

Moreover, we have $\lim_{\tau \to \frac{A_h}{p}^+} y^* = +\infty$, as shown in Figure 6. This indicates that the y^* reaches its minimal value at τ_M. By calculation we have $\exp(\frac{p}{b}\tau_M - \frac{A_h}{b}) = -W(-1, -e^{-1-\frac{A_h}{b}})$, and consequently we have

$$y^*_{\min} = \tau_M \frac{W(-1, -e^{-1-\frac{A_h}{b}})}{1 + W(-1, -e^{-1-\frac{A_h}{b}})} = -\frac{b}{p}W\left(-1, -e^{-1-\frac{A_h}{b}}\right) = Y^h_{\max}. \tag{5.7}$$

Furthermore, it follows from Theorem 3.1 that

$$\tau_M = Y^h_{\max} - \frac{b}{p} > \frac{b}{p} - Y^h_{\min}. \tag{5.8}$$

□

Lemma 5.2 *If* $A_h \le 0$, *then the inequality* $y* < y_2^*$ *holds true naturally.*

Proof If $A_h \le 0$, then the inequality $y* < y_2^*$ can be rewritten as

$$\tau\frac{\exp(\frac{p}{b}\tau - \frac{A_h}{b})}{\exp(\frac{p}{b}\tau - \frac{A_h}{b}) - 1} \le \tau\frac{\exp(\frac{p}{b}\tau)}{\exp(\frac{p}{b}\tau) - 1} < \frac{b + p\tau + \sqrt{b^2 + p^2\tau^2}}{2p}.$$

Rearranging the above inequality yields

$$\left(b+\sqrt{b^2+p^2\tau^2}-p\tau\right)\exp\left[\frac{p}{b}\tau\right]-b-p\tau-\sqrt{b^2+p^2\tau^2}>0. \tag{5.9}$$

Denote $z=\frac{p}{b}\tau>0$, then the above inequality is equivalent to

$$e^z>\frac{1+\sqrt{1+z^2}+z}{1+\sqrt{1+z^2}-z}=z+\sqrt{1+z^2}.$$

Let $F(z)=e^z-(z+\sqrt{1+z^2})$ and we have

$$F(z)>1+z+\frac{1}{2}z^2-\left(z+\sqrt{1+z^2}\right)=1+\frac{1}{2}z^2-\sqrt{1+z^2}>0. \qquad \square$$

To discuss the relations among y^*, $\tau+b/p$, $Y^{h_1}_{\max}$, and $Y^{h_1}_{\min}$ which will be used in this work, we define the following four functions with respect to τ

$$\Im^1_\tau \doteq \tau+\frac{b}{p}-y^*, \qquad \Im^2_\tau \doteq y^*-Y^{h_1}_{\max}, \qquad \Im^3_\tau \doteq y^*-y^*_2, \qquad \Im^4_\tau \doteq y^*-Y^{h_1}_{\min}. \tag{5.10}$$

For the first equation $\Im^1_\tau \doteq \tau+\frac{b}{p}-y^*=0$, substituting y^* into it and arranging the items we can see which is equivalent to the equation $\Im_\tau=0$ (defined by (5.5)). This indicates that the equation $\Im_\tau=0$ has a unique positive root τ_M, *i.e.* the two curves y^* and $\tau+b/p$ with respect to τ intersect at $\tau=\tau_M$, as shown in Figure 6.

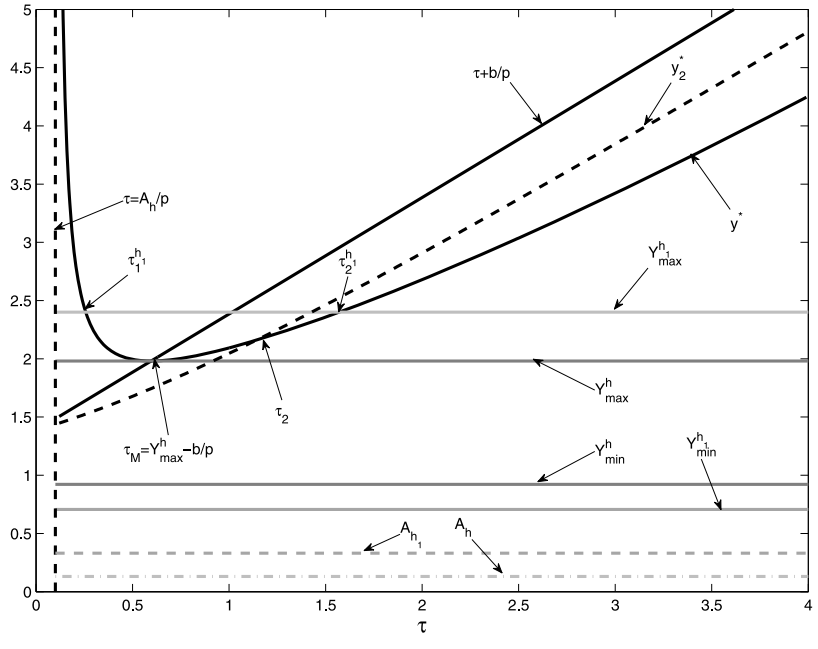

Figure 6 The relations among y^*, y^*_2, $\tau+b/p$, $Y^i_{\min}$, $Y^i_{\max}$ and $i=h,h_1$. All other parameter values are fixed as follows: $b=1.8$, $p=1.3$, $c=0.52$, $\omega=0.1$, $q=0.23$, $\delta=0.3$, $\theta=0.8$, and $V_L=4$.

Substituting y^* into the second function and letting $\Im_\tau^2 = 0$ yield

$$\Im_\tau^2 \doteq y^* - Y_{\max}^{h_1} = \tau \frac{\exp(\frac{p}{b}\tau - \frac{A_h}{b})}{\exp(\frac{p}{b}\tau - \frac{A_h}{b}) - 1} - Y_{\max}^{h_1} = 0. \tag{5.11}$$

Rearranging the above equation, one has

$$\frac{p}{b}\left(\tau - Y_{\max}^{h_1}\right)\exp\left(\frac{p}{b}\left(\tau - Y_{\max}^{h_1}\right)\right) = -\frac{p}{b}Y_{\max}^{h_1}\exp\left(-\frac{p}{b}Y_{\max}^{h_1} + \frac{A_h}{b}\right). \tag{5.12}$$

Substituting $Y_{\max}^{h_1} = -\frac{b}{p}W(-1, -e^{-1-\frac{A_{h_1}}{b}})$ into the right hand side of the above equation according to the equation $W(z)e^{W(z)} = z$ yields

$$-\frac{p}{b}Y_{\max}^{h_1}\exp\left(-\frac{p}{b}Y_{\max}^{h_1} + \frac{A_h}{b}\right) = -e^{-1}e^{-\frac{A_{h_1}-A_h}{b}} = -e^{-1}e^{-\frac{A_1}{b}}.$$

In order to ensure (5.12) has a positive root with respect to τ, the necessary condition is $\tau < Y_{\max}^{h_1}$. Given this and according to the definition of the Lambert W function we can solve it and yield two roots, denoted by $\tau_1^{h_1}$ and $\tau_2^{h_1}$, where

$$\tau_1^{h_1} = Y_{\max}^{h_1} + \frac{b}{p}W\left[-1, -e^{-1}e^{-\frac{A_1}{b}}\right] \tag{5.13}$$

and

$$\tau_2^{h_1} = Y_{\max}^{h_1} + \frac{b}{p}W\left[0, -e^{-1}e^{-\frac{A_1}{b}}\right]. \tag{5.14}$$

Note that $A_{h_1} \geq 0$ indicates that $A_{h_1} \geq A_h > 0$ or $A_{h_1} > 0 \geq A_h$, which means that both $\tau_1^{h_1}$ and $\tau_2^{h_1}$ are well defined. Moreover, if $A_h \leq 0$, then the small root $\tau_1^{h_1}$ disappears and y^* will intersect with $Y_{\min}^{h_1}$ at another point, which will be discussed later.

For the third function $\Im_\tau^3$, we want to find the root of equation $\Im_\tau^3 \doteq y^* - y_2^* = 0$ with respect to τ, *i.e.* the positive root of the following equation:

$$\tau \frac{\exp(\frac{p}{b}\tau - \frac{A_h}{b})}{\exp(\frac{p}{b}\tau - \frac{A_h}{b}) - 1} = \frac{b + p\tau + \sqrt{b^2 + p^2\tau^2}}{2p}. \tag{5.15}$$

It is impossible to solve the above equation directly with respect to τ, so we turn to a discussion of the existence of the positive roots. Note that $\Im_{\tau_M}^1 = \tau_M + \frac{b}{p} - y^*(\tau_M) = 0$ and $y_2^* < \tau + \frac{b}{p}$ for all $\tau > 0$. This indicates that $\Im_{\tau_M}^3 = y^*(\tau_M) - y_2^*(\tau_M) > 0$. Moreover, solving the equation $y_2^* - Y_{\max}^{h_1} = 0$ with respect to τ, denoted by τ^* yields

$$\tau^* = 2Y_{\max}^{h_1}\frac{b - pY_{\max}^{h_1}}{b - 2pY_{\max}^{h_1}} < Y_{\max}^{h_1}.$$

Furthermore, it is easy to see that $\Im_{\tau^*}^3 = y^*(\tau^*) - y_2^*(\tau^*) < 0$. Therefore, according to the monotonicity of the function y^* and y_2^* for $\tau \geq \tau_M$, we conclude that for the equation $\Im_\tau^3 = y^* - y_2^* = 0$ there exists a unique positive root, denoted by τ_2 with $\tau_2 \in (\tau_M, \tau^*)$ and $\tau_2 < \tau_2^{h_1}$, as shown in Figure 6.

Finally, we discuss the existence of the positive root of the equation $\Im_\tau^4 \doteq y^* - Y_{\min}^{h_1} = 0$ for the case $A_h \le 0$. By employing the same methods as those for the equation $\Im_\tau^2 \doteq y^* - Y_{\max}^{h_1} = 0$, it is easy to see that the for the equation $\Im_\tau^4 \doteq y^* - Y_{\min}^{h_1} = 0$ there exists a unique positive root, denoted by $\tau_3^{h_1}$, and

$$\tau_3^{h_1} = Y_{\min}^{h_1} + \frac{b}{p} W\big[0, -e^{-1}e^{-\frac{A_1}{b}}\big]. \tag{5.16}$$

Now we discuss the relations between y^* and $\tau + Y_{is}^{h_1}$ when $A_1 \ge 0$, and the relations between y^* and $\tau + Y_{is}^{h}$ when $A_h \le 0$. That is, we have the following main results.

Lemma 5.3 *If $A_1 \ge 0$, then $y^* < \tau + Y_{is}^{h_1}$ for all $\tau > \tau_2^{h_1}$ and $y^* = \tau + Y_{is}^{h_1}$ at $\tau = \tau_2^{h_1}$. If $A_h \le 0$, then $y^* \le \tau + Y_{is}^{h}$ for all $\tau > 0$.*

Proof First we note that y^* and $Y_{\max}^{h_1}$ intersects at $\tau = \tau_2^{h_1}$, so substituting it into $\tau + Y_{is}^{h_1}$ yields

$$\tau + Y_{is}^{h_1} = \tau_2^{h_1} + Y_{is}^{h_1} = Y_{\max}^{h_1}, \tag{5.17}$$

which indicates that those three functions (*i.e.* y^*, $Y_{\max}^{h_1}$, and $\tau + Y_{is}^{h_1}$) with respect to τ intersect at the same point, *i.e.* $\tau = \tau_2^{h_1}$. Moreover, $\tau_M + Y_{is}^{h_1} = Y_{\max}^{h} - \frac{b}{p} + Y_{is}^{h_1} < Y_{\max}^{h}$. Therefore, we can conclude that if y^* exists then it is no larger than $\tau + Y_{is}^{h_1}$ when $A_1 \ge 0$.

For the second part of Lemma 5.3, it follows from (5.4) that we consider the following equation:

$$\frac{dy^*}{d\tau} = \frac{\exp(\frac{p}{b}\tau - \frac{A_h}{b})[b\exp(\frac{p}{b}\tau - \frac{A_h}{b}) - b - p\tau]}{b[\exp(\frac{p}{b}\tau - \frac{A_h}{b}) - 1]^2} = 1 \tag{5.18}$$

with respect to τ. Rearranging the above equation one has

$$(b - p\tau)\exp\left(\frac{p}{b}\tau - \frac{A_h}{b}\right) = b$$

and solving the above equation one gets the unique positive root when $A_h \le 0$

$$\tau_T = \frac{b}{p} + \frac{b}{p} W\big(-e^{-1+\frac{A_h}{b}}\big) = \frac{b}{p} - Y_{is}^{h}. \tag{5.19}$$

Moreover, we have $y^*(\tau_T) = \frac{b}{p} = \tau_T + Y_{is}^{h}$, which indicates that both functions (*i.e.* y^* and $\tau + Y_{is}^{h}$) are tangent at $\tau = \tau_T$. According to the monotonicity of both functions we conclude that $y^* \le \tau + Y_{is}^{h}$ when $A_h \le 0$ and the equal holds true only at $\tau = \tau_T$. □

5.2 Existence of order-1 limit cycle

In order to provide the detailed sufficient conditions for the existence of a fixed point of the Poincaré map $\mathcal{P}(y_i^+)$, we rearrange the subcases of the cases (C_1)-(C_3) according to the domains of the Poincaré map $\mathcal{P}(y_i^+)$ listed in Table 2 or the domains of the phase set listed in Table 1 or the signs of A_h and A_{h_1}. Thus, we put the subcases with the domain of the

Poincaré map $\mathcal{P}(y_i^+)$ defined by Y_D^1 (or the phase set defined by $\mathcal{N}_1$ or $A_h \le 0$) in together, denoted by subcase (SC_{123}), *i.e.*

$$(\mathrm{SC}_{123}): \quad (\mathrm{C}_1) \text{ with } \theta_1 V_L < x_3^* \text{ or } \theta_1 V_L > x_1^*, (\mathrm{C}_2) \text{ with } \theta_1 V_L \le x_4^* \text{ and } (\mathrm{C}_3). \tag{5.20}$$

We denote the subcase for (C_1) with $A_h > 0$ and $A_{h_1} \ge 0$ as subcase (SC_{11}), *i.e.*

$$(\mathrm{SC}_{11}): \quad (\mathrm{C}_1) \text{ with } V_L < x_{\min}^{h_2} \text{ and } x_{\min} < \theta_1 V_L < x_{\mathrm{mid}}, \tag{5.21}$$

and denote all subcases for (C_1) with $A_h \le 0$ and $A_{h_1} \ge 0$ as subcase (SC_{12}), *i.e.*

$$(\mathrm{SC}_{12}): \begin{cases} (\mathrm{C}_1) \text{ with } V_L < x_{\min}^{h_2} \text{ and } x_3^* \le \theta_1 V_L \le x_{\min}, \\ (\mathrm{C}_1) \text{ with } V_L < x_{\min}^{h_2} \text{ and } x_{\mathrm{mid}} \le \theta_1 V_L \le x_1^*, \\ (\mathrm{C}_1) \text{ with } x_{\min}^{h_2} \le V_L \text{ and } x_3^* \le \theta_1 V_L \le x_1^*. \end{cases} \tag{5.22}$$

The combination of (SC_{11}) and (SC_{12}) is called (SC_1) in this work. Finally, we denote the subcases for (C_2) with $A_h > 0$ as subcase (SC_2), *i.e.*

$$(\mathrm{SC}_2): \quad (\mathrm{C}_2) \text{ with } x_4^* < \theta_1 V_L. \tag{5.23}$$

Based on the important relations discussed before, for the existence of a fixed point of the Poincaré map $\mathcal{P}(y_i^+)$ of model (2.2) and consequently the existence of the order-1 limit cycle we have the following main results.

Theorem 5.1 *If $\tau = 0$ and $A_h = 0$ (here $\theta > 0$), then any y^* in the phase set is a fixed point of the Poincaré map $\mathcal{P}(y_i^+)$. If $\tau = 0$ and $A_h \ne 0$, then $y^* = 0$ is a unique fixed point of the Poincaré map $\mathcal{P}(y_i^+)$.*

If $\tau > 0$, then the fixed point y^* of the Poincaré map $\mathcal{P}(y_i^+)$ is always well defined for (SC_{123}) *with $y^* \in Y_D^1$. If $\tau > \tau_2^{h_1}$, then the fixed point y^* of the Poincaré map $\mathcal{P}(y_i^+)$ exists for* (SC_{11}) *and $y^* \in (Y_{\max}^{h_1}, Y_{is}^{h_1} + \tau]$. If $0 < \tau < \tau_3^{h_1}$ (or $\tau > \tau_2^{h_1}$), then the fixed point y^* of the Poincaré map $\mathcal{P}(y_i^+)$ exists for* (SC_{12}) *and $y^* \in (0, Y_{\min}^{h_1})$ (or $y^* \in (Y_{\max}^{h_1}, Y_{is}^{h_1} + \tau]$). If $\tau \ge \tau_M$, then the fixed point y^* of the Poincaré map $\mathcal{P}(y_i^+)$ exists for* (SC_2) *and $y^* \in [Y_{\max}^h, \frac{b}{p} + \tau]$.*

Proof The results for $\tau = 0$ are true obviously. Since $A_h \le 0$ for (SC_{123}), it follows from Lemma 5.3 that $y^* \le \tau + Y_{is}^h$ for all $\tau > 0$, which indicates that y^* exists in the phase set, *i.e.* $y^* \in Y_D^1$.

If $\tau > \tau_2^{h_1}$, then it follows from the relations between y^* and $Y_{\max}^{h_1}$ that $y^* > Y_{\max}^{h_1}$. Further, according to Lemma 5.3 we have $y^* < Y_{is}^{h_1} + \tau$ for all $\tau > \tau_2^{h_1}$ due to $A_1 \ge 0$ in case (SC_{11}). Thus the fixed point y^* of the Poincaré map $\mathcal{P}(y_i^+)$ exists for (SC_{11}) and $y^* \in (Y_{\max}^{h_1}, Y_{is}^{h_1} + \tau]$.

If $0 < \tau < \tau_3^{h_1}$, then it follows from the relations between y^* and $Y_{\min}^{h_1}$ that $y^* < Y_{\min}^{h_1}$, which means that the fixed point y^* of the Poincaré map $\mathcal{P}(y_i^+)$ exists for (SC_{12}) and $y^* \in (0, Y_{\min}^{h_1})$. If $\tau > \tau_2^{h_1}$, then the result can be proved by using the same methods as those for case (SC_{11}).

If $\tau \ge \tau_M$, then it follows from the relations between y^* and $Y_{\max}^h$ and the relations between y^* and $\frac{b}{p} + \tau$ that $y^* \in [Y_{\max}^h, \frac{b}{p} + \tau]$ and consequently the last part of the results shown in Theorem 5.1 are true. □

Based on the relations discussed before and Theorem 5.1, we have the following main results for the non-existence of a fixed point of the Poincaré map $\mathcal{P}(y_i^+)$ of model (2.2).

Corollary 5.1 *Assume* $\tau > 0$. *The Poincaré map* $\mathcal{P}(y_i^+)$ *does not have a fixed point for case* (SC_{11}) *provided* $\frac{A_h}{p} < \tau \le \tau_2^{h_1}$; *The Poincaré map* $\mathcal{P}(y_i^+)$ *does not have a fixed point for case* (SC_{12}) *provided* $\tau_3^{h_1} \le \tau \le \tau_2^{h_1}$; *The Poincaré map* $\mathcal{P}(y_i^+)$ *does not have a fixed point for case* (SC_2) *provided* $\frac{A_h}{p} < \tau < \tau_M$.

Theorem 5.1 and Corollary 5.1 provide the detailed conditions for the existence and non-existence of a fixed point of the Poincaré map $\mathcal{P}(y_i^+)$ of model (2.2), consequently the existence and non-existence of order-1 limit cycles of model (2.2) can be obtained directly. For the existence and non-existence of a fixed point of model (2.3) we have the following results.

Corollary 5.2 *If* $\tau = 0$ *and* $A_0 = 0$ (*here* $\theta > 0$), *then any* y^* *in the phase set is a fixed point of the Poincaré map* $\mathcal{P}(y_i^+)$ *of model* (2.3). *If* $\tau = 0$ *and* $A_0 \ne 0$, *then* $y^* = 0$ *is a unique fixed point of Poincaré map* $\mathcal{P}(y_i^+)$. *If* $\tau > 0$ *and* $A_0 \le 0$, *then for the Poincaré map defined in the phase set there exists a unique fixed point* $y^* \in Y_D^0$. *If* $A_0 > 0$ *and* $\tau \ge \tau_M$, *then for the Poincaré map* $\mathcal{P}(y_i^+)$ *there exists a unique fixed point* y^* *with* $Y_{\max}^0 \le y^* \le \tau + \frac{b}{p}$. *The Poincaré map* $\mathcal{P}(y_i^+)$ *does not have a fixed point provided* $0 < \frac{A_0}{p} < \tau < \tau_M$.

6 Local and global stability of order-1 limit cycle

To address the stability of y^*, we note that if $\tau = 0$ and $A_h = 0$ (here $\theta > 0$), then y^* is stable but not asymptotically stable. For the case $\tau = 0$ and $A_h \ne 0$ (*i.e.* $y^* = 0$) we will address it as a special case later in more detail. Thus, we first assume that $\tau > 0$ and y^* exists, and we provide the sufficient conditions for the local stability and global stability of the fixed point y^*. Consequently, the global stability of the order-1 limit cycle of model (2.2) can be obtained, which improved on previous results on models with state-dependent feedback control [1, 4].

6.1 Local stability of order-1 limit cycle

Theorem 6.1 *Assume that* $\tau > 0$ *and* y^* *exists. If* $A_h \le 0$ *then the fixed point* y^* *of Poincaré map* $\mathcal{P}(y_i^+)$ *is locally stable*; *If* $A_h > 0$ *then the fixed point* y^* *of Poincaré map* $\mathcal{P}(y_i^+)$ *is locally stable provided*

$$y^* < \frac{b + p\tau + \sqrt{b^2 + p^2\tau^2}}{2p}. \tag{6.1}$$

Proof For convenience, denote $f(y) = -\frac{p}{b}y\exp(-\frac{p}{b}y + \frac{A_h}{b})$, and we have

$$f'(y) = -\frac{p}{b}\exp\left(-\frac{p}{b}y + \frac{A_h}{b}\right)\left[1 - \frac{p}{b}y\right].$$

Moreover, by simple calculation and according to the properties of the Lambert W function we have

$$\begin{aligned}\left.\frac{d\mathcal{P}(y_i^+)}{dy_i^+}\right|_{y_i^+ = y^*} &= -\frac{b}{p}\frac{W(f(y^*))}{f(y^*)(1 + W(f(y^*)))}f'(y^*) \\ &= -\frac{b}{p}\frac{W(f(y^*))}{1 + W(f(y^*))}\left[\frac{1}{y^*} - \frac{p}{b}\right] = \frac{(y^* - \tau)(b - py^*)}{y^*(b - p(y^* - \tau))} \triangleq g(y^*).\end{aligned} \tag{6.2}$$

We first note that if $y^* = \tau + b/p$ then $g(y^*) = -\infty$, which indicates that y^* is unstable. Thus, for the stability of y^*, we only need to focus on the interval $\tau < y^* < \tau + b/p$. Moreover, $|g(y^*)| < 1$ is equivalent to the following inequalities:

$$-1 < \frac{(y^* - \tau)(b - py^*)}{y^*(b - p(y^* - \tau))} < 1, \tag{6.3}$$

which indicates that if the above inequalities hold, then the fixed point y^* is locally stable. Note that we have $y^*(b - p(y^* - \tau)) > 0$ for all $\tau < y^* < \tau + b/p$ and $\tau > 0$. It is easy to show that the right hand side of (6.3) holds true naturally, and the left hand side inequality is equivalent to

$$p\big(y^*\big)^2 - (b + p\tau)y^* + \frac{b\tau}{2} < 0 \tag{6.4}$$

and solving the above inequality we have $y_1^* < y^* < y_2^*$ where

$$y_{1,2}^* = \frac{b + p\tau \mp \sqrt{b^2 + p^2\tau^2}}{2p}.$$

Further, we can show that

$$y_1^* < \tau < y_2^* < \tau + b/p.$$

This indicates that if $\tau < y^* < y_2^*$, then the fixed point y^* of Poincaré map $\mathcal{P}(y_i^+)$ is locally stable. It follows from Lemma 5.2 that $y^* < y_2^*$ holds true naturally if $A_h \le 0$. This completes the proof of Theorem 6.1. □

Corollary 6.1 *Assume that* $\tau > 0$, y^* *exists, and* $A_h > 0$. *If* $y^* \in (y_2^*, \tau + \frac{b}{p}]$, *then the fixed point* y^* *of the Poincaré map* $\mathcal{P}(y_i^+)$ *of model* (2.2) *is unstable*.

Corollary 6.2 *Assume that* $\tau > 0$ *and* y^* *exists. If* $A_0 \le 0$, *then the fixed point* y^* *of the Poincaré map* $\mathcal{P}(y_i^+)$ *of model* (2.3) *is locally stable*; *If* $A_0 > 0$, *then the fixed point* y^* *of Poincaré map* $\mathcal{P}(y_i^+)$ *is locally stable provided* $y^* \in (\tau, y_2^*)$, *and it is unstable when* $y^* \in (y_2^*, \tau + \frac{b}{p}]$.

By combining Theorems 5.1 and 6.1, Corollaries 5.1 and 6.1, and all of the relations discussed in Section 5.1 we can provide the exact conditions for the existence and stability of the fixed point y^* of the Poincaré map $\mathcal{P}(y_i^+)$ of model (2.2) based on the three parameters θ, V_L, and τ. Here for simplification and convenience we employ the signs of A_h and A_{h_1} rather than θ and V_L, and list all results in Table 3.

Here, $\times$ means the sign of A_{h_1} is not necessary for that subcase, NE denotes the nonexistence of a fixed point, EU represents the existence of a fixed point which is unstable, ES shows the existence of a fixed point which is stable, EG denotes the existence of a fixed point which is globally stable, and ENS represents the existence of a fixed point which is neutrally stable. Note that if $\tau = 0$, then for case (SC_{12}) we have $Y_{\min}^{h_1} = Y_{is}^{h_1}$ once $A_h = 0$. Thus, in this subcase, any $y^* \in [0, Y_{\min}^{h_1}) = [0, Y_{is}^{h_1})$ is a fixed point of the Poincaré map $\mathcal{P}(y_i^+)$ of model (2.2), *i.e.* for any solution initiating from $((1 - \theta)V_L, y^*)$ is an order-1 periodic solution which is neutrally stable.

Table 3 Existence and stability of the fixed point y^* of Poincaré map $\mathcal{P}(y_i^+)$

Cases	A_h and A_{h_1}	τ	y^*	Interval of y^*
(SC_{123})	$A_h \le 0, \times$	$\tau > 0$	EG	$Y_D^1 = [\tau, Y_{is}^h + \tau]$
	$A_h < 0, \times$	$\tau = 0$	EG	$y^* = 0$
	$A_h = 0, \times$		ENS	$\forall y^* \in [0, Y_{is}^h]$
(SC_{11})	$A_h > 0, A_{h_1} \ge 0$	$\frac{A_h}{p} < \tau \le \tau_2^{h_1}$	NE	
		$\tau_2^{h_1} < \tau$	ES	$(Y_{\max}^{h_1}, Y_{is}^{h_1} + \tau]$
		$\tau = 0$	EU	$y^* = 0$
(SC_{12})	$A_h \le 0, A_{h_1} \ge 0$	$\tau_3^{h_1} \le \tau \le \tau_2^{h_1}$	NE	
		$0 < \tau < \tau_3^{h_1}$	ES	$(0, Y_{\min}^{h_1})$
		$\tau > \tau_2^{h_1}$	ES	$(Y_{\max}^{h_1}, Y_{is}^{h_1} + \tau]$
	$A_h < 0, \times$	$\tau = 0$	ES	$y^* = 0$
	$A_h = 0, \times$		ENS	$\forall y^* \in [0, Y_{\min}^{h_1})$
(SC_2)	$A_h > 0, \times$	$\frac{A_h}{p} < \tau < \tau_M$	NE	
		$\tau_M \le \tau \le \tau_2$	EU	$[Y_{\max}^h, \frac{b}{p} + \tau]$
		$\tau_2 < \tau$	ES	$[Y_{\max}^h, \frac{b}{p} + \tau]$
		$\tau = 0$	EU	$y^* = 0$

So far, all cases shown in Table 3 have been proved except for the global stability of the fixed point y^* in subcase (SC_{123}) and the stability of $y^* = 0$ for $\tau = 0$, which are our main purposes in the following subsections.

6.2 Global stability of the order-1 limit cycle

For the global stability of the fixed point y^* as well as the order-1 limit cycle of system (2.2), we first focus on the case $\tau > 0$ for (SC_{123}) based on the domains of Poincaré map $\mathcal{P}(y_i^+)$ and the existence of y^*, and we have the following main result.

Theorem 6.2 *Assuming that* $\tau > 0$ *in case* (SC_{123}), *then the fixed point* y^* *of Poincaré map* $\mathcal{P}(y_i^+)$ *exists and satisfies* $\tau < y^* < y_2^*$. *Moreover, it is globally stable once it exists. Consequently, the order-*1 *limit cycle of system* (2.2) *is globally stable.*

Proof Note that we have $A_h \le 0$ for (SC_{123}), and then it follows from Theorem 6.1 and Lemma 5.2 that the fixed point y^* of the Poincaré map $\mathcal{P}(y_i^+)$ exists and satisfies $\tau < y^* < y_2^*$. It is easy to see that the Poincaré map $\mathcal{P}(y_i^+)$ is continuous and differentiable on its domains. Moreover, for any solution initiating from $((1-\theta)V_L, y_0^+)$ with $y_0^+ \notin (\tau, \tau + b/p]$ will reach the phase set $\mathcal{N}_1$ after a single impulsive effect with $y_1^+ \in (\tau, \tau + Y_{is}^h] \subset (\tau, \tau + b/p]$. Further, for all $y \in (\tau, \tau + b/p]$ we have

$$\frac{d\mathcal{P}(y)}{dy} = -\frac{b}{p}\frac{W(f(y))}{f(y)(1+W(f(y)))}f'(y) = -\frac{b}{p}\frac{W(f(y))}{1+W(f(y))}\left[\frac{1}{y} - \frac{p}{b}\right] \triangleq g(y). \tag{6.5}$$

According to the conditions we see that $f(y) \ge -e^{-1}$ for $y \in (\tau, \tau + b/p]$, which indicates that $-1 \le W(f(y)) < 0$. Moreover, if $A_h = 0$, then we have $W(f(b/p)) = -1$ and $\lim_{y \to b/p} g(y) = 0$. Thus there exists a unique $y_e = b/p$ such that $g(y) = 0$, $g(y) < 0$ for all $y > b/p$ and $g(y) > 0$ for all $y < b/p$. In order to prove the global stability of the fixed point y^*, we consider the following two cases:

Case 1 $\tau \ge b/p$.

For this case, we have $-1 < W(f(y)) < 0$ and $g(y) < 0$ for all $y \in (\tau, \tau + b/p]$. Therefore, in order to show the global stability, we only need to prove $g(y) > -1$ for all $y \in (\tau, \tau + b/p]$. It

follows from (6.5) that $g(y) > -1$ is equivalent to the following inequality:

$$W\big(f(y)\big) > \frac{py}{b-2py}. \tag{6.6}$$

It is easy to know that $\frac{py}{b-2py} > -1$ for $y > b/p$, and according to the definition of the Lambert W function the above inequality is equivalent to

$$f(y) > \frac{py}{b-2py}\exp\left(\frac{py}{b-2py}\right)$$

i.e.

$$\frac{2py-b}{b} < \exp\left[\frac{p}{b}y - \frac{py}{2py-b} - \frac{A_h}{b}\right]. \tag{6.7}$$

Thus, we only need to show

$$\frac{2py-b}{b} < \exp\left[\frac{p}{b}y - \frac{py}{2py-b}\right].$$

Denote $u = \frac{p}{b}y$ with $u \in (\frac{p}{b}\tau, 1+\frac{p}{b}\tau] \subseteq (1, 1+\frac{p}{b}\tau]$. Then the above inequality is equivalent to the following inequality:

$$F(u) = (2u-1)\ln(2u-1) - 2u(u-1) < 0,$$

where $F(1) = 0$ and by simple calculation yields

$$F'(u) = 2\big[\ln(2u-1) + 2 - 2u\big], \quad \text{and} \quad F''(u) = \frac{4}{2u-1} - 4 < 0,$$

which indicates that $F'(u) < F'(1) = 0$. This shows that if $\tau \geq b/p$, then we have $-1 < g(y) < 0$ for all $y \in (\tau, \tau + b/p]$ and consequently the fixed point y^* is globally stable.

Case 2 $\tau < b/p$.

For this case, we note that $-1 < g(y) < 0$ for all $y \in (\frac{b}{p}, \frac{b}{p} + \tau]$. Therefore, since we have $g(b/p) = 0$ and in order to prove the global stability of y^* for this case, we only need to show $0 < g(y) < 1$ for all $y \in (\tau, b/p)$. It is easy to see that $g(y) > 0$ holds true for all $y \in (\tau, b/p)$ and $g(y) < 1$ is equivalent to

$$-1 < -\frac{py}{b} < W\big(f(y)\big).$$

Thus, according to the definition of the Lambert W function the above inequality is equivalent to

$$-\frac{p}{b}y\exp\left(-\frac{p}{b}y\right) < -\frac{p}{b}y\exp\left(-\frac{p}{b}y + \frac{A_h}{b}\right),$$

which holds true naturally if $A_h < 0$. Therefore, if $A_h < 0$, then we have $0 \leq g(y) < 1$ for all $y \in (\tau, b/p]$, and consequently the fixed point y^* is globally stable if $\tau < b/p$ and $A_h < 0$.

Finally, if $\tau < b/p$ and $A_h = 0$, then it is easy to see that $y^* \in (\frac{b}{p}, y_2^*)$ and $g(y) = 1$ for all $y \in (\tau, \frac{b}{p})$. Moreover, by simple calculation we have $W(f(y)) = -\frac{py}{b}$ for all $y \in (\tau, \frac{b}{p})$, which

means that for any solution initiating from $((1-\theta)V_L, y_0^+)$ with $y_0^+ < b/p$ we have $y_{i+1}^+ = y_i^+ + \tau$ if $y_i^+ \in (\tau, \frac{b}{p})$. Therefore, there exists a positive integer k_1 such that $y_{k_1}^+ \in (b/p, \tau + b/p]$ and $y_i^+ \in (\tau, b/p)$ for all $i < k_1$. The result follows if we can prove that $y_i^+ \in (b/p, \tau + b/p]$ for all $i \geq k_1$. To do this, we need the following result.

Claim If $y_{k_1}^+ \in (b/p, \tau + b/p]$, then we must have $y_{k_1+1}^+ \in (b/p, \tau + b/p]$.

Proof We employ the following two methods to prove the above claim, which are useful later.

Method 1: Note that

$$y_{k_1+1}^+ = -\frac{b}{p} W\left[-\frac{p}{b} y_{k_1}^+ \exp\left(-\frac{p}{b} y_{k_1}^+\right)\right] + \tau$$

and $y_{k_1+1}^+ \in (b/p, \tau + b/p]$ is equivalent to

$$W\left[-\frac{p}{b} y_{k_1}^+ \exp\left(-\frac{p}{b} y_{k_1}^+\right)\right] < -1 + \frac{p}{b}\tau. \tag{6.8}$$

Thus, if the following inequality:

$$\left(-1 + \frac{p}{b}\tau\right) \exp\left(-1 + \frac{p}{b}\tau\right) > -\frac{p}{b} y \exp\left(-\frac{p}{b} y\right)$$

holds for all $y \in (b/p, \tau + b/p]$, then the inequality (6.8) follows. According to the monotonicity of $-\frac{p}{b} y \exp(-\frac{p}{b} y)$ we only need to show

$$\psi(\tau) \doteq \left(-1 + \frac{p}{b}\tau\right) \exp\left(-1 + \frac{p}{b}\tau\right) + \left(1 + \frac{p\tau}{b}\right) \exp\left[-\left(1 + \frac{p\tau}{b}\right)\right] > 0$$

for all $\tau \in (0, b/p)$.

It is easy to see that $\psi(0) = 0$ and $\psi'(\tau) > 0$. This indicates that $y_{k_1+1}^+ > b/p$ and by induction we have $y_i^+ \in (b/p, \tau + b/p]$ for all $i \geq k_1$.

Method 2: In the following we prove that if $\tau < b/p$ and $A_h = 0$ then $y^* \in (\frac{b}{p} + \frac{\tau}{2}, y_2^*)$. Note that $y^* < y_2^*$ has been proved as in Lemma 5.2, and $y^* > \frac{b}{p} + \frac{\tau}{2}$ is equivalent to

$$y^* = \tau \frac{\exp(\frac{p}{b}\tau)}{\exp(\frac{p}{b}\tau) - 1} > \frac{b}{p} + \frac{\tau}{2} \quad \text{for all } \tau \in (0, b/p). \tag{6.9}$$

Rearranging the above inequality yields

$$\phi(\tau) \doteq \frac{\tau}{2}\left[\exp\left(\frac{p}{b}\tau\right) + 1\right] - \frac{b}{p}\left[\exp\left(\frac{p}{b}\tau\right) - 1\right] > 0$$

with $\phi(0) = 0$, $\phi(b/p) = 3 - e > 0$ and $\phi'(\tau) > 0$. This indicates that the inequality (6.9) holds true. Thus, if $y_{k_1}^+ \in (b/p, \tau + b/p]$, then according to $-1 < g(y) < 0$ for all $y \in (\frac{b}{p}, \frac{b}{p} + \tau]$ we have

$$\left|y_{k_1+1}^+ - y^*\right| = \left|\mathcal{P}\left(y_{k_1}^+\right) - \mathcal{P}\left(y^*\right)\right| = \left|g'(y_*)\right| \left|y_{k_1}^+ - y^*\right| < \left|y_{k_1}^+ - y^*\right|,$$

where $y_* \in (y^*, y_{k_1}^+)$ or $y_* \in (y_{k_1}^+, y^*)$. It follows from $y^* > \frac{b}{p} + \frac{\tau}{2}$ and $\tau < b/p$ that we have $y_{k_1+1}^+ > b/p$. By induction, we conclude that $y_i^+ \in (b/p, \tau + b/p]$ for all $i \geq k_1$.

Therefore, the fixed point y^* is globally stable when $A_h = 0$ and $\tau < b/p$. Based on results shown in Cases 1 and 2, we can see that if the conditions of Theorem 6.2 are true, then the fixed point y^* is globally stable. This completes the proof. □

Remark 6.1 The above two theorems (Theorem 6.1 and Theorem 6.2) have provided the detailed analyses for the existence and stability of fixed point y^* of the Poincaré map $\mathcal{P}(y_i^+)$ and consequently the order-1 limit cycle. Further, we note that the period of the order-1 limit cycle can be analytically determined by using similar methods as those developed in reference [1].

Corollary 6.3 *Assuming that* $\tau > 0$ *and* $A_0 \leq 0$, *then the fixed point* y^* *of Poincaré map* $\mathcal{P}(y_i^+)$ *for model* (2.3) *exists and satisfies* $\tau < y^* < y_2^*$. *Moreover, it is globally stable once it exists. Consequently, the order-*1 *limit cycle of system* (2.3) *is globally stable.*

Before finishing this subsection, we would like to address some special cases of the order-1 limit cycle including the existence of an order-1 homoclinic cycle, and long or short order-1 limit cycles.

Order-1 homoclinic cycle. To address the existence of the order-1 homoclinic cycle, we note that the point $P_1^+ = ((1-\theta)V_L, y^*)$ determined by the fixed point y^* of the Poincaré map $\mathcal{P}(y_i^+)$ must lie in the order-1 Homoclinic cycle (as shown in Figure 7), where y^* is defined by formula (5.2), *i.e.*

$$y^* = \tau \frac{\exp(\frac{p}{b}\tau - \frac{A_h}{b})}{\exp(\frac{p}{b}\tau - \frac{A_h}{b}) - 1}.$$

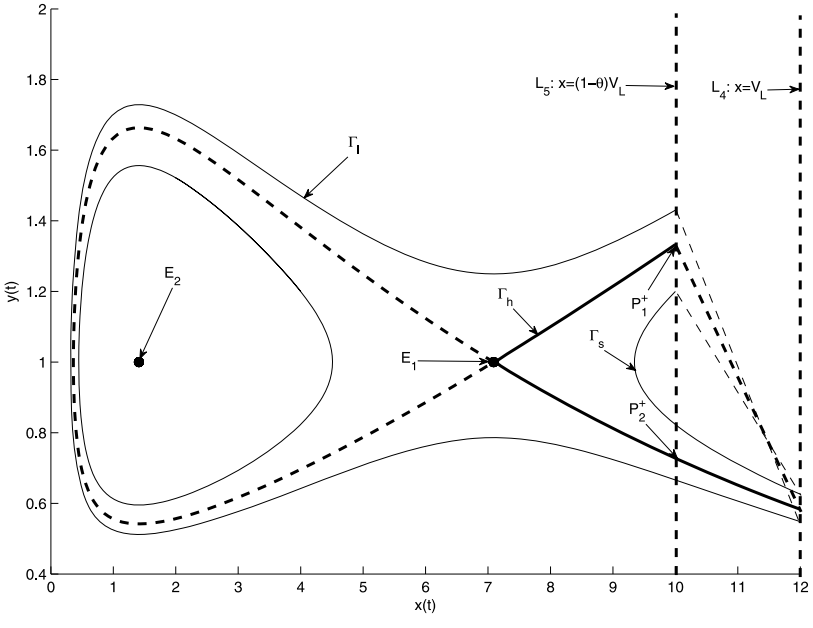

Figure 7 Illustrations of existence of order-1 homoclinic cycle (Γ_h), order-1 long (Γ_l) or short (Γ_s) limit cycle.

Therefore, we have

$$b\ln\left(y^*\right) - py^* - \frac{c}{\omega}\ln\left(1+\omega(1-\theta)V_L\right) + \delta\ln\left((1-\theta)V_L\right) + q(1-\theta)V_L = h_1. \tag{6.10}$$

Then the above equation becomes

$$b\ln\left(y^*\right) - py^* = b\ln(b/p) - b - A_{h_1}.$$

Therefore, if y^* satisfies the above equation, *i.e.* all parameters satisfy the following relation:

$$y^* = \tau\frac{\exp(\frac{p}{b}\tau - \frac{A_h}{b})}{\exp(\frac{p}{b}\tau - \frac{A_h}{b}) - 1} = -\frac{b}{p}W\left(-1, \frac{p}{b}\exp\left(\frac{b\ln(b/p) - b - A_{h_1}}{b}\right)\right) \doteq y_h^*,$$

then for model (2.2) there exists a unique order-1 homoclinic cycle Γ_h, as shown in Figure 7.

Order-1 long or short limit cycle. Based on the existence of the order-1 homoclinic cycle, we see that if the fixed point y^* of Poincaré map is less than the y_h^* and $(1-\theta)V_L > x_1^*$, then we say that model (2.2) has an order-1 short limit cycle Γ_s, as shown in Figure 7. While, if the fixed point y^* of Poincaré map is larger than the y_h^* and $(1-\theta)V_L > x_1^*$, then we say that model (2.2) has an order-1 long limit cycle Γ_l, as shown in Figure 7. The order-1 short or long limit cycle may play a key role in real problems with state-dependent feedback control actions, which tells us how frequently the control tactics should be applied or how to design the control tactics to adjust the period of control actions.

6.3 Boundary order-1 limit cycle and its stability

It follows from Theorem 5.1 that if $\tau = 0$ and $A_h \neq 0$, then $y^* = 0$ is a unique fixed point of Poincaré map $\mathcal{P}(y_i^+)$ (please see Table 3 for details), which indicates that for model (2.2) there exists a unique boundary order-1 limit cycle with initial condition $((1-\theta)V_L, 0)$. Therefore, in this subsection, we address its analytical formula and stability. Note that, if $\tau = 0$ and $A_h \neq 0$, then the derivative of the Poincaré map at $y^* = 0$ is one, which indicates that the stability of $y^* = 0$, which in this case cannot be determined directly.

In model (2.2), let $y(t) = 0$ and $\tau = 0$, then we have the following subsystem:

$$\begin{cases} \frac{dx(t)}{dt} = bx(t), & x < V_L, \\ x(t^+) = (1-\theta)x(t), & x = V_L. \end{cases} \tag{6.11}$$

Solving the first equation with initial condition $x(0^+) = (1-\theta)V_L$ yields

$$x(t) = (1-\theta)V_L\exp(bt)$$

and letting $V_L = (1-\theta)V_L\exp(bT)$ and solving it with respect to T, we have $T = \frac{1}{b}\ln\frac{1}{1-\theta}$. Therefore, model (6.11) has a periodic solution, denoted by $x^T(t)$ and $x^T(t) = (1-\theta)V_L\exp(bt)$ with period T, which means that for model (2.2) there exists a boundary order-1 limit cycle $(x^T(t), 0)$.

To show its stability, we first consider two points $P_1^+ = ((1-\theta)V_L, y_1^+) \in L_5$ and $Q_1 = (V_L, y_2) \in L_4$ with $y_1^+, y_2 \leq b/p$, which lie in the same trajectory of system (2.2), as shown

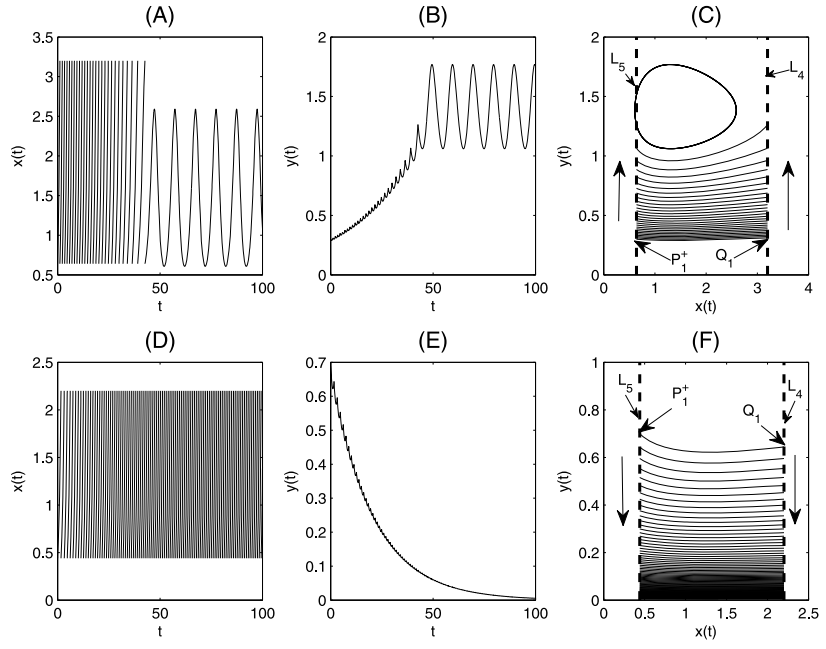

Figure 8 Stability of boundary order-1 limit cycle $(x^T(t), 0)$. (A)-(C) Unstable boundary order-1 limit cycle with $V_L = 3.2$ and $A_h = 0.0495$; **(D)-(F)** Stable boundary order-1 limit cycle with $V_L = 2.2$ and $A_h = -0.0775$. All other parameter values are fixed as follows: $b = 1.8$, $p = 1.3$, $c = 0.52$, $\omega = 0.1$, $q = 0.23$, $\delta = 0.3$, $\theta = 0.8$, $\tau = 0$.

in Figure 8(C) and (F). Moreover, the coordinates of these two points satisfy the following relations:

$$A_h = \frac{c}{\omega}\ln\left(\frac{1+\omega V_L}{1+\omega(1-\theta)V_L}\right) - \delta\ln\left(\frac{1}{1-\theta}\right) - q\theta V_L = b\ln\left(\frac{y_2}{y_1^+}\right) - p\left[y_2 - y_1^+\right]. \tag{6.12}$$

It is easy to see that $y_1^+ \neq y_2$. Otherwise, if $y_1^+ = y_2$ then $A_h = 0$, which contradicts with $A_h \neq 0$. Define function $h(y)$ as $h(y) = b\ln(y) - py$ with $h'(y) = p(\frac{b}{p}\frac{1}{y} - 1)$, which indicates that $h'(y) > 0$ for $y < \frac{b}{p}$. Therefore, if $A_h > 0$, then we have

$$b\ln\left(\frac{y_2^+}{y_1^+}\right) - p\left[y_2^+ - y_1^+\right] > 0 \quad \text{or} \quad b\ln\left(\frac{y_2}{y_1}\right) - p[y_2 - y_1] > 0,$$

here we use $y_2^+ = y_2$ and $y_1^+ = y_1$ due to $\tau = 0$. That is,

$$b\ln\left(y_2^+\right) - py_2^+ > b\ln\left(y_1^+\right) - py_1^+ \quad \text{or} \quad b\ln(y_2) - py_2 > b\ln(y_1) - py_1,$$

which indicate that $y_2^+ > y_1^+$ and $y_2 > y_1$.

Similarly, if $A_h < 0$, then $y_2^+ < y_1^+$ and $y_2 < y_1$ must hold true. In conclusion, we have the following main results for the boundary order-1 limit cycle.

Theorem 6.3 *Let* $\tau = 0$ *and* $A_h \neq 0$. *The boundary order-*1 *limit cycle* $(x^T(t), 0)$ *is globally asymptotically stable for* (SC_{123}), *and it is locally asymptotically stable for* (SC_{12}). *The boundary order-*1 *limit cycle* $(x^T(t), 0)$ *is unstable for* (SC_{11}) *and* (SC_2).

Proof For case (SC_{123}), we assume, without loss of generality, that any solution initiating from phase set $\mathcal{N}_1$ experience infinite impulsive effects, *i.e.* we have $y_k^+ \in (0, Y_{is}^h]$ for all $k \geq 0$. Since $A_h < 0$, it follows from the above discussion that by induction we conclude that y_k^+ is a strictly decreasing sequence with $\lim_{k\to\infty} y_k^+ = y^*$. Moreover, $y^* = 0$ must hold, otherwise it contradicts the uniqueness of $y^* = 0$ in this case. Thus, the boundary order-1 limit cycle $(x^T(t), 0)$ is globally attractive.

So in order to prove Theorem 6.3, we only need to show that it is asymptotically stable. To do this, by using Lemma A.1 we denote $bx(t) - px(t)y(t) \doteq P(x,y)$ and $\frac{cx(t)y(t)}{1+\omega x(t)} - qx(t)y(t) - \delta y(t) \doteq Q(x,y)$, then

$$\begin{aligned}
&\frac{\partial P}{\partial x} = b - py, \qquad \frac{\partial Q}{\partial y} = \frac{cx}{1+\omega x} - qx - \delta,\\
&\frac{\partial a}{\partial x} = -\theta, \qquad \frac{\partial a}{\partial y} = \frac{\partial b}{\partial x} = \frac{\partial b}{\partial y} = 0,\\
&\frac{\partial \phi}{\partial x} = 1, \qquad \frac{\partial \phi}{\partial y} = 0
\end{aligned}$$

and $\triangle_1 = P_+/P = 1 - \theta$. Thus

$$\begin{aligned}
\int_0^T \left(\frac{\partial P}{\partial x} + \frac{\partial Q}{\partial y}\right) dt &= \int_0^T \left(b + \frac{cx^T(t)}{1+\omega x^T(t)} - qx^T(t) - \delta\right) dt\\
&= (b-\delta)t - \frac{(1-\theta)qV_L}{b}\exp(bt) + \frac{c}{\omega b}\ln\left[1+\omega(1-\theta)V_L\exp(bt)\right]\Big|_0^T\\
&= (1-\delta/b)\ln\frac{1}{1-\theta} - \frac{q\theta V_L}{b} + \frac{c}{b\omega}\ln\left(\frac{1+\omega V_L}{1+\omega(1-\theta)V_L}\right)\\
&= \ln\left(\frac{1}{1-\theta}\right) + \frac{1}{b}A_h.
\end{aligned}$$

Therefore,

$$|\mu_2| = (1-\theta)\exp\left(\ln\left(\frac{1}{1-\theta}\right) + \frac{1}{b}A_h\right) = \exp\left(\frac{1}{b}A_h\right),$$

which indicates that the boundary order-1 limit cycle is orbitally asymptotically stable and enjoys the property of asymptotic phase if $A_h < 0$. Thus, the boundary order-1 limit cycle is globally stable if $\tau = 0$ and $A_h \neq 0$ in case (SC_{123}).

The local stability of the boundary order-1 limit cycle for (SC_{12}) is obvious due to the domain of the phase set. The instability of the boundary order-1 limit cycle for (SC_{11}) and (SC_2), is shown since $A_h > 0$, y_k^+ is a strictly increasing sequence and the solution will be free from impulsive effects after finite state-dependent feedback control actions, as shown in Figure 8(C). Thus the results are true. □

Remark 6.2 It is interesting to note that if we let $\tau = 0$ and A_h be a bifurcation parameter, then the unique boundary order-1 limit cycle is stable when $A_h < 0$, and there exists a family of order-1 periodic solutions when $A_h = 0$. As A_h increases and goes beyond zero (*i.e.* $A_h > 0$), then the boundary order-1 limit cycles disappear. These results indicate that if $\tau = 0$, then the Poincaré map $\mathcal{P}(y_i^+)$ undergoes a Fold bifurcation at $(y^*, A_h) = (0,0)$.

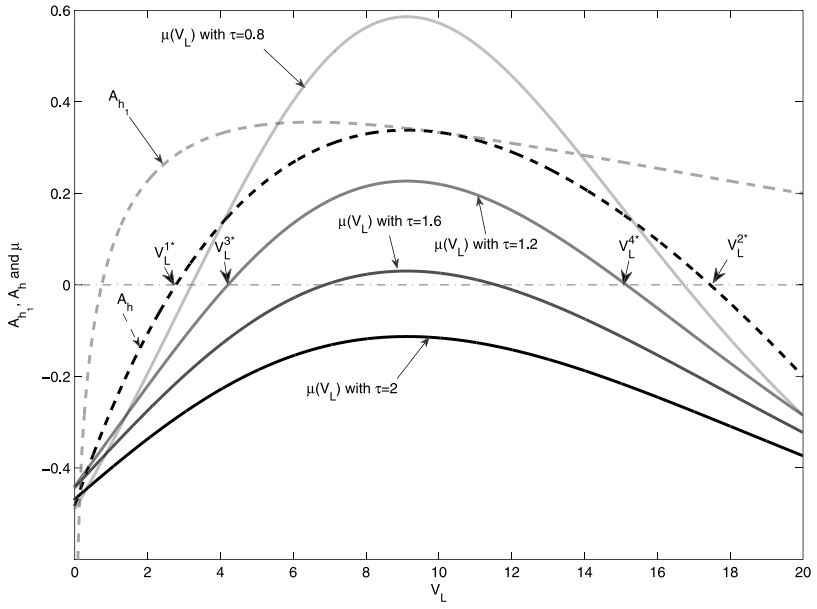

Figure 9 The plots of A_{h_1}, A_h, and μ as V_L varies for different τ. All other parameter values are fixed as follows: $b = 1.8$, $p = 1.3$, $c = 0.52$, $\omega = 0.1$, $q = 0.23$, $\delta = 0.3$, $\theta = 0.8$.

Moreover, if the A_h is considered as a function of V_L, then there are two critical values V_L^{1*} and V_L^{2*} such that $A_h = 0$, as shown in Figure 9.

To confirm the main results obtained in Theorem 6.3, we fixed the parameter values as those in Figure 8, and we can see that if $A_h > 0$, then the impulsive points and its phase points of trajectory shown in Figure 8(C) are two monotonically increasing sequences, and eventually the trajectory approaches a closed orbit which frees it from impulsive effects. While if $A_h < 0$, then the impulsive points and its phase points of trajectory shown in Figure 8(F) are two monotonically decreasing sequences, and eventually the trajectory tends to the boundary order-1 limit cycle $(x^T(t), 0)$.

Corollary 6.4 *If $\tau = 0$ and $A_0 \neq 0$, then there exists a unique boundary order-1 limit cycle $(x^T(t), 0)$ for model (2.3). Furthermore, if $A_0 > 0$, then the order-1 limit cycle $(x^T(t), 0)$ is unstable; if $A_0 < 0$, then the order-1 limit cycle $(x^T(t), 0)$ is globally asymptotically stable.*

7 Flip bifurcation and existence of order-2 limit cycle

Investigating the existence or non-existence of the limit cycle with order no less than 1 for models with state-dependent feedback control is challenging, but this problem has been addressed for some special cases [1]. Thus, in the following two sections we will focus on the existence and non-existence of order-2 limit cycles for model (2.2) and provide some sufficient conditions or necessary conditions on this topic.

According to the stability analyses of the fixed point y^* of the Poincaré map $\mathcal{P}(y_i^+)$ that if $\tau > 0$ and $A_h \leq 0$, then the fixed point y^* is locally stable or globally stable once it exists. However, it follows from Theorem 6.1 that if $\tau > 0$, $A_h > 0$ and y^* exists, then the fixed

point y^* of the Poincaré map $\mathcal{P}(y_i^+)$ is locally stable provided

$$y^* < \frac{b + p\tau + \sqrt{b^2 + p^2\tau^2}}{2p} = y_2^*. \tag{7.1}$$

Therefore, we can define the following flip bifurcation curve with respect to threshold value V_L when $\tau > 0$ and $A_h > 0$:

$$\mu(V_L) = y^* - \frac{b + p\tau + \sqrt{b^2 + p^2\tau^2}}{2p} = y^* - y_2^*, \tag{7.2}$$

which indicates that if $\mu = 0$, then we have $g(y^*) = -1$, and the positive fixed point y^* loses its stability at $\mu = 0$. In order to consider the existence of a flip bifurcation of model (2.2), we choose the threshold V_L as a bifurcation parameter and define $G(y, V_L) = \mathcal{P}(y_i^+)$ as the one parameter maps, correspondingly we denote $f(y, V_L) = -\frac{p}{b}y\exp(-\frac{p}{b}y + \frac{A_h}{b})$. Then we first solve the equation $\mu(V_L) = 0$ with respect to A_h, yielding

$$A_h = \frac{c}{\omega}\ln\left(\frac{1 + \omega V_L}{1 + \omega(1-\theta)V_L}\right) - \delta\ln\left(\frac{1}{1-\theta}\right) - q\theta V_L = p\tau - b\ln\left(\frac{y_2^*}{y_2^* - \tau}\right) > 0. \tag{7.3}$$

Now we discuss the existence of positive roots of the above equation with respect to V_L and consequently the positive roots for the equation $\mu(V_L) = 0$. To show this, we denote

$$F_A(V_L) = \frac{c}{\omega}\ln\left(\frac{1 + \omega V_L}{1 + \omega(1-\theta)V_L}\right) - \delta\ln\left(\frac{1}{1-\theta}\right) - q\theta V_L$$

and we have the following results.

Lemma 7.1 *Let* $V_L^2 = \frac{-2q+q\theta+\sqrt{B}}{2(1-\theta)q\omega}$ *with* $B = \theta^2q^2 + 4qc - 4\theta qc$. *If* $A_h > 0$, *then there are two positive roots of the equation* $F_A(V_L) = 0$, *denoted by* V_L^{1*} *and* V_L^{2*}, *such that* $F_A(V_L) > 0$ *for all* $V_L \in (V_L^{1*}, V_L^{2*})$. *Further, if* $F_A(V_L^2) > p\tau - b\ln(\frac{y_2^*}{y_2^*-\tau})$, *then the equation* $\mu(V_L) = 0$ *exists with two positive roots, denoted by* V_L^{3*} *and* $V_L^{4^*}$ (*as shown in Figure* 9), *and* $V_L^{1*} < V_L^{3*} < V_L^{4^*} < V_L^{2*}$. *Moreover,* $F_A'(V_L^{3*}) > 0$ *and* $F_A'(V_L^{4*}) < 0$.

Proof It is easy to see that $F_A(0) < 0$ and $F_A(+\infty) = -\infty$. Taking the derivative of $F_A(V_L)$ with respect to V_L yields

$$F_A'(V_L) = \frac{\theta[c - q(1 + \omega V_L)(1 + (1-\theta)\omega V_L)]}{(1 + \omega V_L)(1 + \omega V_L - \omega\theta V_L)}$$

and solving $F_A'(V_L) = 0$ yields two roots V_L^1, V_L^2 with

$$V_L^1 = \frac{-2q + q\theta - \sqrt{B}}{2(1-\theta)q\omega}, \qquad V_L^2 = \frac{-2q + q\theta + \sqrt{B}}{2(1-\theta)q\omega},$$

where $B = \theta^2q^2 + 4qc - 4\theta qc$. Note that $V_L^1 < \frac{-1}{(1-\theta)\omega} < \frac{-1}{\omega} < 0$, thus only the V_L^2 may be the desirable maximal extreme point of the function $F_A(V_L)$. Moreover, $V_L^2 > 0$ is equivalent to

$$-2q + q\theta + \sqrt{B} > 0.$$

Rearranging the above inequality we have: if $c > q$, then $V_L^2 > 0$ holds true. This indicates that if x_1^* and x_2^* exist (*i.e.* $c - q - \delta\omega > 2\sqrt{q\omega\delta}$), then for the function $F_A(V_L)$ there always exists a unique maximal extreme point V_L^2. Thus, the results for the function $F_A(V_L)$ and the function $\mu(V_L)$ are correct. □

Theorem 7.1 *Assuming that* $\tau > 0$, $A_h > 0$, y^* *exists and* $F_A(V_L^2) > p\tau - b\ln(\frac{y_2^*}{y_2^*-\tau})$, *then the family* $G(y, V_L)$ *undergoes a flip bifurcation at* (y_2^*, V_L^{3*}), *while the family* $G(y, V_L)$ *cannot undergo a flip bifurcation at* (y_2^*, V_L^{4*}).

Proof It is easy to see that $G(y_2^*, V_L^*) = y_2^*$ for $V_L^* = V_L^{3*}$ and $V_L^* = V_L^{4*}$. Further

$$\begin{aligned}
&\frac{\partial G(y,V_L)}{\partial y}\bigg|_{(y,V_L)=(y_2^*,V_L^*)} = -\frac{b}{p}\frac{W(f(y,V_L))}{1+W(f(y,V_L))}\left[\frac{1}{y}-\frac{p}{b}\right]\bigg|_{(y,V_L)=(y_2^*,V_L^*)} = -1,\\
&\frac{\partial^2 G(y,V_L)}{\partial y\,\partial V_L}\bigg|_{(y,V_L)=(y_2^*,V_L^*)} = -\frac{F_A'(V_L)(b-py)}{bpy}\frac{W(f(y,V_L))}{[1+W(f(y,V_L))]^3}\bigg|_{(y,V_L)=(y_2^*,V_L^*)}\\
&\qquad = \frac{bF_A'(V_L^*)(b-py_2^*)(y_2^*-\tau)}{y_2^*[b-p(y_2^*-\tau)]^3}.
\end{aligned}$$

It follows from the relations $\tau < y_2^* < \tau + b/p$ that $y_2^* - \tau > 0$ and $b - p(y_2^* - \tau) > 0$. Therefore, according to the signs of $F_A'(V_L^{3*})$ and $F_A'(V_L^{4*})$ we have $\frac{\partial^2 G(y,V_L)}{\partial y\,\partial V_L}|_{(y,V_L)=(y_2^*,V_L^{3*})} < 0$ provided $y_2^* > b/p$ and $\frac{\partial G^2(y,V_L)}{\partial y\,\partial V_L}|_{(y,V_L)=(y_2^*,V_L^{4*})} < 0$ provided $y_2^* < b/p$. Further, if $A_h > 0$, then $y^* = y_2^* > \frac{b}{p}$, and it follows from Lemmas A.2-A.3 that the family $G(y, V_L)$ undergoes a flip bifurcation at (y_2^*, V_L^{3*}). In contrast, the family $G(y, V_L)$ cannot undergo a flip bifurcation at (y_2^*, V_L^{4*}). This completes the proof. □

To address the stability of a flip bifurcation (supercritical or subcritical bifurcation), we need to calculate $\frac{\partial^3 G^2}{\partial x^3}(y, V_L)$ and to determine its sign at (y_2^*, V_L^*), which is quite complex. Thus, we turn to, equivalently, a calculation of the Schwarzian derivative of the map $M(x)$, which is defined as follows [99–101]:

$$SM(x) = \frac{M'''(x)}{M'(x)} - \frac{3}{2}\left[\frac{M''(x)}{M'(x)}\right]^2.$$

By complex calculation, we have (denote $W_1 = W(f(y_2^*, V_L^*))$)

$$SG(y_2^*) = \frac{-p^2(y_2^*)^2[(py_2^*-2b)^2+2b^2](1+4W_1) - b^3(4py_2^*-b)W_1^2[(W_1+2)^2+2]}{b^2(y_2^*)^2(b-py_2^*)^2(1+W_1)^4},$$

which indicates that if $SG(y_2^*) < 0$ (*i.e.* $\frac{\partial^3 G^2}{\partial x^3}(y_2^*, V_L^{3*}) < 0$), then the family $G(y, V_L)$ undergoes a supercritical flip bifurcation at (y_2^*, V_L^{3*}); If $SG(y_2^*) > 0$ (*i.e.* $\frac{\partial^3 G^2}{\partial x^3}(y_2^*, V_L^{3*}) > 0$), then the family $G(y, V_L)$ undergoes a subcritical flip bifurcation at (y_2^*, V_L^{3*}).

As an example, we choose the parameter values as shown in Figure 10, then we have $V_L^{3*} = 6.872$, $V_L^{4*} = 11.578$, and $y^* = 2.5503$. Moreover, $x_1^* = 10$, $x_2^* = 1.304$, $A_h = 0.303$, $A_{h_1} = 0.356$, $Y_{\min}^h = 0.728$, $Y_{\max}^h = 2.350$, $Y_{\min}^{h_1} = 0.686$, $Y_{\max}^{h_1} = 2.446$, and $\tau + b/p = 2.986$. This indicates that the phase set is defined by $\mathcal{N}_2^h$ and $y^* \in [Y_{\max}^h, \tau + b/p]$ with $V_L = 6 < x_1^*$.

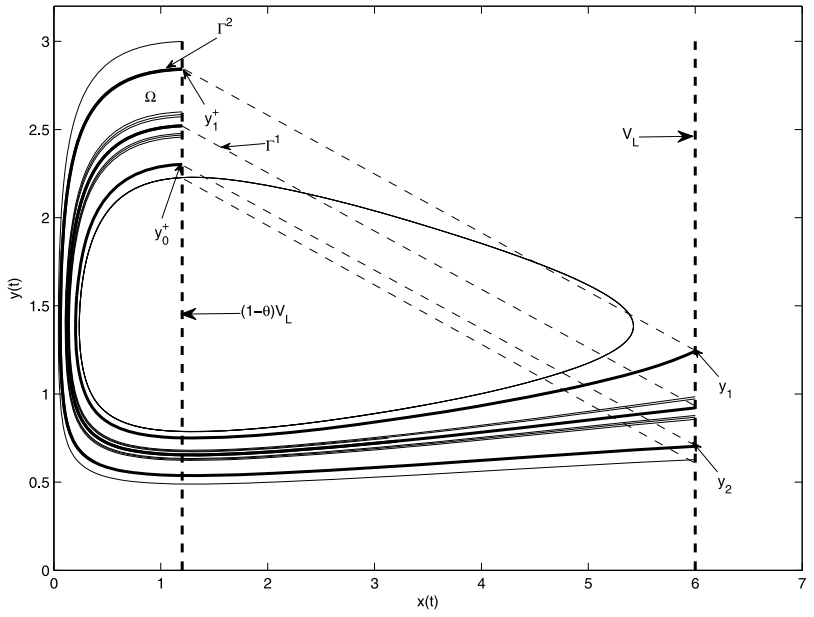

Figure 10 An unstable order-2 limit cycle and a stable order-1 limit cycle: $b = 1.8$, $p = 1.3$, $c = 0.52$, $\omega = 0.1$, $q = 0.23$, $\delta = 0.3$, $\theta = 0.8$, $\tau = 1.6$, $V_L = 6$. The initial value for Γ^2 is 2.3017 and the initial value for Γ^1 is 2.5213.

By further calculations we have

$$\frac{\partial^2 G}{\partial x\,\partial \alpha}\left(y^*, V_L^{3*}\right) \approx -0.1850 < 0, \qquad \frac{\partial^3 G^2}{\partial x^3}\left(y^*, V_L^{3*}\right) \approx 18.258 > 0.$$

Therefore, the subcritical flip bifurcation occurs at point (y^*, V_L^{3*}), and there exists a constant $\epsilon > 0$ such that the Poincaré map has an orbit of period two which is unstable for $V_L^{1*} < V_L^{3*} - \epsilon < V_L < V_L^{3*}$. Consequently, for the model (2.2) there exists an unstable order-2 limit cycle, as shown in Figure 10.

Corollary 7.1 (Flip bifurcation of model (2.3)) *Assume that $\tau > 0$ and y^* exists. If $A_0 > 0$, then the family $G(y, V_L)$ undergoes a flip bifurcation at (y_2^*, V_L^0), where*

$$V_L^0 = \frac{p\tau}{c\theta} + \frac{\delta}{c\theta}\ln\left(\frac{1}{1-\theta}\right) - \frac{b}{c\theta}\ln\left(\frac{y_2^*}{y_2^* - \tau}\right). \tag{7.4}$$

Proof Substituting $A_0 = c\theta V_L - \delta\ln(\frac{1}{1-\theta})$ into y^* and solving the equation $\mu(V_L) = 0$ with respect to V_L yield one critical value V_L^0, where

$$V_L^0 = \frac{p\tau}{c\theta} + \frac{\delta}{c\theta}\ln\left(\frac{1}{1-\theta}\right) - \frac{b}{c\theta}\ln\left(\frac{y_2^*}{y_2^* - \tau}\right) \tag{7.5}$$

and $V_L^0 > 0$ holds true due to $A_0 > 0$. It is easy to see that $G(y_2^*, V_L^0) = y_2^*$ and

$$\left.\frac{\partial G(y, V_L)}{\partial y}\right|_{(y,V_L)=(y_2^*, V_L^0)} = -\frac{b}{p}\frac{W(f(y, V_L))}{1 + W(f(y, V_L))}\left[\frac{1}{y} - \frac{p}{b}\right]\Bigg|_{(y,V_L)=(y_2^*, V_L^0)} = -1,$$

$$\left.\frac{\partial^2 G(y,V_L)}{\partial y\,\partial V_L}\right|_{(y,V_L)=(y_2^*,V_L^0)} = -\frac{c\theta(b-py)}{bpy}\frac{W(f(y,V_L))}{[1+W(f(y,V_L))]^3}\Bigg|_{(y,V_L)=(y_2^*,V_L^0)}$$
$$= \frac{bc\theta(b-py_2^*)(y_2^*-\tau)}{y_2^*[b-p(y_2^*-\tau)]^3}.$$

It follows from $\tau < y_2^* < \tau + b/p$ that $\frac{\partial^2 G(y,V_L)}{\partial y\,\partial V_L}|_{(y,V_L)=(y_2^*,V_L^0)} < 0$. This indicates that the family $G(y,V_L)$ undergoes a flip bifurcation at (y_2^*, V_L^0) due to $y_2^* > b/p$ when $A_0 > 0$. □

Similarly, it is difficult to calculate the $\frac{\partial^3 G^2}{\partial x^3}(y_2^*, V_L^0)$ for model (2.3) and to determine its sign, so we turn to a calculation of the Schwarzian derivative and we have (denote $W_1 = W(f(y_2^*, V_L^0))$)

$$SG(y_2^*) = \frac{-p^2(y_2^*)^2[(py_2^*-2b)^2+2b^2](1+4W_1) - b^3(4py_2^*-b)W_1^2[(W_1+2)^2+2]}{b^2(y_2^*)^2(b-py_2^*)^2[1+W_1]^4}.$$

8 The necessary condition for the existence of an order-2 limit cycle

Evidence for the existence of an order-2 limit cycle, as discussed in Section 7, which can bifurcate from an order-1 limit cycle through a subcritical flip bifurcation, and some special cases for the existence of an order-2 limit cycle will be discussed in Section 11. Moreover, we note that the order-2 limit cycles can only appear in cases (SC_{11}) and (SC_2), because $|g(y)| < 1$ for all y lying in the domains of Poincaré map $\mathcal{P}$ if $A_h \le 0$. Therefore, for the necessary condition of existence of an order-2 limit cycle we only need to focus on cases (SC_{11}) and (SC_2), which will be addressed later. So we would like to discuss the relations between order-2 and order-1 limit cycles first.

8.1 The relations between order-2 limit cycle and order-1 limit cycle

In this section, we assume that for model (2.2) there exists an order-2 limit cycle, as shown in Figure 10 with $P_0^+ = ((1-\theta)V_L, y_0^+)$, $P_1^+ = ((1-\theta)V_L, y_1^+)$ and $y_0^+ \neq y_1^+$, and we denote the corresponding points lying in impulsive set $\mathcal{M}$ as $Q_0 = (V_L, y_1)$ and $Q_1 = (V_L, y_2)$ with $y_2^+ = y_0^+$. Without loss of generality, we let $y_1^+ > y_0^+$ and focus on case (SC_2), *i.e.* $V_L < x_1^*$ and $x_4^* < (1-\theta)V_L$, as shown in Table 3. For case (SC_{11}), we can obtain the same results by using the methods developed in this section. Therefore, for case (SC_2) there are three possibilities: (i) $y_1^+ > y_0^+ \ge Y_{\max}^h > b/p$; (ii) $y_1^+ \ge Y_{\max}^h > b/p > Y_{\min}^h \ge y_0^+$; (iii) $b/p > Y_{\min}^h \ge y_1^+ > y_0^+$.

Lemma 8.1 *Assuming* (SC_2) (*i.e.* $V_L < x_1^*$ *and* $x_4^* < (1-\theta)V_L$) *and model* (2.2) *has an order-*2 *limit cycle, then Cases* (ii) *and* (iii) *cannot occur.*

Proof Here we first prove that case (iii) cannot hold true and case (ii) will be proved in Section 8.2. Assume $b/p > Y_{\min}^h \ge y_1^+ > y_0^+$. If model (2.2) has an order-2 limit cycle O_2 with initiating value P_0^+, then the two line segments $\overline{Q_2P_0^+}$ and $\overline{Q_1P_1^+}$ satisfy $\overline{Q_2P_0^+} \parallel \overline{Q_1P_1^+}$, which is impossible due to $y_2^+ = y_0^+$. Thus, we conclude that case (iii) cannot appear if for model (2.2) there exists an order-2 limit cycle under condition (SC_2). □

The following theorem shows the relations between the existence of an order-2 limit cycle and the existence of an order-1 limit cycle. Similar results and proofs have already been published [1].

Theorem 8.1 *Assuming* (SC_2) (*i.e.* $V_L < x_1^*$ *and* $x_4^* < (1-\theta)V_L$), *then the existence of an order-*2 *limit cycle of model* (2.2) *indicates the existence of an order-*1 *limit cycle of model* (2.2).

Proof According to the definition of the Poincaré map, for system (2.2) the existence of an order-2 limit cycle implies that (y_0^+, y_1^+) satisfies

$$\begin{aligned} y_0^+ &= -\frac{b}{p} W\left(-\frac{p}{b} y_1^+ \exp\left(-\frac{p}{b} y_1^+ + \frac{A_h}{b}\right)\right) + \tau, \\ y_1^+ &= -\frac{b}{p} W\left(-\frac{p}{b} y_0^+ \exp\left(-\frac{p}{b} y_0^+ + \frac{A_h}{b}\right)\right) + \tau, \end{aligned} \tag{8.1}$$

with $y_0^+ \neq y_1^+$, *i.e.*,

$$\begin{aligned} y_1^+ \exp\left(-\frac{p}{b} y_1^+ + \frac{A_h}{b}\right) &= \left(y_0^+ - \tau\right) \exp\left(-\frac{p}{b}\left(y_0^+ - \tau\right)\right), \\ y_0^+ \exp\left(-\frac{p}{b} y_0^+ + \frac{A_h}{b}\right) &= \left(y_1^+ - \tau\right) \exp\left(-\frac{p}{b}\left(y_1^+ - \tau\right)\right). \end{aligned} \tag{8.2}$$

To prove Theorem 8.1, according to Table 3 we need to prove that the existence of an order-2 limit cycle indicates that $\tau > \frac{A_h}{p}$ and $\tau \geq \tau_M$. It follows from Lemma 8.1 that we have: (i) $y_1^+ > y_0^+ \geq Y_{\max}^h > b/p$; (ii) $y_1^+ \geq Y_{\max}^h > b/p > Y_{\min}^h \geq y_0^+$. This shows $y_1^+ \geq Y_{\max}^h$ in both cases. It follows from (8.1) that

$$Y_{\max}^h \leq y_1^+ = -\frac{b}{p} W\left(-\frac{p}{b} y_0^+ \exp\left(-\frac{p}{b} y_0^+ + \frac{A_h}{b}\right)\right) + \tau,$$

i.e.

$$\tau \geq Y_{\max}^h + \frac{b}{p} W\left(-\frac{p}{b} y_0^+ \exp\left(-\frac{p}{b} y_0^+ + \frac{A_h}{b}\right)\right) \geq Y_{\max}^h - \frac{b}{p} = \tau_M.$$

Moreover, we can prove that if for model (2.2) there exists an order-2 limit cycle, then we must have $A_h < p\tau$, and consequently the y^* defined by (5.2) is well defined with $y^* \in [Y_{\max}^h, \tau + \frac{b}{p}]$. Otherwise if $A_h \geq p\tau$, it follows from the two equations (8.2) that we have the following inequalities:

$$y_0^+ \exp\left(-\frac{p}{b}\left(y_0^+ - \tau\right)\right) \leq \left(y_1^+ - \tau\right) \exp\left(-\frac{p}{b}\left(y_1^+ - \tau\right)\right) \tag{8.3}$$

and

$$y_1^+ \exp\left(-\frac{p}{b}\left(y_1^+ - \tau\right)\right) \leq \left(y_0^+ - \tau\right) \exp\left(-\frac{p}{b}\left(y_0^+ - \tau\right)\right). \tag{8.4}$$

From a combination of (8.3) and (8.4) we get

$$y_0^+ y_1^+ \leq \left(y_1^+ - \tau\right)\left(y_0^+ - \tau\right),$$

which implies $y_1^+ + y_0^+ \le \tau$. This contradicts $y_1^+ \ge \tau$, $y_0^+ \ge \tau$ and $y_0^+ + y_1^+ > 2\tau$ due to $y_0^+, y_1^+ \in \mathcal{N}$. Therefore, $\tau > A_h/p$ and $\tau \ge Y^h_{\max} - b/p$ indicate that y^* is well defined and consequently the existence of an order-1 limit cycle follows. This completes the proof. □

Remark 8.1 If $y_0^+, y_1^+ \in [Y^h_{\max}, \tau + b/p]$ (*i.e.* case (i)), as shown in Figure 10, then it is easy to prove that the existence of an order-2 limit cycle indicates the existence of an order-1 limit cycle. That is, the region Ω shown in Figure 10 satisfies all the conditions of the Poincaré-Bendixson theorem of impulsive semi-dynamic systems [60]. However, this method cannot be applied when case (ii) occurs, because the domains of the Poincaré map are separated into two segments, *i.e.* $y_i^+ \in [\tau, Y^h_{\min}] \cup [Y^h_{\max}, b/p + \tau]$. Therefore, if we want to employ the Poincaré-Bendixson theorem of impulsive semi-dynamic systems, then we must exclude case (ii), as mentioned before which will be proved later by using the necessary condition of existence of an order-2 limit cycle.

8.2 The necessary condition for the existence of an order-2 limit cycle

Although we cannot provide the simple sufficient conditions for the existence of an order-2 limit cycle as those for the existence of an order-1 limit cycle, the necessary conditions shown in the following theorem are quite useful.

Theorem 8.2 *The necessary condition for the existence of an order-*2 *limit cycle of model* (2.2) *is that* y_0^+ *and* y_1^+ *are the two roots of the following equation*:

$$f_2(y) = y(y-\tau)\exp\left(-\frac{2p}{b}y\right) = c, \quad y > \tau, \tag{8.5}$$

where $0 < c < f_2(y_2^*)$ *and* $y_2^* = \frac{b+p\tau+\sqrt{b^2+p^2\tau^2}}{2p}$ (*defined in* (5.3)) *with* $y_0^+ < y_2^* < y_1^+$.

Proof Assume that model (2.2) has an order-2 limit cycle, *i.e.*, y_0^+ and y_1^+ lie in the domains of the Poincaré map $\mathcal{P}$ with $y_0^+ \ne y_1^+$ and satisfy (8.2). Therefore, dividing both sides of (8.2) simultaneously, one has

$$y_1^+\left(y_1^+ - \tau\right)\exp\left(-\frac{2p}{b}y_1^+\right) = y_0^+\left(y_0^+ - \tau\right)\exp\left(-\frac{2p}{b}y_0^+\right), \tag{8.6}$$

which indicates that the above equation must hold if for model (2.2) there exists an order-2 limit cycle. According to the symmetry of both sides, we can define the function $f_2(y)$ given by (8.5) for all $y > \tau$ due to both y_0^+ and y_1^+ being larger than τ.

Taking the derivative of the function $f_2(y)$ with respect to y yields

$$f_2'(y) = -\frac{\exp(-\frac{2p}{b}y)}{b}\left[2py^2 - 2(b+p\tau)y + b\tau\right]. \tag{8.7}$$

Solving the equation $f_2'(y) = 0$ yields two roots which are just the same as y_1^* and y_2^*, *i.e.*

$$y_{1,2}^* = \frac{b + p\tau \mp \sqrt{b^2 + p^2\tau^2}}{2p}$$

and only the $y_2^* = \frac{b+p\tau+\sqrt{b^2+p^2\tau^2}}{2p}$ is a feasible root which satisfies $\tau < y_2^* < \tau + b/p$. It is easy to see that the function $f_2(y)$ reaches its maximum value at $y = y_2^*$. Moreover, we have $f_2(\tau) = 0$

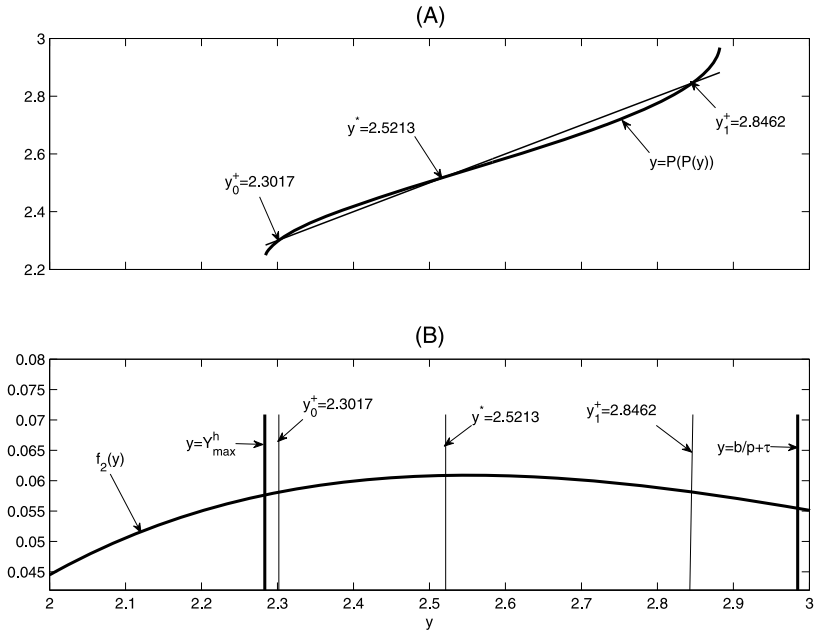

Figure 11 Illustration of the necessary condition of existence of an order-2 limit cycle. The parameter values are as follows: $b = 1.8$, $p = 1.3$, $c = 0.52$, $\omega = 0.1$, $q = 0.23$, $\delta = 0.3$, $\theta = 0.8$, $\tau = 1.6$, $V_L = 6$.

and $f_2(y) \to 0$ as $y \to +\infty$. Thus, for any $0 < c < f_2(y_2^*)$, there are two roots y_0^+ and y_1^+ such that $f_2(y_0^+) = f_2(y_1^+)$ (as shown in Figure 11), *i.e.* (8.6) holds. This completes the proof. □

In order to show the necessary condition of the existence of an order-2 limit cycle, we plot the second iteration of Poincaré map $\mathcal{P}(y)$ with the parameter set as those shown in Figure 11(A). Obviously, with the given parameter values, for the Poincaré map $\mathcal{P}(y)$ there exists a period two solution, as shown in Figure 11(A). At the same time, we plot the function $f_2(y)$ in Figure 11(B) and we have $f_2(y_0^+) = f_2(y_1^+)$ with $Y_{\max}^h < y_0^+ < y_1^+ < \frac{b}{p} + \tau$, which indicates the necessary condition of the existence of an order-2 limit cycle holds true.

Remark 8.2 Note that the existence of an order-2 limit cycle strictly depends on the y_2^*, once the two roots y_0^+ and y_1^+ of $f_2(y) = c$ coincide, *i.e.* $y_0^+ = y_1^+ = y_2^*$, then we have $y^* = y_2^*$ at which point the flip bifurcation occurs. All these results confirm that the existence of an order-2 limit cycle associates with the flip bifurcation at y_2^*. Moreover, the function $f_2(y)$ only depends on the three parameters b, p, and τ, which is independent of control parameters V_L and θ.

Note that the family $G(y, V_L)$ undergoes a flip bifurcation at (y_2^*, V_L^{3*}) and according to Lemma 7.1 and Figure 9 that the A_h is a monotonic increasing function of V_L in the neighborhood of V_L^{3*}, which indicates that $Y_{\max}^h$ is a monotonic increasing function, while $Y_{\min}^h$ is a monotonic decreasing function, as shown in Figure 12. Thus, there is less likelihood that the order-2 limit cycle exists as V_L passes through the critical V_L^{3*} and decreases. In particular, for a given parameter set, the ranges of initial values y_0^+ and y_1^+ for existence of an order-2 limit cycle can be determined. For example, if we fixed the parameters as those in Figure 9 and Figure 12, then the flip bifurcation occurs at $(2.5503, 6.972)$, at which we have $Y_{\max}^h = 2.3504 \doteq Y_m^1$ and $f_2(Y_m^1) = 0.0592$. Thus, we can determine the value Y_M^1 by solving

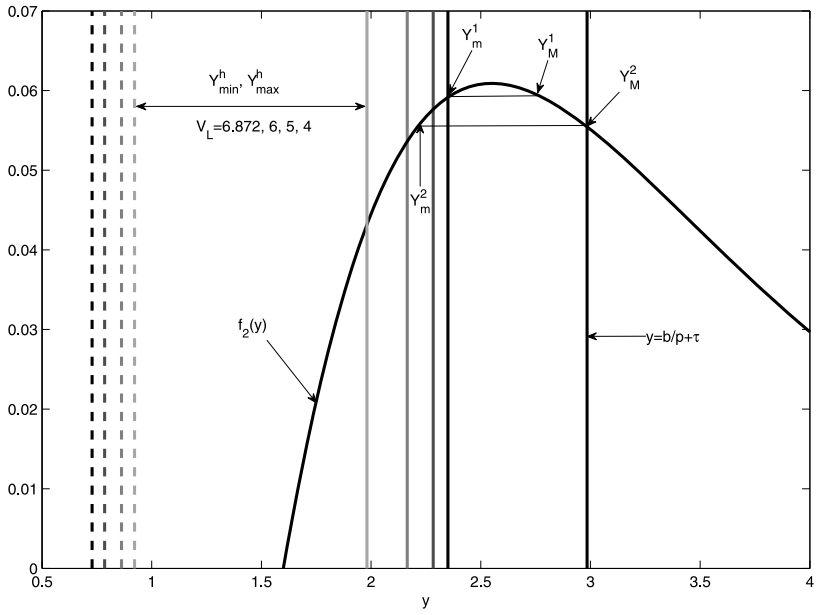

Figure 12 Illustration of initial domains of the existence of an order-2 limit cycle for case (i), *i.e.* $y_1^+ > y_0^+ \geq Y^h_{\max} > b/p$. Four lines for $y = Y^h_{\min}$ and $y = Y^h_{\max}$ related to different V_L are plotted. The parameter values are as follows: $b = 1.8$, $p = 1.3$, $c = 0.52$, $\omega = 0.1$, $q = 0.23$, $\delta = 0.3$, $\theta = 0.8$, $\tau = 1.6$, and $V_L = 6.872, 6, 5, 4$.

the equation $f_2(y) = 0.0592$, *i.e.* we have $Y^1_M = 2.7768$. Similarly, since $f_2(b/p + \tau) = 0.0555$ with $b/p + \tau = 2.9846 \doteq Y^2_M$, we can determine Y^2_m by solving the equation $f_2(y) = 0.0555$, *i.e.* we have $Y^2_m = 2.2134$. Therefore, as V_L passes through the critical V_L^{3*} and decreases, the initial values for the existence of an order-2 limit cycle can only be in the following intervals: $y_0^+ \in [Y^2_m, Y^1_m]$ and $y_1^+ \in [Y^1_M, Y^2_M]$. For this case we see that both y_0^+ and y_1^+ are larger than $Y^h_{\max} > b/p$, *i.e.* case (i) occurs here.

Based on the necessary condition of existence of an order-2 limit cycle, we can prove case (ii) in Lemma 8.1.

Proof of case (ii) *in Lemma* 8.1 Now we turn to a proof of the second case (*i.e.* case (ii)) cannot happen in Lemma 8.1, *i.e.* we ask under what necessary conditions we could have $y_1^+ \geq Y^h_{\max} > b/p > Y^h_{\min} \geq y_0^+$ (case (ii) here) if for model (2.2) there exists an order-2 limit cycle. Note that $\tau < Y^h_{\min}$ must hold if case (ii) occurs. Thus, based on the necessary condition we must have

$$f_2\big(Y^h_{\min}\big) > f_2(\tau + b/p). \tag{8.8}$$

Let $z = -e^{-1-\frac{A_h}{b}}$, then we have

$$\begin{aligned} f_2\big(Y^h_{\min}\big) &= Y^h_{\min}\big(Y^h_{\min} - \tau\big)\exp\left(-\frac{2p}{b}Y^h_{\min}\right) \\ &= -\frac{b}{p}\left(-\frac{bW(z)}{p} - \tau\right)\frac{z^2}{W(z)} \\ &= \frac{b}{p}\left(\frac{b}{p} + \frac{\tau}{W(z)}\right)\exp\left(-2 - \frac{2A_h}{b}\right) \end{aligned}$$

and

$$f_2(\tau + b/p) = \frac{b}{p}\left(\frac{b}{p} + \tau\right)\exp\left(-2 - \frac{2p\tau}{b}\right).$$

Thus, $f_2(Y^h_{\min}) > f_2(\tau + b/p)$ is equivalent to the following inequality ($\tau < Y^h_{\min}$, $0 < A_h < p\tau$):

$$\left(\frac{b}{p} + \frac{\tau}{W(z)}\right)\exp\left(-\frac{2A_h}{b}\right) > \left(\frac{b}{p} + \tau\right)\exp\left(-\frac{2p\tau}{b}\right). \tag{8.9}$$

It is easy to show $(\frac{b}{p} + \frac{\tau}{W(z)}) > 0$. Note that if $A_h = 0$, then the left hand side becomes $\frac{b}{p} - \tau$. So we first claim that $\frac{b}{p} - \tau < (\frac{b}{p} + \tau)\exp(-\frac{2p\tau}{b})$. To do this, we define

$$f_3(\tau) = \frac{b}{p} - \tau - \left(\frac{b}{p} + \tau\right)\exp\left(-\frac{2p\tau}{b}\right).$$

By calculation we have $f_3(0) = 0$ and $f_3'(\tau) = -1 + (1 + \frac{2p\tau}{b})\exp(-\frac{2p\tau}{b}) < 0$. This indicates that the inequality (8.9) cannot hold true if $A_h = 0$. Further, we denote that

$$f_4(A_h) = \left(\frac{b}{p} + \frac{\tau}{W(z)}\right)\exp\left(-\frac{2A_h}{b}\right),$$

and

$$f_4'(A_h) = \frac{\exp(-\frac{2A_h}{b})[\tau p + 2bW(z) + 2\tau pW(z) + 2bW(z)^2]}{-bpW(z)(1 + W(z))}.$$

It follows from $\tau < Y^h_{\min} = -\frac{b}{p}W(z)$ that

$$\tau p + 2bW(z) + 2\tau pW(z) + 2bW(z)^2 < W(z)\big[b + 2\tau p + 2bW(z)\big] < 0.$$

This shows that the inequality (8.9) cannot hold true for all $A_h > 0$, and consequently if for model (2.2) there exists an order-2 limit cycle, then case (ii) cannot occur too. Thus, we prove case (ii) in Lemma 8.1. □

Corollary 8.1 *If for model* (2.2) *there exists an order-*2 *limit cycle, then the order-*2 *and order-*1 *limit cycles coexist. Moreover, the non-existence of the order-*1 *limit cycle implies the non-existence of the order-*2 *limit cycle.*

Proof According to the proof of Lemma 8.1 that only case (i), *i.e.* $y_1^+ > y_0^+ \geq Y^h_{\max} > b/p$, is feasible if for model (2.2) there exists an order-2 limit cycle. Consequently, it follows from Remark 8.1 that the region Ω indicated in Figure 10 satisfies the Poincaré-Bendixson theorem of impulsive semi-dynamic systems [58]. Thus, the existence of the order-2 limit cycle indicates the existence of the order-1 limit cycle. □

The necessary condition also tells us that the order-2 limit cycle will disappear as V_L is decreasing or τ is increasing. Moreover, we can obtain similar results to those shown in this section for model (2.3) and we do not repeat them here.

9 Finite state-dependent feedback control actions

To address the global dynamic behavior of model (2.2) completely, for cases (SC_1) and (SC_2) we need to know under which conditions the solution initiating from $((1-\theta)V_L, y_0^+)$, where $y_0^+ \in Y_D^h$ or $Y_D^{h_1}$, will be free from impulsive effects after finite state-dependent feedback control actions. That is, whether there exists a positive integer k_1, such that $y_{k_1}^+ \in [Y_{\min}^{h_1}, Y_{\max}^{h_1}]$ for case (SC_1) or $y_{k_1}^+ \in (Y_{\min}^h, Y_{\max}^h)$ for case (SC_2). This is not only important for determining the global dynamics, but also it is crucial for our real life problems considered in the present work.

Therefore, in this section we will focus on finding the conditions under which all solutions of model (2.2) with initial value $((1-\theta)V_L, y_0^+)$ will be free from impulsive effects after finite state-dependent feedback control actions. For convenience, we denote the boundary of closed trajectory Γ_h (or homoclinic cycle Γ_{h_1}) as $\partial\Omega_h$ (or $\partial\Omega_{h_1}$) and its interior as $\operatorname{Int}\Omega_h$ (or $\operatorname{Int}\Omega_{h_1}$).

9.1 Finite state-dependent feedback control actions for case (SC_2)

Based on the results shown in Section 6, in particular the results shown in Table 3, we have the following main theorem with respect to finite state-dependent feedback control actions for model (2.2) under case (SC_2). Note that all trajectories from $\operatorname{Int}\Omega_h$ are free from impulsive effects, and $\operatorname{Int}\Omega_h$ is an invariant set of system (2.2) under case (SC_2).

Theorem 9.1 *For case* (SC_2), *if* $\frac{A_h}{p} < \tau < \tau_M$ *then any solution initiating from* $((1-\theta)V_L, y_0^+)$ *with* $y_0^+ > 0$ *will experience finite state-dependent feedback control actions and enter into* $\operatorname{Int}\Omega_h$ *eventually.*

Proof For any solution initiating from $((1-\theta)V_L, y_0^+)$ with $y_0^+ \le \tau$ or $y_0^+ > \tau + \frac{b}{p}$ will enter into the region $\mathcal{N}_2^h$ after a single impulsive effect, *i.e.* $y_1^+ \in Y_D$. It follows from $\tau < \tau_M = Y_{\max}^h - \frac{b}{p}$ that there are two possibilities: (a) $y_1^+ \in (Y_{\min}^h, Y_{\max}^h)$, and (b) $y_1^+ \in (\tau, Y_{\min}^h]$. For case (a), it is easy to see the results shown in Theorem 9.1 are true, and the solution initiating from $((1-\theta)V_L, y_0^+)$ at most experiences an impulsive effect once only before entering into $\operatorname{Int}\Omega_h$.

For case (b), without loss of generality, we assume the solution initiating from $((1-\theta)V_L, y_0^+)$ experiences impulsive effects k times and we will prove that k is finite. Otherwise, if k is infinite, then we must have $y_k^+ \in (\tau, Y_{\min}^h]$ for all $k > 1$ due to $\tau < \tau_M$. We note that

$$y_i^+ = -\frac{b}{p} W\left(-\frac{p}{b} y_{i-1}^+ \exp\left(-\frac{p}{b} y_{i-1}^+ + \frac{A_h}{b}\right)\right) + \tau, \quad i = 1, 2, \ldots, k.$$

It follows from the definition of the function $f(y)$, *i.e.* $f(y) = -\frac{p}{b} y \exp(-\frac{p}{b} y + \frac{A_h}{b})$, then we have

$$f'(y) = -\frac{p}{b} \exp\left(-\frac{p}{b} y + \frac{A_h}{b}\right)\left(1 - \frac{p}{b} y\right),$$

which means that $f'(y) > 0$ if $y > b/p$, and $f'(y) < 0$ if $y < b/p$. Moreover, the Lambert $\mathrm{W}(z)$ function is a strictly increasing function for $z \in [-e^{-1}, 0)$.

Therefore, if the inequality $y_2^+ < y_1^+$ holds, then it follows from the monotonicity of the functions of the Lambert W and f that

$$\tau < y_k^+ < y_{k-1}^+ < \cdots < y_2^+ < y_1^+ < y_0^+ \le Y_{\min}^h \tag{9.1}$$

and if the inequality $y_2^+ > y_1^+$ holds, then

$$\tau < y_1^+ < y_2^+ < \cdots < y_{k-1}^+ < y_k^+ \le Y_{\min}^h. \tag{9.2}$$

Thus, the limitation

$$\lim_{k\to\infty} y_k^+ = y^*$$

exists with $y^* \in (\tau, Y_{\min}^h]$. According to the continuity of the Lambert W function on the interval $(\tau, Y_{\min}^h]$ we can see that

$$y^* = -\frac{b}{p} W\left(-\frac{p}{b} y^* \exp\left(-\frac{p}{b} y^* + \frac{A_h}{b}\right)\right) + \tau,$$

which indicates that y^* is a fixed point of the Poincaré map $\mathcal{P}(y_i^+)$ and this contradicts the non-existence of the equilibrium, as shown in Table 3. Further, the non-existence of the equilibrium y^* clarifies that inequalities (9.1) cannot hold true. Therefore, only the inequalities shown in (9.2) can occur, *i.e.* the sequence y_k^+ with $k \ge 1$ is strictly monotonically increasing, and it will enter into $\operatorname{Int}\Omega_h$ after finite impulsive effects, as shown in Figure 13(A). □

Corollary 9.1 *For case* (SC_2), *if* $0 < \tau < \tau_M$ *then any solution initiating from* $((1-\theta)V_L, y_0^+)$ *with* $y_0^+ > 0$ *will experience finite state-dependent feedback control actions and enter into* $\operatorname{Int}\Omega_h$ *eventually.*

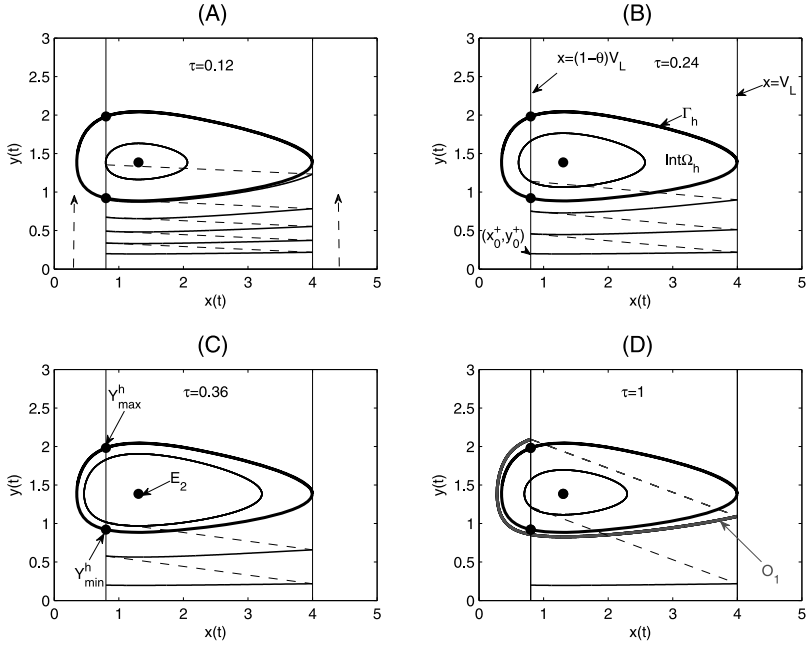

Figure 13 Illustration of Theorem 9.1 with parameter values $b = 1.8$, $p = 1.3$, $c = 0.52$, $\omega = 0.1$, $q = 0.23$, $\delta = 0.3$, $\theta = 0.8$, $V_L = 4$. The solution shown in each subplot starting at $((1-\theta)V_L, 0.2)$, $\frac{A_h}{b} = 0.1005$, $\tau_M = 0.5965$, and $Y_{\min}^h = 0.9219$, $Y_{\max}^h = 1.9811$.

In Figure 13, we show the effects of different values of τ on the finite impulsive effects of solutions. It follows from Figure 13(A)-(C) that if the solution initiating from the same initial point $((1-\theta)V_L, 0.2)$, then the smaller τ is, the greater the number of impulsive effects that it has. Note that not all solutions will enter into $\operatorname{Int}\Omega_h$ after finite impulsive effects once the τ increases and exceeds the τ_M, because there exists an order-1 limit cycle which could be stable or unstable, as shown in Figure 13(D) and Table 3. If so, for model (2.2) there may exist multiple attractors including a stable order-1 limit cycle (indicated as O_1 in Figure 13(D)) and $\operatorname{Int}\Omega_h$. Thus, the question is what are their regions of attraction, and we will address this question in the following sections.

9.2 Finite state-dependent feedback control actions for case (SC_1)

Note that all trajectories from $\operatorname{Int}\Omega_{h_1} \cup \partial\Omega_{h_1}$ are free from impulsive effects for case (SC_1), and $\operatorname{Int}\Omega_{h_1} \cup \partial\Omega_{h_1}$ is an invariant set of system (2.2) under case (SC_1). In the following we provide the results for the two subcases of (SC_1) separately.

Theorem 9.2 *For case* (SC_{11}), *if* $\frac{A_h}{p} < \tau \le \tau_2^{h_1}$ *then any solution initiating from* $((1-\theta)V_L, y_0^+)$ *with* $y_0^+ > 0$ *will experience finite state-dependent feedback control actions and enter into* $\operatorname{Int}\Omega_{h_1} \cup \partial\Omega_{h_1}$ *eventually.*

Proof Note that for case (SC_{11}) we have $V_L \ge x_1^*$, thus the line $x = V_L$ intersects with the right branch trajectory of homoclinic cycle Γ_{h_1} at two points, as shown in Figure 14 (gray lines). The vertical coordinate of the small intersection point is $Y_{\max}^{h_1} - \tau_2^{h_1}$, and the rest of the proof of Theorem 9.2 is complete and is the same as was used in the proof of Theorem 9.1, so we omit the details. □

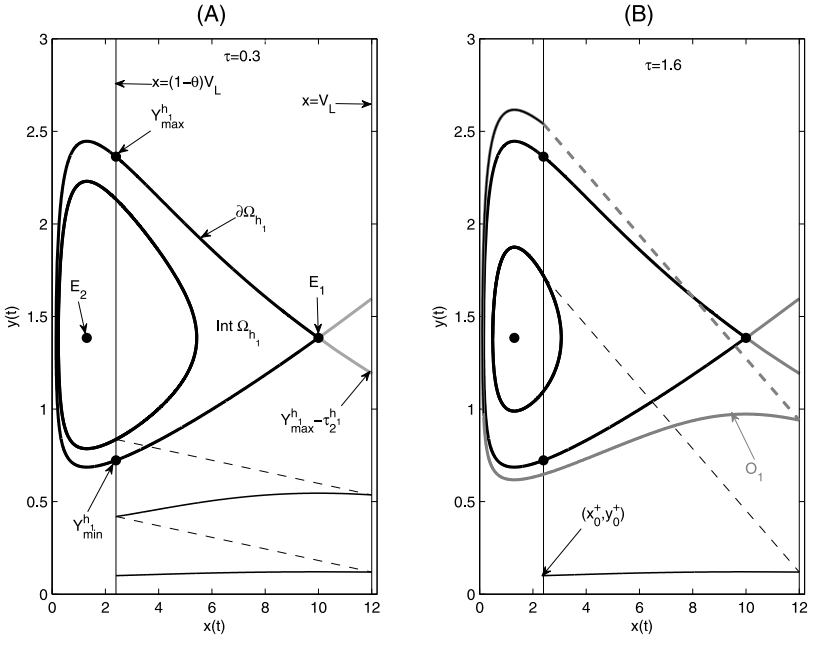

Figure 14 Illustration of Theorem 9.2 with parameter values $b = 1.8$, $p = 1.3$, $c = 0.52$, $\omega = 0.1$, $q = 0.23$, $\delta = 0.3$, $\theta = 0.8$, $V_L = 12$. We have $\tau = 0.3$ **(A)** and $\tau = 1.6$ **(B)**. The solution shown in each subplot starting at $((1-\theta)V_L, 0.1)$, $\frac{A_h}{b} = 0.2235$, $\tau_2^{h_1} = 1.1701$ and $Y_{\min}^{h_1} = 0.7229$, $Y_{\max}^{h_1} = 2.3628$, $y^* = 2.5399$ for subplot **(B)**.

Corollary 9.2 *For case* (SC_{11}), *if* $0 < \tau \le \tau_2^{h_1}$ *then any solution initiating from* $((1-\theta)V_L, y_0^+)$ *with* $y_0^+ > 0$ *will experience finite state-dependent feedback control actions and enter into* $\operatorname{Int}\Omega_{h_1} \cup \partial\Omega_{h_1}$ *eventually.*

In Figure 14(A), we show that if $\frac{A_h}{p} < \tau \le \tau_2^{h_1}$, then all solutions initiating from $((1-\theta)V_L, y_0^+)$ will be free from impulsive effects and enter into the invariant set $\operatorname{Int}\Omega_{h_1} \cup \partial\Omega_{h_1}$ after finite state-dependent feedback control actions. However, once the τ is increasing and exceeds the threshold value $\tau_2^{h_1}$, then multiple attractors may exist (as shown in Figure 14(B)) and their regions of attraction will also be addressed later.

Similarly, for subcase (SC_{12}) we have the following main results on the finite state-dependent feedback control actions.

Theorem 9.3 *For case* (SC_{12}), *if* $\tau_3^{h_1} \le \tau \le \tau_2^{h_1}$ *then any solution initiating from* $((1-\theta)V_L, y_0^+)$ *with* $y_0^+ > 0$ *will experience finite state-dependent feedback control actions and enter into* $\operatorname{Int}\Omega_{h_1} \cup \partial\Omega_{h_1}$ *eventually.*

By using the same methods as those in the proof of Theorem 9.1 and Theorem 9.2 we can prove Theorem 9.3. Note that for subcase (SC_{12}) multiple attractors can exist for $\tau < \tau_3^{h_1}$ and $\tau > \tau_2^{h_1}$.

10 Non-existence of order-k ($k \ge 3$) limit cycles

It follows from Table 3 and the results shown in Section 9 that the dynamical behavior for case (SC_{11}) with $\tau > \tau_2^{h_1}$, case (SC_2) with $\tau \ge \tau_M$ and case (SC_{12}) with $\tau < \tau_3^{h_1}$ or $\tau > \tau_2^{h_1}$ could be complex. In order to address the possible complex dynamics in more detail, the non-existence of order-k ($k \ge 3$) limit cycles of model (2.2) will be investigated in this section. Thus, without loss of generality, we assume that $y_0^+ \ne y_1^+ \ne y_2^+$ and the solution of system (2.2) with initial value $((1-\theta)V_L, y_0^+)$ experiences impulses k ($k \ge 3$) times. Then there exists a positive integer n such that $k = 2n$ or $k = 2n+1$.

For convenience we denote the set $\mathcal{K} = \{0, 1, 2, 3, \ldots\} = \mathcal{K}_1 \cup \mathcal{K}_2$, where $\mathcal{K}_1 = \{l_1, l_2, \ldots\}$ and $\mathcal{K}_2 = \{m_1, m_2, \ldots\}$ are two real subsets of set $\mathcal{K}$. Further, we denote $\mathcal{Y} = \{y_k^+ | k \in \mathcal{K}\}$, $\overline{\mathcal{Y}} = \{y_l^+ | y_l^+ \ge b/p, l \in \mathcal{K}_1\}$ and $\underline{\mathcal{Y}} = \{y_m^+ | y_m^+ < b/p, m \in \mathcal{K}_2\}$, respectively.

10.1 Generalized results

We first prove the following generalized results before giving the main results in this section. Note that results similar to those shown in the following first two Lemmas have been proved in [1]. For completeness and independence we briefly provide details of the proofs here.

Lemma 10.1 *Assume that* $\tau \ge \frac{b}{p}$. *One of the following cases must hold* (*where, without loss of generality, we assume k is an odd number*).

(a) $y_1^+ < y_0^+ < y_2^+$. *Then*

$$\frac{b}{p} < y_{2n+1}^+ < y_{2n-1}^+ < \cdots < y_3^+ < y_1^+ < y_0^+ < y_2^+ < y_4^+ < \cdots < y_{2n}^+.$$

(b) $y_1^+ < y_2^+ < y_0^+$. *Then*

$$\frac{b}{p} < y_1^+ < y_3^+ < \cdots < y_{2n+1}^+ < y_{2n}^+ < y_{2(n-1)}^+ < \cdots < y_4^+ < y_2^+ < y_0^+.$$

(c) $y_2^+ < y_0^+ < y_1^+$. *Then*

$$\frac{b}{p} < y_{2n}^+ < y_{2(n-1)}^+ < \cdots < y_4^+ < y_2^+ < y_0^+ < y_1^+ < y_3^+ < \cdots < y_{2n+1}^+.$$

(d) $y_0^+ < y_2^+ < y_1^+$. *Then*

$$\frac{b}{p} < y_0^+ < y_2^+ < \cdots < y_{2(n-1)}^+ < y_{2n}^+ < y_{2n+1}^+ < y_{2n-1}^+ < \cdots < y_3^+ < y_1^+.$$

Further, if $A_h \le 0$, *then only cases* (b) *and* (d) *can occur.*

Proof Assume that the solution of system (2.2) with initial value (x_0^+, y_0^+) experiences impulses k ($k \ge 3$) times and $k = 2n + 1$. Note that $\tau \ge \frac{b}{p}$ and

$$\begin{aligned}
y_1^+ &= -\frac{b}{p} W\left(-\frac{p}{b} y_0^+ \exp\left(-\frac{p}{b} y_0^+ + \frac{A_h}{b}\right)\right) + \tau, \\
y_2^+ &= -\frac{b}{p} W\left(-\frac{p}{b} y_1^+ \exp\left(-\frac{p}{b} y_1^+ + \frac{A_h}{b}\right)\right) + \tau, \\
y_3^+ &= -\frac{b}{p} W\left(-\frac{p}{b} y_2^+ \exp\left(-\frac{p}{b} y_2^+ + \frac{A_h}{b}\right)\right) + \tau.
\end{aligned} \tag{10.1}$$

It follows from the monotonicity of the Lambert W function and $f(y)$ that we have $y_2^+ > y_1^+$ if $\frac{b}{p} < y_1^+ < y_0^+$. For the relations between y_2^+ and y_0^+ there are two possibilities.

If $y_2^+ > y_0^+$ then the inequalities $y_1^+ < y_0^+ < y_2^+$ hold, which implies that $\frac{b}{p} < y_3^+ < y_1^+$. Again we have

$$y_4^+ = -\frac{b}{p} W\left(-\frac{p}{b} y_3^+ \exp\left(-\frac{p}{b} y_3^+ + \frac{A_h}{b}\right)\right) + \tau, \tag{10.2}$$

it follows that we have $\frac{b}{p} < y_3^+ < y_1^+ < y_0^+ < y_2^+ < y_4^+$. By induction, the inequalities

$$\frac{b}{p} < y_{2n+1}^+ < y_{2n-1}^+ < \cdots < y_3^+ < y_1^+ < y_0^+ < y_2^+ < y_4^+ < \cdots < y_{2n}^+ \tag{10.3}$$

hold, and case (a) follows. If $y_2^+ < y_0^+$ then by the same method as above we can prove that case (b) holds.

If $\frac{b}{p} < y_0^+ < y_1^+$ then there are two cases corresponding to cases (c) and (d) which can be proved similarly. According to the proof of Theorem 6.2 we have $-1 < g(y) < 0$ for all $y \in (\tau, \tau + b/p]$, which indicates that if $A_h \le 0$, then only the cases (b) and (d) can occur. □

Lemma 10.2 *If* $\tau \ge \frac{b}{p}$, *then for model* (2.2) *there does not exist an order-k* ($k \ge 3$) *limit cycle other than the order-*1 *and order-*2 *limit cycles.*

Proof The existence of order-1 periodic solutions and order-2 limit cycles has been shown in previous sections. For the non-existence of order-k ($k \ge 3$) limit cycles, since $\tau \ge \frac{b}{p}$, without loss of generality, we can assume $\frac{b}{p} < y_0^+$ and the trajectory of system (2.2) with initial value $((1 - \theta)V_L, y_0^+)$ experiences impulses k times. Denote the coordinates of all

impulsive points $P_i^+ = ((1-\theta)V_L, y_i^+)$ in the phase set corresponding to $Q_i = (V_L, y_{i+1})$ ($i = 0,1,2,\ldots,k$) in impulsive set, then the line segments $\overline{Q_iP_i^+}$ satisfy

$$\overline{Q_0P_0^+} \parallel \overline{Q_1P_1^+} \parallel \overline{Q_2P_2^+} \parallel \cdots \parallel \overline{Q_kP_k^+}. \tag{10.4}$$

Assume that system (2.2) has an order-k ($k \geq 3$) limit cycle, then we have

$$y_0^+ \neq y_1^+ \neq \cdots \neq y_{k-1}^+, \qquad y_k^+ = y_0^+.$$

Lemma 10.1 states that there are only four possible sequences of y_i^+ ($i = 0,1,2,\ldots,k$). Thus $y_0^+ = y_k^+$ cannot hold for $k \geq 3$ due to (10.4). This contradiction shows that for system (2.2) an order-k ($k \geq 3$) limit cycle does not exist if $\tau \geq \frac{b}{p}$. □

Lemma 10.3 *If $\tau < \frac{b}{p}$ and inequality $y_1^+ < y_0^+ < \frac{b}{p}$ holds, then for model* (2.2) *a limit cycle with order no less than* 2 *does not exist.*

Proof If $\tau < \frac{b}{p}$ and the inequalities $y_1^+ < y_0^+ < \frac{b}{p}$ hold, then it follows from the monotonicity of the Lambert W(z) function and f that

$$\tau < y_k^+ < y_{k-1}^+ < \cdots < y_2^+ < y_1^+ < y_0^+ < \frac{b}{p}. \tag{10.5}$$

Taking the same notations as those in the proof of Lemma 10.2 we have the same relations as shown in (10.4). Combining with (10.5) we conclude that an order-k ($k \geq 2$) limit cycle does not exist for model (2.2). □

Remark 10.1 (Open problem proposed in [1]) Assume $\tau < \frac{b}{p}$, $y_0^+ < y_1^+ < \frac{b}{p}$ and any trajectory from (x_0^+, y_0^+) experiences impulses k times ($k \geq 3$). If $y_k^+ \leq \frac{b}{p}$, then from the monotonicity of the Lambert W function and f we have

$$y_0^+ < y_1^+ < \cdots < y_k^+ \leq \frac{b}{p}.$$

Further, if $k \to \infty$, then it is easy to show that there exists an unique asymptotically stable order-1 limit cycle and then for model (2.2) a limit cycle with order no less than 3 does not exist. If there exists a $j < k$ such that $y_{j-1}^+ \leq \frac{b}{p}$ and $y_j^+ > \frac{b}{p}$, then we cannot determine whether for model (2.2) there exists a limit cycle with order no less than 2 or not in this way. This is also an open problem proposed in [1] for model (2.3), which will be solved in this paper.

Lemma 10.4 *If $\tau < \frac{b}{p}$, $y_{k_1}^+ \in (b/p, \tau + b/p]$ and $A_h \geq 0$, then we must have $y_{k_1+1}^+ \in (b/p, \tau + b/p]$.*

Proof Note that

$$y_{k_1+1}^+ = -\frac{b}{p} W\left[-\frac{p}{b} y_{k_1}^+ \exp\left(-\frac{p}{b} y_{k_1}^+ + \frac{A_h}{b}\right)\right] + \tau$$

and $y^+_{k_1+1} \in (b/p, \tau + b/p]$ is equivalent to

$$W\left[-\frac{p}{b}y^+_{k_1}\exp\left(-\frac{p}{b}y^+_{k_1}+\frac{A_h}{b}\right)\right] < -1+\frac{p}{b}\tau. \tag{10.6}$$

Thus, if the following inequality:

$$\left(-1+\frac{p}{b}\tau\right)\exp\left(-1+\frac{p}{b}\tau\right) > -\frac{p}{b}y\exp\left(-\frac{p}{b}y+\frac{A_h}{b}\right)$$

holds for all $y \in (b/p, \tau + b/p]$, then the inequality (10.6) follows. Equivalently, we only need to show

$$\left(-1+\frac{p}{b}\tau\right)\exp\left(-1+\frac{p}{b}\tau\right) > -\frac{p}{b}y\exp\left(-\frac{p}{b}y\right),$$

which has been proven in Theorem 6.2. This indicates that $y^+_{k_1+1} > b/p$ and by induction we have $y^+_i \in (b/p, \tau + b/p]$ for all $i \geq k_1$. □

Lemma 10.5 *If* $A_h \geq 0$ *then* $y^* > \frac{b}{p} + \frac{\tau}{2}$.

Proof Note that $y^* > \frac{b}{p} + \frac{\tau}{2}$ is equivalent to

$$y^* = \tau\frac{\exp(\frac{p}{b}\tau - \frac{A_h}{b})}{\exp(\frac{p}{b}\tau - \frac{A_h}{b}) - 1} \geq \tau\frac{\exp(\frac{p}{b}\tau)}{\exp(\frac{p}{b}\tau) - 1} > \frac{b}{p} + \frac{\tau}{2}. \tag{10.7}$$

Rearranging the above inequality yields

$$\phi(\tau) \doteq \frac{\tau}{2}\left[\exp\left(\frac{p}{b}\tau\right)+1\right] - \frac{b}{p}\left[\exp\left(\frac{p}{b}\tau\right)-1\right] > 0$$

with $\phi(0) = 0$, $\phi(b/p) = \frac{b}{2p}[3 - e] > 0$ and $\phi'(\tau) > 0$. This indicates that the inequality (10.7) holds true if $A_h \geq 0$. □

10.2 Non-existence of a limit cycle with order no less than 3

Now we assume that the solution of model (2.2) experiences infinite pulse effects and we have the following main results.

Theorem 10.1 *For model* (2.2) *a limit cycle with order no less than* 3 *does not exist.*

Proof It follows from Theorem 5.1 and Theorem 6.3 that if $\tau = 0$ and $A_h = 0$, then any solution initiating from $((1-\theta)V_L, y^+_0)$ with $y^+_0 \in Y_D$ (or Y^h_D or $Y^{h_1}_D$) and $y^+_0 < b/p$ is an order-1 periodic solution; if $A_h \neq 0$ then the unique boundary order-1 limit cycle is either stable (locally or globally) or unstable. Further, according to Lemma 10.3 and Remark 10.1 it is easy to see that if $\tau = 0$ then for model (2.2) a limit cycle with order no less than 2 does not exist.

If $\tau > 0$ then it follows from Theorem 6.2 that the unique order-1 limit cycle is globally stable under condition (SC_{123}), which indicates that for model (2.2) an order-k ($k \geq 2$) limit cycle does not exist in this case.

For case (SC_2), if $0 < \tau < \tau_M$ then any solution initiating from $((1-\theta)V_L, y_0^+)$ with $y_0^+ > 0$ will experience finite state-dependent feedback control actions and enter into $\operatorname{Int}\Omega_h$ eventually. If so, for model (2.2) no limit cycle or periodic solution exists for this case. In the following we prove that if $\tau \geq \tau_M$, then for model (2.2) no limit cycle with order no less than 3 exists for case (SC_2).

In fact if $\tau_M \geq b/p$ then $y_k^+ \geq Y_{\max}^h \geq b/p$ for $k \in \mathcal{K}$ must hold, and according to Lemma 10.2 the result follows. If $\tau_M < b/p$ and for any solution which experiences infinite pulse effects under case (SC_2), then note that $A_h > 0$ and we claim that it is impossible that all $y_k^+ \leq Y_{\min}^h < b/p$ for $k \in \mathcal{K}$. Otherwise, according to $\tau < y_k^+ \leq Y_{\min}^h < b/p$ we conclude that

$$\lim_{k\to\infty} y_k^+ = y^* \in \left[\tau, Y_{\min}^h\right]$$

and y^* is a fixed point of Poincaré map $\mathcal{P}$, which contradicts $y^* > \frac{b}{p} + \frac{\tau}{2}$ due to Lemma 10.5.

Therefore, for the series y_k^+ we have either all $y_k^+ \geq b/p$ (*i.e.* $y_k^+ \geq Y_{\max}^h$) for $k \in \mathcal{K}$ or $\mathcal{Y} = \overline{\mathcal{Y}} \cup \underline{\mathcal{Y}}$. If the former case occurs, then we have all $y_k^+ > \frac{b}{p}$. It follows from Lemma 10.2 that model (2.2) does not have any limit cycle with order no less than 2. If the latter case occurs, then without loss of generality we assume $y_0^+ < Y_{\min}^h < b/p$ and claim that there must exist the smallest positive integer j such that $y_j^+ \leq Y_{\min}^h$ and $y_{j+1}^h \geq Y_{\max}^h$. Otherwise, we have $y_k^+ \leq Y_{\min}^h < b/p$ for $k \in \mathcal{K}$ and this is impossible based on discussions above. Therefore, $y_{j+1}^+ \geq Y_{\max}^h > b/p$ must hold true. Based on Lemma 10.4 we conclude the $y_k^+ \geq Y_{\max}^h \geq b/p$ for $k \geq j+1$ and once again according to Lemma 10.2 for model (2.2) a limit cycle with order no less than 3 does not exist.

For case (SC_{11}), we can employ the same methods as those for case (SC_2) to prove that for model (2.2) a limit cycle with order no less than 3 does not exist. So we omit the details here.

For case (SC_{12}), it follows from Theorem 9.3 that if $\tau_3^{h_1} \leq \tau \leq \tau_2^{h_1}$, then any solution initiating from $((1-\theta)V_L, y_0^+)$ with $y_0^+ > 0$ will experience finite state-dependent feedback control actions and enter into $\operatorname{Int}\Omega_{h_1} \cup \partial\Omega_{h_1}$ eventually. Thus, for model (2.2) no limit cycle or periodic solution exists if $\tau_3^{h_1} \leq \tau \leq \tau_2^{h_1}$.

If $0 < \tau < \tau_3^{h_1}$, then it follows from Table 3 that $A_h \leq 0$ and the unique fixed point y^* exists and it is stable with $\tau < y^* < Y_{\min}^{h_1}$. Without loss of generality we assume $y_0^+ < Y_{\min}^{h_1}$ because if $y_0^+ > Y_{\max}^{h_1}$, then y_1^+ should be less than $Y_{\min}^{h_1}$ due to $\tau < \tau_3^{h_1}$, as shown in Figure 15(A). Note that $Y_{\min}^{h_1} - \tau_3^{h_1} = Y_{is}^{h_1}$ and consequently we have $y_k^+ < Y_{\min}^{h_1}$ for all $k \in \mathcal{K}$. Moreover, there are two possibilities: (a) $y_0^+ > y^*$; and (b) $y_0^+ < y^*$. For case (a), according to the uniqueness of the y^* and its stability the sequence y_k^+ is monotonically decreasing with $\lim_{k\to\infty} y_k^+ = y^*$, and for case (b) the sequence y_k^+ is monotonically increasing with $\lim_{k\to\infty} y_k^+ = y^*$. These results indicate that model (2.2) does not have any limit cycle with order no less than 2.

If $\tau > \tau_2^{h_1}$, then we consider the following two cases: (a) $\tau > \tau_2^{h_1}$ and $\tau \geq Y_{\min}^{h_1}$, and (b) $\tau_2^{h_1} < \tau < Y_{\min}^{h_1}$. For case (a), it is easy to see that $y_k^+ \geq Y_{\max}^{h_1}$ for all $k \geq 1$, which, according to Lemma 10.2, indicates that model (2.2) does not have any limit cycle with order no less than 2. For case (b), taking a point $Q_1(V_L, Y_{\min}^{h_1} - \tau) \in \mathcal{M}_2$ related to the phase point $P_1((1-\theta)V_L, Y_{\min}^{h_1}) \in \mathcal{N}_2^{h_1}$, and taking a point $P_0((1-\theta)V_L, y_M^+) \in \mathcal{N}_2^{h_1}$ with $y_M^+ > Y_{\max}^{h_1}$ which lies in the same trajectory with Q_1 (as shown in Figure 15(B)), *i.e.* we have

$$b\ln\left(\frac{Y_{\min}^{h_1} - \tau}{y_0^+}\right) - p\left[Y_{\min}^{h_1} - \tau - y_0^+\right] = A_h.$$

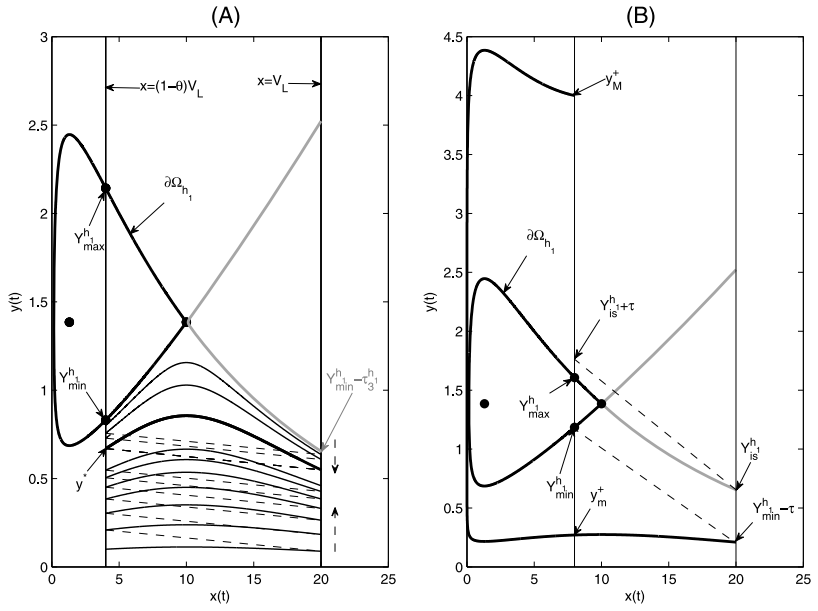

Figure 15 Existence of periodic solution for case (SC_{12}). (A) Numerical simulations for case (SC_{12}) with $\tau < \tau_3^{h_1}$. The parameter values are $b = 1.8$, $p = 1.3$, $c = 0.52$, $\omega = 0.1$, $q = 0.23$, $\delta = 0.3$, $\theta = 0.8$, $V_L = 20$, and $\tau = 0.12$. Here $A_{h_1} = 0.1998$, $A_h = -0.1997$, $\tau_2^{h_1} = 1.4887$, $\tau_3^{h_1} = 0.1758$, $\tau_2^{h_1} = 1.1701$, $Y_{\min}^{h_1} = 0.8304$, $Y_{\max}^{h_1} = 2.1433$, $y^* = 0.6692$. **(B)** Illustration for case (SC_{12}) with $\tau > \tau_2^{h_1}$.

Solving it with respect to y_M^+ yields

$$y_M^+ = -\frac{b}{p} W\left[-1, -\frac{p}{b}\left(Y_{\min}^{h_1} - \tau\right) \exp\left(-\frac{p}{b}\left(Y_{\min}^{h_1} - \tau\right) + \frac{A_h}{b}\right)\right].$$

Now we prove $y_M^+ > Y_{is}^{h_1} + \tau$. It follows from $A_1 = A_{h_1} - A_h$ and the monotonicity of the Lambert W function that $Y_{\min}^{h_1} > Y_{is}^{h_1}$. Thus, if we can prove $y_M^+ > Y_{\min}^{h_1} + \tau$ then the result follows. In fact, $y_M^+ > Y_{\min}^{h_1} + \tau$ is equivalent to

$$-\frac{p}{b}\left(Y_{\min}^{h_1} - \tau\right) \exp\left(-\frac{p}{b}\left(Y_{\min}^{h_1} - \tau\right) + \frac{A_h}{b}\right) > -\frac{p}{b}\left(Y_{\min}^{h_1} + \tau\right) \exp\left(-\frac{p}{b}\left(Y_{\min}^{h_1} + \tau\right)\right).$$

Note that $A_h \le 0$ in this case and rearranging the above inequality yields

$$Y_{\min}^{h_1} - \tau < \left(Y_{\min}^{h_1} + \tau\right) \exp\left(-\frac{2p\tau}{b}\right) \quad \text{for } \tau < Y_{\min}^{h_1},$$

which can easily be proved.

Therefore, the sequence y_k^+ for any solution initiating from $((1-\theta)V_L, y_0^+)$ with $y_0^+ \in [y_m^+, y_M^+]$, which experiences infinite pulse effects, satisfies $y_k^+ > Y_{\max}^{h_1}$ for $k \ge 1$. For the solution with $y_0^+ \notin [y_m^+, y_M^+]$, there must exist a positive integer j such that $y_j^+ \in [y_m^+, y_M^+]$ and consequently we have $y_k^+ > Y_{\max}^{h_1}$ for $k \ge j+1$. According to Lemma 10.2, model (2.2) does not have any limit cycle with order no less than 3.

Thus, according to results for cases (a) and (b) that if $\tau > \tau_2^{h_1}$ then model (2.2) does not have any order-k ($k > 2$) limit cycle. In conclusion, we have proved that model (2.2) does

not have a limit cycle with order no less than 3 for all cases, and consequently the result shown in Theorem 10.1 is true. □

Corollary 10.1 *For* (SC_{12}), *if* $0 < \tau < \tau_3^{h_1}$, *then for model* (2.2) *there exists a unique order*-1 *limit cycle which is globally stable with respect to the phase set* $\mathcal{N}_2^{h_1}$.

Corollary 10.2 *For model* (2.3) *a limit cycle with order no less than* 3 *does not exist*.

It follows from [1] that the result shown in Corollary 10.2 for model (2.3) has also been addressed and the proof provided only for $\tau \geq b/p$, and a conjecture for $\tau < b/p$ has been proposed. Thus, in this paper we have solved this problem completely.

11 Multiple attractors and their basins of attraction, interior structure

Based on the key parameters θ, V_L, and τ, we can investigate the dynamics of model (2.2) and model (2.3) in terms of different parameter spaces (*i.e.* (SC_{123}), (SC_1) and (SC_2)) and the critical values of τ. So far, the dynamics for (SC_1) and (SC_2) have not been solved completely. For example: the global existence of order-2 limit cycles and their stabilities have not been solved yet. Moreover, as mentioned in Section 9, for certain intervals of τ model (2.2) there exist multiple attractors including an order-1 limit cycle and invariant set $\operatorname{Int}\Omega_h$ or $\operatorname{Int}\Omega_{h_1} \cup \partial\Omega_{h_1}$, and the question is how to determine the basins of attraction once multiple attractors exist in model (2.2). Note that for some special cases this question for model (2.3) has been discussed in [1]. Thus, we will focus on those points in this section, aiming to find all the types of multiple attractors for system (2.2) and their regions of attraction.

11.1 Multiple attractors and their basins of attraction for (SC_2)

To address the existence of multiple attractors of model (2.2) for (SC_2), it follows from Table 3 that the parameter τ can be divided into two parts: (a) $\tau \in I_\tau^1 = (0, \tau_M)$ and (b) $\tau \in I_\tau^2 = [\tau_M, \tau_2] \cup (\tau_2, +\infty)$. If $\tau \in I_\tau^1$, then according to Theorem 9.1 and Corollary 9.1 the set $\operatorname{Int}\Omega_h$ is a unique global attractor of model (2.2) under case (SC_2). Thus, we assume $\tau \in I_\tau^2$ in this subsection. That is, we have $\tau_M \leq \tau$ and in the following we consider two cases: (a) $\tau_M \leq \tau < b/p$ and (b) $\max\{\tau_M, b/p\} \leq \tau$.

Case (a): For case (a), denote the coordinate of point $Q_0 = (V_L, \frac{b}{p})$. Since $\tau < \frac{b}{p}$, we can cut off the segment $\overline{Q_0Q_1}$ on L_4 below Q_0 equal to τ. Then there must exist a trajectory (closed or non-closed) Γ_{Q_1} through the point $Q_1 = (V_L, \frac{p}{b} - \tau)$ which intersects with the line L_5 at two points $P_5^+ = ((1-\theta)V_L, y_5^+)$ and $P_4^+ = ((1-\theta)V_L, y_4^+)$, where

$$\Gamma_{Q_1}: \quad H(x,y) = b\ln\left(\frac{b}{p} - \tau\right) - p\left(\frac{b}{p} - \tau\right) - \frac{c}{\omega}\ln(1+\omega V_L) + \delta\ln(V_L) + qV_L. \tag{11.1}$$

Substituting $x = (1-\theta)V_L$ into the Γ_{Q_1} shows that y_4^+ and y_5^+ are the two roots of the following equation:

$$b\ln(y) - py = b\ln\left(\frac{b}{p} - \tau\right) - p\left(\frac{b}{p} - \tau\right) - A_h, \tag{11.2}$$

and solving the above equation with respect to y we have

$$\begin{aligned} y_4^+ &= -\frac{b}{p} W\left(-1, -\frac{p}{b}\left(\frac{b}{p}-\tau\right)e^{-\frac{p}{b}(\frac{b}{p}-\tau)-\frac{A_h}{b}}\right), \\ y_5^+ &= -\frac{b}{p} W\left(-\frac{p}{b}\left(\frac{b}{p}-\tau\right)e^{-\frac{p}{b}(\frac{b}{p}-\tau)-\frac{A_h}{b}}\right) \end{aligned} \tag{11.3}$$

for $\tau_M \le \tau < b/p$. Note that both y_4^+ and y_5^+ are well defined due to $A_h > 0$ for (SC_2). For the relations among y_4^+, y_5^+ and τ, we have the following results.

Lemma 11.1 *For* (SC_2), *if* $\tau_M \le \tau < b/p$, *then we have the following inequalities*:

$$y_4^+ - \frac{b}{p} > \frac{b}{p} - y_5^+ > \tau. \tag{11.4}$$

Proof It follows from Theorem 3.1 that we have $y_4^+ - \frac{b}{p} > \frac{b}{p} - y_5^+$. Thus, to prove the inequalities (11.4) we only need to show $\frac{b}{p} - y_5^+ > \tau$, which is equivalent to the following inequality:

$$\frac{b}{p} + \frac{b}{p} W\left(-\frac{p}{b}\left(\frac{b}{p}-\tau\right)e^{-\frac{p}{b}(\frac{b}{p}-\tau)-\frac{A_h}{b}}\right) > \tau. \tag{11.5}$$

According to the definition of the Lambert W function and its monotonicity, the inequality (11.5) becomes as follows:

$$\left(\frac{p\tau}{b}-1\right)e^{\frac{p\tau}{b}-1-\frac{A_h}{b}} > \left(\frac{p\tau}{b}-1\right)e^{\frac{p\tau}{b}-1},$$

which holds true due to $\tau < \frac{b}{p}$ and $A_h > 0$. □

Denote the region Ω_{Q_1} bounded by the trajectory Γ_{Q_1}, two line segments $\overline{P_1^+P_4^+}$ and $\overline{Q_0Q_1}$ and a piece of closed trajectory Γ_h, *i.e.* arc $\widehat{Q_0P_1^+}$. Then we have the following results.

Theorem 11.1 *For* (SC_2), *if* $\tau_M \le \tau < b/p$, *then the set* Ω_{Q_1} *is an attractor whose region of attraction is the basic phase set* $\mathcal{N}$, *as shown in Figure* 16. *Moreover, the unique order*-1 *limit cycle* $O_1 \subset \Omega_{Q_1}$ *if* $\tau_M < \tau < b/p$. *In particular, if* $\tau = \tau_M$, *then the arc* $\widehat{Q_0P_1^+}$ *becomes an order*-1 *periodic solution*.

Proof It follows from Lemma 11.1 that for (SC_2) and all $\tau_M \le \tau < b/p$ the three line segments $\overline{Q_0Q_1}$, $\overline{P_0^+P_4^+}$ and $\overline{P_0^+P_5^+}$ satisfy the following relations:

$$\tau = |\overline{Q_0Q_1}| < \left|\overline{P_0^+P_5^+}\right| < \left|\overline{P_0^+P_4^+}\right|,$$

where $|\cdot|$ denotes the length of line segment. This indicates that the point P_3^+ must lie below the point P_4^+, and consequently the region Ω_{Q_1} is an invariant set of model (2.2). By using methods similar to those used in Theorem 9.1 we can show that any trajectory initiating from the basic phase set $\mathcal{N}$ and out of the line segment $\overline{P_5^+P_4^+}$ will enter into the region Ω_{Q_1} after finite impulsive effects. Moreover, the unique fixed point y^* of the Poincaré map $\mathcal{P}$ is well defined with $y^* \in [Y_{\max}^h, \tau + \frac{b}{p})$ in this case, as shown in Table 3. Thus, all results in Theorem 11.1 are true. □

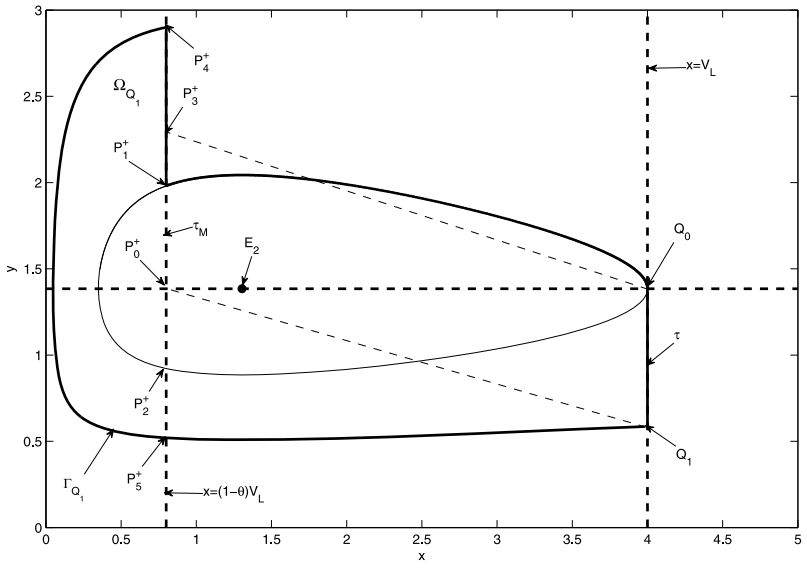

Figure 16 Attractor and its basin of attraction for case (SC_2) with $\tau_M \le \tau < b/p$. The parameter values are $b = 1.8$, $p = 1.3$, $c = 0.52$, $\omega = 0.1$, $q = 0.23$, $\delta = 0.3$, $\theta = 0.8$, $V_L = 4$, and $\tau = 0.7988$.

Remark 11.1 In Theorem 6.1 of [1], only the special case (*i.e.* $(1-\theta)V_L = x_2^*$) for model (2.3) has been proven. However, in Theorem 11.1 we have proved that the results for model (2.2) hold true for all $(1-\theta)V_L > x_4^*$ and of course hold true for model (2.3) under case (SC_2) and $\tau_M \le \tau < b/p$.

It follows from Figure 16 that a smaller attractor of model (2.2) under conditions of Theorem 11.1 may exist. Thus, we aim to find the smaller attractor in the following and its regions of attraction. Note that the coordinate of point $P_3^+ = ((1-\theta)V_L, b/p + \tau)$, and there exists a trajectory $\Gamma_{P_3^+}$ through the point P_3^+ which will intersect with the impulsive set at point Q_3 and $Q_3 = (V_L, y_3)$, where

$$\begin{aligned}\Gamma_{P_3^+}: \quad H(x,y) = {} & b\ln\left(\frac{b}{p}+\tau\right) - p\left(\frac{b}{p}+\tau\right) \\ & - \frac{c}{\omega}\ln\big(1+\omega(1-\theta)V_L\big) + \delta\ln\big((1-\theta)V_L\big) + q(1-\theta)V_L \end{aligned} \tag{11.6}$$

and y_3 is the smaller root of the following equation:

$$b\ln(y) - py = b\ln\left(\frac{b}{p}+\tau\right) - p\left(\frac{b}{p}+\tau\right) + A_h. \tag{11.7}$$

Solving the above equation with respect to y yields

$$y_3 = -\frac{b}{p}W\left(-\frac{p}{b}\left(\frac{b}{p}+\tau\right)e^{-\frac{p}{b}(\frac{b}{p}+\tau)+\frac{A_h}{b}}\right). \tag{11.8}$$

It is interesting to note that if there exists a $\tau \in (\tau_M, b/p)$ such that the equation

$$y_3 + \tau = Y_{\max}^h = -\frac{b}{p}W\big(-1, -e^{-1-\frac{A_h}{b}}\big) \tag{11.9}$$

holds, then for model (2.2) an order-2 limit cycle exists. Thus, we first address this.

Note that if we consider the y_3 as a function of τ, then we have

$$y_3(\tau_M) = -\frac{b}{p} W\left(-e^{-1-\frac{A_h}{b}} e^{\frac{A_h}{b}}\right) = \frac{b}{p},$$

which indicates that $y_3 + \tau = Y^h_{\max}$ at $\tau = \tau_M$. Thus, if there exists a $\tau \in (\tau_M, b/p)$ such that the above equation holds, then model (2.2) has an order-2 limit cycle. Taking the derivative of y_3 with respect to τ we can see that y_3 is monotonically decreasing for $\tau \in [\tau_M, b/p)$, where

$$\frac{dy_3}{d\tau} = \frac{p\tau}{b+p\tau} \frac{W(-\frac{p}{b}(\frac{b}{p}+\tau)e^{-\frac{p}{b}(\frac{b}{p}+\tau)+\frac{A_h}{b}})}{1+W(-\frac{p}{b}(\frac{b}{p}+\tau)e^{-\frac{p}{b}(\frac{b}{p}+\tau)+\frac{A_h}{b}})}. \tag{11.10}$$

Moreover, it is easy to see that $\frac{dy_3}{d\tau} < 1$ at $\tau = \tau_M$. These results show that for (11.9) there exists a positive root in the interval $\tau \in (\tau_M, b/p)$ provided $y_3(b/p) > Y^h_{\max} - \frac{b}{p} = \tau_M$, denoted by τ_2^*. Thus, we have the following result on the existence of an order-2 limit cycle.

Lemma 11.2 *For* (SC_2), *if* $\tau \in [\tau_M, b/p)$, *then there exists a* $\tau_2^* \in (\tau_M, b/p)$ *such that model* (2.2) *has an order-*2 *limit cycle provided* $y_3(b/p) > Y^h_{\max} - \frac{b}{p} = \tau_M$.

By using methods similar to those used in Theorem 11.1, we have the following results.

Theorem 11.2 *For* (SC_2), *if* τ_2^* *exists and* $\tau = \tau_2^*$, *then the set* Ω_{O_2} *bounded by the order-*2 *limit cycle and two line segments* $\overline{P_1^+P_3^+}$ *and* $\overline{Q_0Q_3}$ *and the set* Ω_{Q_0} *which is the interior of the closed curve* Γ_h *are two invariant sets. Moreover, the set* $\Omega_{O_2} \cup \Omega_{Q_0}$ *is an attractor whose region of attraction is basic phase set* $\mathcal{N}$, *as shown in Figure* 17.

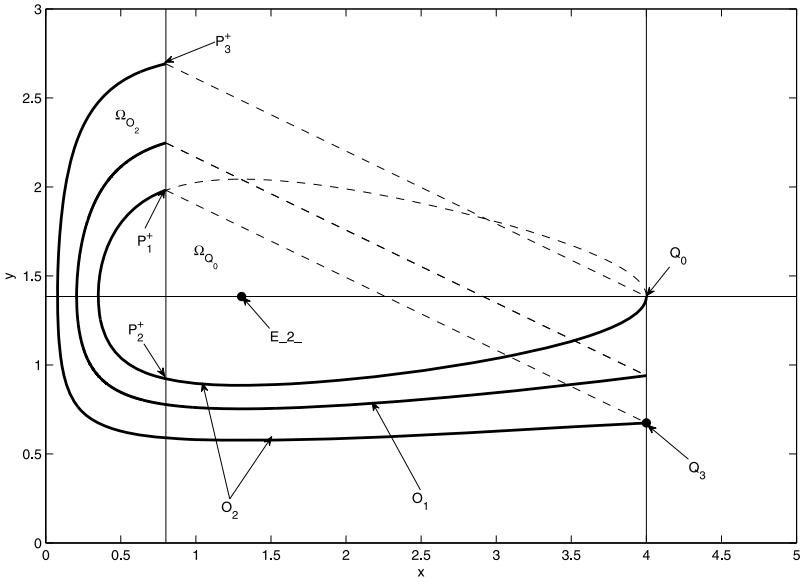

Figure 17 The existence of an order-2 limit cycle for case (SC_2) with $\tau_M \le \tau < b/p$. The parameter values are $b = 1.8$, $p = 1.3$, $c = 0.52$, $\omega = 0.1$, $q = 0.23$, $\delta = 0.3$, $\theta = 0.8$, $V_L = 4$, and $\tau_2^* = 1.307$.

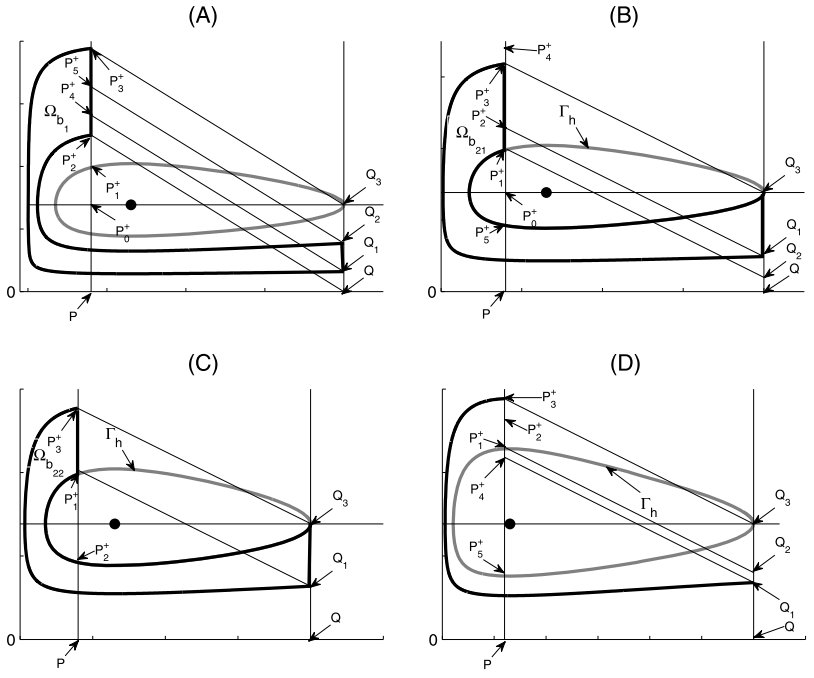

Figure 18 Positive invariant sets and attractors for case (b), *i.e.* $\max\{\tau_M, b/p\} \le \tau$.

Therefore, to address the existence of the attractor for cases (SC_2) with $\tau \in [\tau_M, b/p)$ (*i.e.* case (a)) completely, we need to discuss the following three subcases: (a_1) $y_3(b/p) > Y^h_{\max} - \frac{b}{p} = \tau_M$ and $\tau \in [\tau_M, \tau_2^*)$; ($a_2$) $y_3(b/p) > Y^h_{\max} - \frac{b}{p} = \tau_M$ and $\tau \in [\tau_2^*, b/p)$; (a_3) $y_3(b/p) < Y^h_{\max} - \frac{b}{p} = \tau_M$. By using the same methods as those in Theorem 11.1 the three subcases can be studied and the attractors and their regions of attraction can be obtained similarly, so we omit them here.

Case (b): $\max\{\tau_M, b/p\} \le \tau$.

To discuss the existence of the attractors and their regions of attraction, we consider the following two subcases: (b_1) $\max\{\tau_M, b/p, Y^h_{\max}\} \le \tau$; ($b_2$) $\max\{\tau_M, b/p\} \le \tau < Y^h_{\max}$.

For both subcases (b_1) and (b_2), we can take a point P_3^+ in the line L_5 (*i.e.* $x = (1-\theta)V_L$) with $|P_0^+P_3^+| = \tau$, and P_3^+ must lie above the point P_1^+ due to $\max\{\tau_M, b/p\} \le \tau$, as shown in Figure 18(A). Consider a trajectory through the point P_3^+. As t increases, the trajectory $\Gamma_{P_3^+}$ will intersect with the line L_4 (*i.e.* $x = V_L$) at point $Q_1 = (V_L, y_1)$, and the analytical formula for y_1 can easily be obtained according to the first integral and the Lambert W function. So for simplicity we do not provide the analytical formula for the coordinates of all points used here.

Therefore, for subcase (b_1), we can measure off $|PP_2^+|$ on L_5 equal to τ. There exists a trajectory through $P_2^+ = ((1-\theta)V_L, \tau)$ that intersects with the line L_4 at point $Q_2 = (V_L, y_2)$.

Since $Q_3 \in \mathcal{M}$, then $I(Q_3) = P_3^+ = ((1-\theta)V_L, \frac{b}{p} + \tau) \in \mathcal{N}_2^h$. Connect Q and P_2^+, Q_3 and P_3^+, draw the lines $\overline{Q_1P_4^+}$ and $\overline{Q_2P_5^+}$ such that

$$\overline{QP_2^+} \parallel \overline{Q_1P_4^+} \parallel \overline{Q_2P_5^+} \parallel \overline{Q_3P_3^+}. \tag{11.11}$$

Then we have

$$\begin{aligned}
&\overline{QQ_1} \subset M, \qquad I(\overline{QQ_1}) = \overline{P_2^+P_4^+} \subset \mathcal{N}_2^h,\\
&\overline{Q_1Q_2} \subset M, \qquad I(\overline{Q_1Q_2}) = \overline{P_4^+P_5^+} \subset \mathcal{N}_2^h,\\
&\overline{Q_2Q_3} \subset M, \qquad I(\overline{Q_2Q_3}) = \overline{P_5^+P_3^+} \subseteq \mathcal{N}_2^h.
\end{aligned} \tag{11.12}$$

Denote the horseshoe-like set Ω_{b_1} bounded by the two pieces of trajectories, *i.e.* arc $\widehat{P_3^+Q_1}$ and arc $\widehat{P_2^+Q_2}$, and two line segments $\overline{P_2^+P_3^+}$ and $\overline{Q_1Q_2}$, then Ω_{b_1} is a positive invariant set, as shown in Figure 18(A).

Note that any trajectory initiating from $\mathcal{N}_2^h$ either stays in the positive invariant Ω_{b_1} or jumps into it after a single impulsive effect. This implies that the horseshoe-like positive invariant set Ω_{b_1} is an attractor whose region of attraction is $\mathcal{N}_2^h$, as shown in Figure 18(A). Therefore, we have the following results for subcase (b_1).

Theorem 11.3 *For* (SC_2), *if* $\max\{\tau_M, b/p, Y_{\max}^h\} \le \tau$, *then the horseshoe-like positive invariant set* Ω_{b_1} *is an attractor whose region of attraction is the set* $\mathcal{N}_2^h$.

The interesting question arising here is what the interior structure of the horseshoe-like positive invariant set Ω_{b_1} is, and we have the following main results.

Theorem 11.4 *For* (SC_2), *assume that* $\max\{\tau_M, b/p, Y_{\max}^h\} \le \tau$. *Let* $\Pi_{z_0^+}(t)$ *be a trajectory of model* (2.2) *from the initial point* $z_0^+ = (x_0^+, y_0^+) \in \overline{P_2^+P_3^+} \subset \mathcal{N}_2^h$. *Then one of the following cases holds*:

(i) $\Pi_{z_0^+}$ *is an order-*1 *limit cycle*;
(ii) $\Pi_{z_0^+}$ *is an order-*2 *limit cycle*;
(iii) $\lim_{t\to\infty} \rho(\Pi_{z_0^+}(t) - O_1) = 0$;
(iv) $\lim_{t\to\infty} \rho(\Pi_{z_0^+}(t) - O_2) = 0$,

where O_i $(i = 1, 2)$ *denote the order-i limit cycles contained in the interior of horseshoe-like attractor* Ω_{b_1}.

Proof It follows from Theorem 11.3 that the set Ω_{b_1} is a positive invariant set. Moreover, the point $((1-\theta)V_L, y^*)$ must lie in the line segment $\overline{P_2^+P_3^+}$, and consequently the fixed point y^* of the Poincaré map $\mathcal{P}$ satisfies $y_2^+ < y^* < y_3^+$, where y_2^+ and y_3^+ are the vertical coordinates of two points P_2^+ and P_3^+. In fact, based on the Poincaré map $\mathcal{P}(y_k^+)$ we can define the following successor function:

$$d(s) = \mathcal{P}(s) - s, \quad s \in \mathcal{N}_2^h, \tag{11.13}$$

and it is easy to see that

$$d\big(y_3^+\big) = \mathcal{P}\big(y_3^+\big) - y_3^+ = y_4^+ - y_3^+ < 0, \qquad d\big(y_2^+\big) = \mathcal{P}\big(y_2^+\big) - y_2^+ = y_5^+ - y_2^+ > 0,$$

where y_4^+ and y_5^+ are the vertical coordinates of two points P_4^+ and P_5^+. This implies that there exists a point $P^* = ((1-\theta)V_L, y^{**})$ lying between P_2^+ and P_3^+ such that $d(y^{**}) = 0$ according to the continuity of the function $d(s)$ on the set $\mathcal{N}_2^h$. Thus, y^{**} is a fixed point of

the Poincaré map $\mathcal{P}$, and consequently we have $y^* = y^{**}$ due to the uniqueness of the fixed point. Therefore, the following inequalities:

$$y_2^+ < y_4^+ < y^* < y_5^+ < y_3^+$$

hold true.

Further, any solution initiating from the line segment $\overline{P_4^+P_5^+}$ will reach the line segment $\overline{Q_1Q_2}$, and then their phase points must lie in the interior of the line segment $\overline{P_4^+P_5^+}$. This means that the line segment $\overline{P_4^+P_5^+}$ is an attractor of the phase set $\mathcal{N}_2^h$ for case (b_1). Similarly, the vertical coordinates of the successor points P_6^+ and P_7^+ for two points P_4^+ and P_5^+ satisfy

$$y_2^+ < y_4^+ < y_6^+ < y^* < y_7^+ < y_5^+ < y_3^+.$$

By induction, we have

$$Y_{\max}^h < y_2^+ < \cdots < y_{2k}^+ < \cdots < y^* < \cdots < y_{2k+1}^+ < \cdots < y_5^+ < y_3^+ = \frac{b}{p} + \tau. \tag{11.14}$$

The inequalities (11.14) indicate that there exist two constants y_1^*, y_2^* such that

$$\lim_{k\to\infty} y_{2k+1} = y_1^* \geq y^*, \qquad \lim_{k\to\infty} y_{2k} = y_2^* \leq y^*. \tag{11.15}$$

Therefore, according to the uniqueness of y^* we have either $y_1^* = y^* = y_2^*$ or $y_1^* > y^* > y_2^*$. If the former case occurs, then the trajectory $\Pi_{z_0^+}(t)$ tends to the order-1 limit cycle; if the later case occurs, then the trajectory $\Pi_{z_0^+}(t)$ tends to an order-2 limit cycle. □

It follows from the relations discussed in Section 5.1 and the necessary conditions of the existence of an order-2 limit cycle discussed in Section 8.2 that we have the following results.

Corollary 11.1 *For* (SC_2), *if* $\max\{\tau_M, b/p, Y_{\max}^h\} \leq \tau \leq \tau_2$, *then the unique order-*2 *limit cycle of model* (2.2) *is globally stable with respect to the phase set* $\mathcal{N}_2^h$.

Proof It follows from Figure 6 and the relations discussed in Section 5.1 that if the conditions of Corollary 11.1 hold, then for (SC_2) the order-1 limit cycle is unstable. Thus, if the order-2 limit cycle is unique, then it follows from the proof of Theorem 11.4 that the results of Corollary 11.1 are true. □

Corollary 11.2 *For* (SC_2), *if* $\max\{\tau_M, b/p, Y_{\max}^h\} \leq \tau$ *and model* (2.2) *does not have any order-*2 *periodic solution* (*i.e.* $y_1^* = y_2^*$), *then the order-*1 *limit cycle is globally stable with respect to the phase set* $\mathcal{N}_2^h$.

For subcase (b_2), as shown in Figure 18(B)-(D), connect Q_3 and $P_3^+ = ((1-\theta)V_L, \frac{b}{p} + \tau)$, draw the line $\overline{P_1^+Q_2}$ such that $\overline{Q_3P_3^+} \parallel \overline{Q_2P_1^+}$. Then we have the following three possibilities:

(b_{21}): Q_1 lies above Q_2, as shown in Figure 18(B), where $Q_1 = (V_L, y_1)$ and $Q_2 = (V_L, Y_{\max}^h - \tau)$. Draw the line $\overline{Q_1P_2^+}$ such that

$$\overline{Q_3P_3^+} \parallel \overline{Q_1P_2^+} \parallel \overline{Q_2P_1^+}.$$

Then there exists a trajectory Γ_{Q_2} through Q_2 which intersects the vertical line L_5 at P_4^+ above P_3^+, and we have

$$\begin{aligned}
&\overline{Q_1Q_3} \subset M, \qquad I(\overline{Q_1Q_3}) = \overline{P_2^+P_3^+} \subseteq \mathcal{N}_2^h,\\
&\overline{Q_2Q_1} \subset M, \qquad I(\overline{Q_2Q_1}) = \overline{P_1^+P_2^+} \subseteq \mathcal{N}_2^h,\\
&\overline{QQ_2} \subset M, \qquad I(\overline{QQ_2}) \subset \overline{P_0^+P_1^+} \nsubseteq \mathcal{N}_2^h.
\end{aligned}$$

Denote the horseshoe-like set $\Omega_{b_{21}}$ bounded by the two sections of trajectories, *i.e.* arc $\widehat{P_3^+Q_1}$ and arc $\widehat{P_1^+Q_3}$, and two line segments $\overline{P_1^+P_3^+}$ and $\overline{Q_1Q_3}$, then $\Omega_{b_{21}}$ is a positive invariant set, as shown in Figure 18(B).

Note that any trajectory $\Pi_{z_0^+}(t)$ with z_0^+ lying in the line segment $\overline{P_3^+P_4^+}$ will jump into the horseshoe-like positive invariant set $\Omega_{b_{21}}$ after one impulsive effect, and any trajectory $\Pi_{z_0^+}(t)$ with initial point above the point P_4^+ will jump into the interior of closed curve Γ_h after one impulsive effect and then be free from impulsive effects.

(b_{22}): Q_1 coincides with Q_2, as shown in Figure 18(C). By the same method as subcase (b_{21}) we can show that the horseshoe-like set $\Omega_{b_{22}}$ is a positive invariant set whose boundary is an order-2 limit cycle or periodic solution. Moreover, no other trajectory enters into the interior of this invariant set from outside.

(b_{23}): Q_1 lies below Q_2, as shown in Figure 18(D). For this case, we cannot separate the attractors into two subsets as those shown in subcases (b_{21}) and (b_{22}).

The interior structures of the positive invariant sets $\Omega_{b_{21}}$ and $\Omega_{b_{22}}$ can be addressed and the results are the same as those shown in Theorem 11.4 can be obtained similarly. For more detailed analyses, please see reference [1].

11.2 Multiple attractors and their basins of attraction for (SC_{11}) and (SC_{12})

Based on the previous investigations, for the existence of multiple attractors of both (SC_{11}) and (SC_{12}) we only need to study cases when $\tau > \tau_2^{h_1}$, and then two subcases should be considered, *i.e.* $\tau_2^{h_1} < \tau \le b/p$ and $\max\{\tau_2^{h_1}, b/p\} < \tau$. Moreover, the latter case $\max\{\tau_2^{h_1}, b/p\} < \tau$ can be separated into two subcases: (c_1) $\max\{\tau_2^{h_1}, b/p, Y_{\max}^{h_1}\} < \tau$; ($c_2$) $\max\{\tau_2^{h_1}, b/p\} < \tau < Y_{\max}^{h_1}$. These can be investigated by using the same methods as those in Section 12, and similar results could be obtained, so we omit them here.

12 Discussion

In order to describe the human actions for real word applications such as pest or virus control and disease treatment, impulsive semi-dynamic systems can be used, which can provide a natural description for threshold control strategies. It is quite challenging to apply the qualitative theorems of impulsive semi-dynamic systems to investigate real life problems completely, although some special cases of model (2.2) (say $\omega = 0$ and $q = 0$) have been investigated [1, 4, 58]. In particular, the existence of an order-1 limit cycle and its local stability, and the non-existence of limit cycles with order no less than 3 have been studied. Moreover, the methods developed in [1, 4] have been used to investigate different models arising from several application domains including chemostat cultures [6, 43, 66], epidemiology [19, 30], and IPM strategies [72, 73]. But only very special cases such as any solution that experiences an infinite number of pulse actions have been addressed. That is, few modeling studies have been completed for all possible dynamics of models with state-dependent feedback control due to the complexity [1].

Therefore, a commonly used mathematical model with state-dependent feedback control has been proposed and analyzed here by employing the definition and properties of impulsive semi-dynamical systems. The main purpose was to develop novel analytical techniques and to provide comprehensive qualitative analyses for all possible dynamics on the whole parameter space, of particular interest being the effects of the key parameters related to integrated control tactics on the dynamic behavior.

To achieve our aims, we employed the definition of the Lambert W function and its properties and the first integral of ODE model (3.1). The exact analytical formula of the Poincaré map determined by the impulsive point series in the phase set and its domain for each case has been provided. The key points are: (i) The impulsive set and phase set have been analyzed and determined firstly on different parameter spaces, please see Table 1 for details; (ii) The effects of key parameters θ, τ and V_L on the signs of A_h and A_{h_1}, and consequently on the domains of the Poincaré map have been completely addressed, as shown in Table 2; (iii) The different parameter spaces for the existence, uniqueness and local stability of the order-1 limit cycle have been provided completely, as shown in Table 3. We realize that the above three points are the basis for solving all of the dynamic behavior of model (2.2).

Based on different parameter spaces defined in Table 3, the proof of the global stability of the order-1 limit cycle with respect to the basic phase set is possible, and our results show that the local stability of an order-1 limit cycle indicates the global stability for case (SC_{123}). In particular, the sufficient conditions for the global stability of the boundary order-1 limit cycle have been obtained for the first time, which can be used to compare the efficiency of a single control tactic alone with the efficiency of more than one integrated control measure. Further, the existence of an order-2 limit cycle can be determined by the flip bifurcation. Although it is hard to find generalized conditions for the existence of an order-2 limit cycle, the necessary conditions for the existence of an order-2 limit cycle have been investigated in more detail, which can be used to address the non-existence of an order-2 limit cycle. Moreover, the sufficient conditions for any trajectory initiating from the phase set which will be free from impulsive effects after finite state-dependent feedback control actions were studied, and the results show that the order-k ($k \geq 3$) limit cycle does not exist and so one open problem in reference [1] has been solved here. Finally, multiple attractors and their basins of attraction and the interior structure of horseshoe-like attractors have been investigated.

Compared with the previous studies mentioned in the introduction, we can see that the innovative analytical techniques developed in this paper are as follows: (i) Exact domains for impulsive and phase sets; (ii) The definition of the Poincaré map in the phase set; (iii) Methods for proving the global stability of the order-1 limit cycle including the boundary order-1 limit cycle; (iv) The necessary condition for the existence of an order-2 limit cycle; (v) Finite state-dependent feedback control actions for all cases have been addressed; (vi) The non-existence of limit cycles with order no less than 3 has been shown. We believe that these methods could easily be employed to study more generalized models with state-dependent feedback control.

The models with state-dependent feedback control cannot only provide natural descriptions of real life problems, but can also result in the rich dynamics of models. Our results have provided some fundamental theoretical conclusions that could be of applied impor-

tance to real life problems. For instance, under some conditions any solution of our main model (2.2) will jump into a positive invariant set and then stabilize with an order 1 or order 2 limit cycle or become free from impulsive effects. At this stage, the system becomes inert with respect to further impulsive effects and so, in theory, the control purposes can be successfully achieved by a sequence of one, two or a few impulsive actions or, alternatively, by periodic interventions. Note that the analytical formula for the period can be calculated based on the initial values by employing the same methods as those used in [2].

Although it is reasonable to assume that the carrying capacity of the pest population could be infinity due to the threshold level considered in the model being quite small compared with the carrying capacity, the disadvantages of this work are: (i) the Lambert W function and its properties are needed for defining the Poincaré map; and (ii) the first integral of the ODE model plays a key role in most of the results. Therefore, if the carrying capacity is a constant rather than $+\infty$, then the first integral of the generalized model does not exist any more, and consequently the Lambert W function cannot be used. Thus, the question is how to extend all analytical techniques developed in this paper to investigate more generalized models with state-dependent feedback control. For our near future work, we will focus on model (2.2) with a constant carrying capacity and different releasing strategies and other models arising from different application fields.

Appendix: Some important definitions

Definition A.1 The Lambert W function is defined to be a multivalued inverse of the function $z \mapsto ze^z$ satisfying

$$\text{Lambert W}(z)\exp\big(\text{Lambert W}(z)\big) = z.$$

For simplicity, we denote it by W. Note that if $z > -1$ then the function $z\exp(z)$ has the positive derivative $(z+1)\exp(z)$. Define the inverse function of $z\exp(z)$ restricted on the interval $[-1,\infty)$ to be $W(0,z) \doteq W(z)$. Similarly, we define the inverse function of $z\exp(z)$ restricted on the interval $(-\infty,-1]$ to be $W(-1,z)$, the two real branches of the Lambert W function, $W(z)$, $W(-1,z)$ and their domains. The branch $W(z)$ is defined on the interval $[-e^{-1},+\infty)$ and it is a monotonically increasing function with respect to z, while the branch $W(-1,z)$ is defined on the interval $[-e^{-1},0)$ and it is a monotonically decreasing function with respect to z. Note that both branches are defined in the common interval $[-e^{-1},0)$ with $W(z) > W(-1,z)$ for $z \in (-e^{-1},0)$, $W(-e^{-1}) = W(-1,-e^{-1}) = -1$ and $W(e) = 1$, as shown in Figure 19.

Planar impulsive semi-dynamical systems and preliminaries. The generalized planar impulsive semi-dynamical systems with state-dependent feedback control can be described as follows:

$$\begin{cases} \left.\begin{aligned} \tfrac{dx(t)}{dt} &= P(x,y),\\ \tfrac{dy(t)}{dt} &= Q(x,y), \end{aligned}\right\} & (x,y) \notin \mathcal{M},\\ \left.\begin{aligned} x^+ &= x + I_1(x,y),\\ y^+ &= y + I_2(x,y), \end{aligned}\right\} & (x,y) \in \mathcal{M}, \end{cases} \tag{A.1}$$

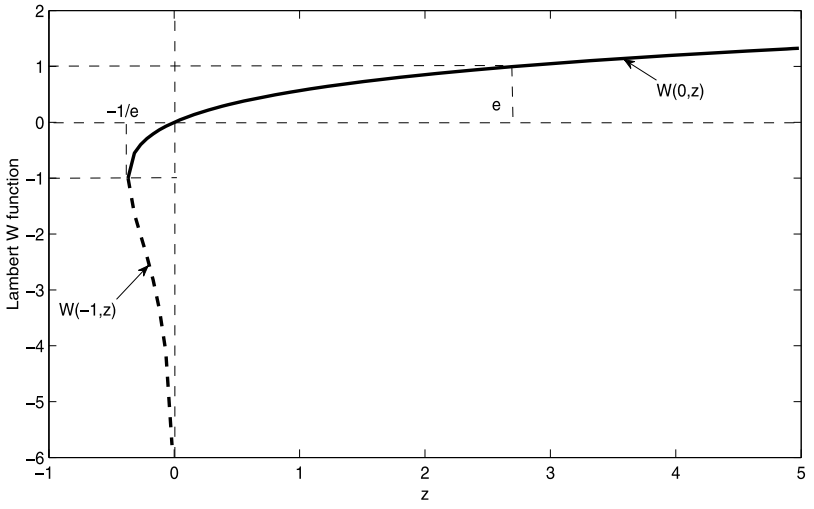

Figure 19 The two real branches of the Lambert W function, $W(0,z)$ and $W(-1,z)$, and their domains.

where $(x,y) \in R^2$, and P, Q, I_1, I_2 are continuous functions from R^2 into R, $\mathcal{M} \subset R^2$ denotes the impulsive set. For each point $z(x,y) \in \mathcal{M}$, the map $I : R^2 \to R^2$ is defined by

$$I(z) = z^+ = \left(x^+, y^+\right) \in R^2, \quad x^+ = x + I_1(x,y), y^+ = y + I_2(x,y),$$

and z^+ is called an impulsive point of z.

Let $\mathcal{N} = I(\mathcal{M})$ be the phase set (*i.e.* for any $z \in \mathcal{M}$, $I(z) = z^+ \in \mathcal{N}$), and $\mathcal{N} \cap \mathcal{M} = \emptyset$. System (A.1) is generally known as a planar impulsive semi-dynamical system. We note that system (2.2) is an impulsive semi-dynamical system, where impulsive set $\mathcal{M} = \{(x,y) \in R_+^2 | x = V_L, 0 \le y \le \frac{b}{p}\}$ is a closed subset of R_+^2 and continuous function $I : (V_L, y) \in \mathcal{M} \to (x^+, y^+) = ((1-\theta)V_L, y+\tau) \in R_+^2$. It follows that the phase set $\mathcal{N} = I(\mathcal{M}) = \{(x^+, y^+) \in R_+^2 | x^+ = (1-\theta)V_L, y^+ \in Y_D\}$ with $Y_D = [\tau, \frac{b}{p} + \tau]$. Unless otherwise specified in the following we assume the initial point $(x_0^+, y_0^+) \in \mathcal{N}$. In the present work we call $\mathcal{M}$ and $\mathcal{N}$ the basic impulsive set and the phase set of model (2.2), respectively.

In the following we briefly list some definitions related to impulsive semi-dynamical systems, which are used in this work.

Let (X, Π, R_+) or (X, Π) be a semi-dynamical system [101, 102], where X is a metric space, R_+ is the set of all non-negative reals. For any $z \in X$, the function $\Pi_z : R_+ \to X$ defined by $\Pi_z(t) = \Pi(z,t)$ is clearly continuous such that $\Pi(z,0) = z$ for all $z \in X$, and $\Pi(\Pi(z,t),s) = \Pi(z,t+s)$ for all $z \in X$ and $t, s \in R_+$. The set

$$C^+(z) = \left\{\Pi(z,t) | t \in R_+\right\}$$

is called the positive orbit of z. For any set $M \subset X$, let

$$M^+(z) = C^+(z) \cap M - \{z\} \quad \text{and} \quad M^-(z) = G(z) \cap M - \{z\},$$

where

$$G(z) = \cup\left\{G(z,t) | t \in R_+\right\} \quad \text{and} \quad G(z,t) = \left\{w \in X | \Pi(w,t) = z\right\}$$

is the attainable set of z at $t \in R_+$. Finally, we set $M(z) = M^+(z) \cup M^-(z)$. Before discussing the dynamical behavior of system (3.1), we need the following definitions and lemmas [52, 53, 55, 103–105].

Definition A.2 An impulsive semi-dynamical system $(X, \Pi; M, I)$ consists of a continuous semi-dynamical system (X, Π) together with a nonempty closed subset M (or impulsive set) of X and a continuous function $I : M \to X$ such that the following property holds:

(i) No point $z \in X$ is a limit point of $M(z)$,

(ii) $\{t | G(z,t) \cap M \neq \emptyset\}$ is a closed subset of R_+.

Throughout the paper, we denote the points of discontinuity of Π_z by $\{z_n^+\}$ and call z_n^+ an impulsive point of z_n.

We define a function Φ from X into the extended positive reals $R_+ \cup \{\infty\}$ as follows: let $z \in X$, if $M^+(z) = \emptyset$ we set $\Phi(z) = \infty$, otherwise $M^+(z) \neq \emptyset$ and we set $\Phi(z) = s$, where $\Pi(x,t) \notin M$ for $0 < t < s$ but $\Pi(z,s) \in M$.

Definition A.3 A trajectory Π_z in (X, Π, M, I) is said to be periodic of period T_k and order k if there exist non-negative integers $m \geq 0$ and $k \geq 1$ such that k is the smallest integer for which $z_m^+ = z_{m+k}^+$ and $T_k = \sum_{i=m}^{m+k-1} \Phi(z_i) = \sum_{i=m}^{m+k-1} s_i$.

For simplicity, we denote a periodic trajectory of period T_k and order k by an order-k periodic solution. An order-k periodic solution is called an order-k limit cycle if it is isolated.

For more details of the concepts and properties of continuous dynamical systems and impulsive dynamical systems; see [52, 64, 101, 102, 106].

Lemma A.1 (Analog of Poincaré criterion [107]) *The order-k limit cycle* $x = \xi(t)$, $y = \eta(t)$ *of system*

$$\begin{cases} \frac{dx}{dt} = P(x,y), & \frac{dy}{dt} = Q(x,y) \quad \text{if } \phi(x,y) \neq 0, \\ \triangle x = a(x,y), & \triangle y = b(x,y) \quad \text{if } \phi(x,y) = 0 \end{cases}$$

is orbitally asymptotically stable and enjoys the property of asymptotic phase if the multiplier μ_2 *satisfies the condition* $|\mu_2| < 1$. *Here*

$$\mu_2 = \prod_{k=1}^{q} \triangle_k \exp\left[\int_0^T \left(\frac{\partial P}{\partial x}\big(\xi(t), \eta(t)\big) + \frac{\partial Q}{\partial y}\big(\xi(t), \eta(t)\big)\right) dt\right],$$

$$\triangle_k = \frac{P_+(\frac{\partial b}{\partial y}\frac{\partial \phi}{\partial x} - \frac{\partial b}{\partial x}\frac{\partial \phi}{\partial y} + \frac{\partial \phi}{\partial x}) + Q_+(\frac{\partial a}{\partial x}\frac{\partial \phi}{\partial y} - \frac{\partial a}{\partial y}\frac{\partial \phi}{\partial x} + \frac{\partial \phi}{\partial y})}{P\frac{\partial \phi}{\partial x} + Q\frac{\partial \phi}{\partial y}},$$

and P, Q, $\frac{\partial a}{\partial x}$, $\frac{\partial a}{\partial y}$, $\frac{\partial b}{\partial x}$, $\frac{\partial b}{\partial y}$, $\frac{\partial \phi}{\partial x}$, $\frac{\partial \phi}{\partial y}$ *are calculated at the point* $(\xi(\tau_k), \eta(\tau_k))$ *and* $P_+ = P(\xi(\tau_k^+), \eta(\tau_k^+))$, $Q_+ = Q(\xi(\tau_k^+), \eta(\tau_k^+))$.

Lemma A.2 (Supercritical flip bifurcation [108]) *Let* $G : U \times I \to R$ *define a one-parameter family of maps, where* G *is* C^r *with* $r \geq 3$, *and* U, I *are open intervals containing* 0. *Assume*

(1) $G(0,\alpha) = 0$ *for all* α;
(2) $\frac{\partial G}{\partial x}(0,0) = -1$;
(3) $\frac{\partial^2 G}{\partial x\,\partial \alpha}(0,0) < 0$;
(4) $\frac{\partial^3 G^2}{\partial x^3}(0,0) < 0$.

Then there are $\alpha_1 < 0 < \alpha_2$ *and* $\epsilon > 0$ *such that*:

(i) *If* $\alpha_1 < \alpha \leq 0$, *then* G_α *has a unique fixed point at the origin, and no orbit of period two in* $(-\epsilon,\epsilon)$. *The fixed point is asymptotically stable.*

(ii) *If* $0 < \alpha < \alpha_2$, *then* G_α *has a unique fixed point at the origin, and a unique orbit of period two in* $(-\epsilon,\epsilon)$. *The fixed point is unstable and the orbit of period two is asymptotically stable.*

Lemma A.3 (Subcritical flip bifurcation [108]) *Replace the inequality* (4) *in Lemma* A.2 *by* $\frac{\partial^3 G^2}{\partial x^3}(0,0) > 0$. *Then there exist* $\alpha_1 < 0 < \alpha_2$ *and* $\epsilon > 0$ *such that*:

(i) *If* $\alpha_1 < \alpha < 0$, *then* G_α *has a unique fixed point at the origin, and a unique orbit of period two in* $(-\epsilon,\epsilon)$. *The fixed point is asymptotically stable and the orbit of period two is unstable.*

(ii) *If* $0 \leq \alpha < \alpha_2$, *then* G_α *has a unique fixed point at the origin, and no orbit of period two in* $(-\epsilon,\epsilon)$. *The fixed point is unstable.*

Competing interests
The authors declare that they have no competing interests.

Authors' contributions
ST and WP designed the study and carried out the analysis. ST, WP, RC, and JW contributed to writing the paper. ST performed numerical simulations. All authors read and approved the final manuscript.

Author details
[1]School of Mathematics and Information Science, Shaanxi Normal University, Xi'an, 710062, P.R. China. [2]Natural Resources Institute, University of Greenwich at Medway, Central Avenue, Chatham Maritime, Chatham, Kent ME4 4TB, UK. [3]Centre for Disease Modelling, York University, Toronto, Ontario M3J 1P3, Canada.

Acknowledgements
We would like to thank Prof. Chengzhi Li for helping us to prove Theorem 3.1 that greatly improved the presentation of this paper. This work was partially supported by the National Natural Science Foundation of China (NSFCs 1171199, 11471201), and by the Fundamental Research Funds for the Central Universities (GK201003001, GK201401004).

Received: 6 February 2015 Accepted: 7 October 2015 Published online: 16 October 2015

References

1. Tang, SY, Cheke, RA: State-dependent impulsive models of integrated pest management (IPM) strategies and their dynamic consequences. J. Math. Biol. **50**, 257-292 (2005)
2. Tang, SY, Chen, LS: Modelling and analysis of integrated pest management strategy. Discrete Contin. Dyn. Syst., Ser. B **4**, 759-768 (2004)
3. Tang, SY, Xiao, YN, Cheke, RA: Multiple attractors of host-parasitoid models with integrated pest management strategies: eradication, persistence and outbreak. Theor. Popul. Biol. **73**, 181-197 (2008)
4. Tang, SY, Xiao, YN, Chen, LS, Cheke, RA: Integrated pest management models and their dynamical behaviour. Bull. Math. Biol. **67**, 115-135 (2005)
5. Liang, JH, Tang, SY, Nieto, JJ, Cheke, RA: Analytical methods for detecting pesticide switches with evolution of pesticide resistance. Math. Biosci. **245**, 249-257 (2013)
6. Nie, LF, Teng, ZD, Hu, L: The dynamics of a chemostat model with state dependent impulsive effects. Int. J. Bifurc. Chaos **21**, 1311-1322 (2011)
7. Tang, SY, Cheke, RA: Models for integrated pest control and their biological implications. Math. Biosci. **215**, 115-125 (2008)
8. Tang, SY, Liang, JH, Tan, YS, Cheke, RA: Threshold conditions for interated pest management models with pesticides that have residual effects. J. Math. Biol. **66**, 1-35 (2013)
9. Tang, SY, Tang, GY, Cheke, RA: Optimum timing for integrated pest management: modelling rates of pesticide application and natural enemy releases. J. Theor. Biol. **264**, 623-638 (2010)
10. Wei, CJ, Zhang, SW, Chen, LS: Impulsive state feedback control of cheese whey fermentation for single-cell protein production. J. Appl. Math. **2013**, Article ID 354095 (2013)
11. Lou, J, Lou, YJ, Wu, JH: Threshold virus dynamics with impulsive antiretroviral drug effects. J. Math. Biol. **65**, 623-652 (2012)

12. Maggioloa, F, Airoldia, M, Callegaro, A, et al.: CD4 cell-guided scheduled treatment interruptions in HIV-infected patients with sustained immunologic response to HAART. AIDS **23**, 799-807 (2009)
13. Miron, RE, Smith, RJ: Modelling imperfect adherence to HIV induction therapy. BMC Infect. Dis. **10**, 6 (2010)
14. Smith RJ: Adherence to antiretroviral HIV drugs: how many doses can you miss before resistance emerges? Proc. R. Soc. Lond. B, Biol. Sci. **273**, 617-624 (2006)
15. Smith RJ, Schwartz, EJ: Predicting the potential impact of a cytotoxic *T*-lymphocyte HIV vaccine: how often should you vaccinate and how strong should the vaccine be? Math. Biosci. **212**, 180-187 (2008)
16. Smith RJ, Wahl, LM: Distinct effects of protease and reverse transcriptase inhibition in an immunological model of HIV-1 infection with impulsive drug effects. Bull. Math. Biol. **66**, 1259-1283 (2004)
17. Yang, YP, Xiao, YN: Threshold dynamics for compartmental epidemic models with impulses. Nonlinear Anal., Real World Appl. **13**, 224-234 (2012)
18. Cappuccio, A, Castiglione, F, Piccoli, B: Determination of the optimal therapeutic protocols in cancer immunotherapy. Math. Biosci. **209**, 1-13 (2007)
19. Huang, MZ, Li, JX, Song, XY, Guo, HJ: Modeling impulsive injections of insulin: towards artificial pancreas. SIAM J. Appl. Math. **72**, 1524-1548 (2012)
20. Panetta, JC, Adam, J: A mathematical model of cycle-specific chemotherapy. Math. Comput. Model. **22**, 67-82 (1995)
21. Tang, SY, Xiao, YN: One-compartment model with Michaelis-Menten elimination kinetics and therapeutic window: an analytical approach. J. Pharmacokinet. Biopharm. **34**, 807-827 (2007)
22. Tolic, IM, Mosekilde, E, Sturis, J: Modeling the insulin-glucose feedback system: the significance of pulsatile insulin secretion. J. Theor. Biol. **207**, 361-375 (2000)
23. Agur, Z, Cojocaru, L, Mazor, G, Anderson, RM, Danon, YL: Pulse mass measles vaccination across age cohorts. Proc. Natl. Acad. Sci. USA **90**, 11698-11702 (1993)
24. Choisy, M, Guégan, JF, Rohani, P: Dynamics of infectious diseases and pulse vaccination: teasing apart the embedded resonance effects. Physica D **223**, 26-35 (2006)
25. d'Onofrio, A: Stability properties of pulse vaccination strategy in SEIR epidemic model. Math. Biosci. **179**, 57-72 (2002)
26. Lu, ZH, Chi, XB, Chen, LS: The effect of constant and pulse vaccination on SIR epidemic model with horizontal and vertical transmission. Math. Comput. Model. **36**, 1039-1057 (2002)
27. Fishman, S, Marcus, R: A model for spread of plant disease with periodic removals. J. Math. Biol. **21**, 149-158 (1984)
28. Shulgin, B, Stone, L, Agur, Z: Pulse vaccination strategy in the SIR epidemic model. Bull. Math. Biol. **60**, 1123-1148 (1998)
29. Stone, L, Shulgin, B, Agur, Z: Theoretical examination of the pulse vaccination policy in the SIR epidemic model. Math. Comput. Model. **31**, 207-215 (2000)
30. Tang, SY, Xiao, YN, Cheke, RA: Dynamical analysis of plant disease models with cultural control strategies and economic thresholds. Math. Comput. Simul. **80**, 894-921 (2010)
31. Tang, SY, Xiao, YN, Clancy, D: New modelling approach concerning integrated disease control and cost-effectivity. Nonlinear Anal., Theory Methods Appl. **63**, 439-471 (2005)
32. Terry, AJ: Pulse vaccination strategies in a metapopulation SIR model. Math. Biosci. Eng. **7**, 455-477 (2010)
33. Chacron, MJ, Pakdaman, K, Longtin, A: Interspike interval correlations, memory, adaptation, and refractoriness in a leaky integrate and fire model with threshold fatigue. Neural Comput. **15**, 253-278 (2003)
34. Ermentrout, GB, Kopell, N: Multiple pulse interactions and averaging in systems of coupled neural oscillators. J. Math. Biol. **29**, 195-217 (1991)
35. FitzHugh, R: Impulses and physiological states in theoretical models of nerve membrane. Biophys. J. **1**, 445-466 (1961)
36. Goel, P, Ermentrout, B: Synchrony, stability, and firing patterns in pulse-coupled oscillators. Physica D **163**, 191-216 (2002)
37. Hindmarsh, JL, Rose, RM: A model of the nerve impulse using two first-order differential equations. Nature **296**, 162-164 (1982)
38. Izhikevich, EM: Class 1 neural excitability, conventional synapses, weakly connected networks, and mathematical foundations of pulse-coupled models. IEEE Trans. Neural Netw. **10**, 499-507 (1999)
39. Mirollo, RE, Strogatz, SH: Synchronization of pulse-coupled biological oscillators. SIAM J. Appl. Math. **50**, 1645-1662 (1990)
40. Nagumo, J, Arimoto, S, Yoshizawa, S: An active pulse transmission line simulating nerve axon. Proc. IRE **50**, 2061-2070 (1962)
41. d'Onofrio, A: On pulse vaccination strategy in the SIR epidemic model with vertical transmission. Appl. Math. Lett. **18**, 729-732 (2005)
42. Gao, SJ, Chen, LS, Teng, ZD: Impulsive vaccination of an SEIRS model with time delay and varying total population size. Bull. Math. Biol. **69**, 731-745 (2007)
43. Sun, KB, Tian, Y, Chen, LS, Kasperski, A: Nonlinear modelling of a synchronized chemostat with impulsive state feedback control. Math. Comput. Model. **52**, 227-240 (2010)
44. Van Lenteren, JC: Integrated pest management in protected crops. In: Integrated Pest Management. Chapman & Hall, London (1995)
45. Van Lenteren, JC, Woets, J: Biological and integrated pest control in greenhouses. Annu. Rev. Entomol. **33**, 239-250 (1988)
46. Jarad, F, Abdeljawad, T, Baleanu, D: Higher order fractional variational optimal control problems with delayed arguments. Appl. Math. Comput. **218**, 9234-9240 (2012)
47. Mobayen, S: Robust tracking controller for multivariable delayed systems with input saturation via composite nonlinear feedback. Nonlinear Dyn. **76**, 827-838 (2014)
48. Mobayen, S: An LMI-based robust tracker for uncertain linear systems with multiple time-varying delays using optimal composite nonlinear feedback technique. Nonlinear Dyn. **80**, 917-927 (2015)
49. Doha, EH, Bhrawy, AH, Baleanu, D, et al.: An efficient numerical scheme based on the shifted orthonormal Jacobi polynomials for solving fractional optimal control problems. Adv. Differ. Equ. **2015**, Article ID 15 (2015). doi:10.1186/s13662-014-0344-z

50. Bainov, DD, Simeonov, PS: Systems with Impulsive Effect: Stability, Theory and Applications. Wiley, New York (1989)
51. Benchohra, M, Henderson, J, Ntouyas, S: Impulsive Differential Equations and Inclusions. Hindawi Publishing Corporation, New York (2006)
52. Kaul, SK: On impulsive semidynamical systems. J. Math. Anal. Appl. **150**, 120-128 (1990)
53. Kaul, SK: On impulsive semidynamical systems III: Lyapunov stability. In: Recent Trends in Differential Equations. World Scientific Series in Applicable Analysis, vol. 1, pp. 335-345. World Scientific, River Edge (1992)
54. Kaul, SK: Stability and asymptotic stability in impulsive semidynamical systems. J. Appl. Math. Stoch. Anal. **7**, 509-523 (1994)
55. Lakshmikantham, V, Bainov, DD, Simeonov, PS: Theory of Impulsive Differential Equations. Series in Modern Mathematics. World Scientific, Singapore (1989)
56. Melin, J: Does distribution theory contain means for extending Poincaré-Bendixson theory. J. Math. Anal. Appl. **303**, 81-89 (2004)
57. Qi, JG, Fu, XL: Existence of limit cycles of impulsive differential equations with impulses as variable times. Nonlinear Anal., Theory Methods Appl. **44**, 345-353 (2011)
58. Zeng, GZ, Chen, LS, Sun, LH: Existence of periodic solution of order one of planar impulsive autonomous system. J. Comput. Appl. Math. **186**, 466-481 (2006)
59. Bonotto, EM: Flows of characteristic 0^+ in impulsive semidynamical systems. J. Math. Anal. Appl. **332**, 81-96 (2007)
60. Bonotto, EM, Federson, M: Limit sets and the Poincaré-Bendixson theorem in impulsive semidynamical systems. J. Differ. Equ. **244**, 2334-2349 (2008)
61. Bonotto, EM, Federson, M: Topological conjugation and asymptotic stability in impulsive semidynamical systems. J. Math. Anal. Appl. **326**, 869-881 (2007)
62. Bonotto, EM, Grulha, NG Jr: Lyapunov stability of closed sets in impulsive semidynamical systems. Electron. J. Differ. Equ. **2010**, 78 (2010)
63. Chellaboina, VS, Bhat, SP, Haddad, WM: An invariance principle for nonlinear hybrid and impulsive dynamical systems. Nonlinear Anal., Theory Methods Appl. **53**, 527-550 (2003)
64. Matveev, AS, Savkin, AV: Qualitative Theory of Hybrid Dynamical Systems. Birkhäuser, Cambridge (2000)
65. Bonotto, EM: LaSalle's theorems in impulsive semidynamical systems. Nonlinear Anal., Theory Methods Appl. **71**, 2291-2297 (2009)
66. Tian, Y, Sun, KB, Kasperski, A, Chen, LS: Nonlinear modelling and qualitative analysis of a real chemostat with pulse feeding. Discrete Dyn. Nat. Soc. **2010**, Article ID 640594 (2010)
67. Meng, XZ, Li, ZQ: The dynamics of plant disease models with continuous and impulsive cultural control strategies. J. Theor. Biol. **266**, 29-40 (2010)
68. Chen, LS: Pest control and geometric theory of semi-dynamical systems. J. Beihua Univ. Nat. Sci. **12**, 1-9 (2011)
69. Jiang, GR, Lu, QS, Qian, LN: Complex dynamics of a Holling type II prey-predator system with state feedback control. Chaos Solitons Fractals **31**, 448-461 (2007)
70. Li, YF, Xie, DL, Cui, A: Complex dynamics of a predator-prey model with impulsive state feedback control. Appl. Math. Comput. **230**, 395-405 (2014)
71. Nie, LF, Peng, JG, Teng, ZD, Hu, L: Existence and stability of periodic solution of a Lotka-Volterra predator-prey model with state-dependent impulsive effects. J. Comput. Appl. Math. **224**, 544-555 (2009)
72. Tian, Y, Sun, KB, Chen, LS: Modelling and qualitative analysis of a predator-prey system with state-dependent impulsive effects. Math. Comput. Simul. **82**, 318-331 (2011)
73. Wei, CJ, Chen, LS: Periodic solution of prey-predator model with Beddington-DeAngelis functional response and impulsive state feedback control. J. Appl. Math. **2012**, Article ID 607105 (2012)
74. Pedigo, LP, Higley, LG: A new perspective of the economic injury level concept and environmental quality. Am. Entomol. **38**, 12-20 (1992)
75. Bunimovich-Mendrazitsky, S, Byrne, H, Stone, L: Mathematical model of pulsed immunotherapy for superficial bladder cancer. Bull. Math. Biol. **70**, 2055-2076 (2008)
76. Bunimovich-Mendrazitsky, S, Claude Gluckman, J, Chaskalovic, J: A mathematical model of combined bacillus Calmette-Guerin (BCG) and interleukin (IL)-2 immunotherapy of superficial bladder cancer. J. Theor. Biol. **277**, 27-40 (2011)
77. Panetta, JC: A mathematical model of periodically pulsed chemotherapy: tumor recurrence and metastasis in a competitive environment. Bull. Math. Biol. **58**, 425-447 (1996)
78. Wei, HC: A numerical study of a mathematical model of pulsed immunotherapy for superficial bladder cancer. Jpn. J. Ind. Appl. Math. **30**, 441-452 (2013)
79. Wei, HC, Hwang, SF, Lin, JT, Chen, TJ: The role of initial tumor biomass size in a mathematical model of periodically pulsed chemotherapy. Comput. Math. Appl. **61**, 3117-3127 (2011)
80. Wei, HC, Lin, JT: Periodically pulsed immunotherapy in a mathematical model of tumor-immune interaction. Int. J. Bifurc. Chaos **23**, 1-13 (2013)
81. Staccato Study Group, Swiss HIV Cohort Study: CD4 guided scheduled treatment interruption compared to continuous therapy: results of the staccato trial. Lancet **368**, 459-465 (2006)
82. El-Sadr, WM, Lundgren, JD, Neaton, JD: $CD4^+$ count-guided interruption of antiretroviral treatment. The strategies for management of antiretroviral therapy (SMART) study group. N. Engl. J. Med. **355**, 2283-2296 (2006)
83. Mailleret, L, Lemesle, V: A note on semi-discrete modelling in the life sciences. Philos. Trans. R. Soc. A, Math. Phys. Eng. Sci. **367**, 4779-4799 (2009)
84. Tang, SY, Xiao, YN, Wang, N, Wu, HL: Piecewise HIV virus dynamic model with $CD4^+$ *T* cell count guided therapy: I. J. Theor. Biol. **308**, 123-134 (2012)
85. Fleming, GF, Meropol, NJ, Rosner, GL, et al.: A phase I trial of escalating doses of trastuzumab combined with daily subcutaneous interleukin 2: report of cancer and leukemia group B 9661. Clin. Cancer Res. **8**, 3718-3727 (2002)
86. INSIGHT-ESPRIT Study Group, SILCAAT Scientific Committee: Interleukin-2 therapy in patients with HIV infection. N. Engl. J. Med. **361**, 1549-1559 (2009)
87. Miron, RE, Smith, RJ: Resistance to protease inhibitors in a model of HIV-1 infection with impulsive drug effects. Bull. Math. Biol. **76**, 59-97 (2014)

88. Pau, AK, Tavel, JA: Therapeutic use of interleukin-2 in HIV-infected patients. Curr. Opin. Pharmacol. **2**, 433-439 (2002)
89. Choh, Y, Ignacio, M, Sabelis, MW, Janssen, A: Predator-prey role reversals, juvenile experience and adult antipredator behaviour. Sci. Rep. **2**, 1-6 (2012)
90. Ives, AR, Dobson, AP: Antipredator behaviour and the population dynamics of simple predator-prey systems. Am. Nat. **130**, 431-447 (1987)
91. Janssen, A, Faaraji, F, van der Hammen, T, Magalhães, S, Sabelis, MW: Interspecific infanticide deters predators. Ecol. Lett. **5**, 490-494 (2002)
92. Saito, Y: Prey kills predator: counter attack success of a spider mite against its specific phytoseiid predator. Exp. Appl. Acarol. **2**, 47-62 (1986)
93. Ramao-Jiliberto, R, Frodden, E, Aránguiz-Acuña, A: Pre-encounter versus post-encounter inducible defense in predator-prey systems. Ecol. Model. **200**, 99-108 (2007)
94. Komarova, NL, Barnes, E, Klenerman, P, Wodarz, D: Boosting immunity by antiviral drug therapy: a simple relationship among timing, efficacy, and success. Proc. Natl. Acad. Sci. USA **100**, 1855-1860 (2003)
95. Kuznetsov, VA, Makalkin, IA, Taylor, MA, Perelson, AS: Nonlinear dynamics of immunogenic tumors: parameter estimation and global bifurcation analysis. Bull. Math. Biol. **56**, 295-321 (1994)
96. Mukhopadhyay, B, Bhattacharyya, R: Modelling phytoplankton allelopathy in a nutrient-plankton model with spatial heterogeneity. Ecol. Model. **198**, 163-173 (2006)
97. Pei, YZ, Lv, YF, Li, CG: Evolutionary consequences of harvesting for a two-zooplankton one-phytoplankton system. Appl. Math. Model. **36**, 1752-1765 (2012)
98. Corless, RM, Gonnet, GH, Hare, DEG, Jeffrey, DJ, Knuth, DE: On the Lambert W function. Adv. Comput. Math. **5**, 329-359 (1996)
99. de Melo, W, van Strien, S: One-Dimensional Dynamics. Springer, New York (1993)
100. de Melo, W, van Strien, S: One-dimensional dynamics: the Schwarzian derivative and beyond. Bull., New Ser., Am. Math. Soc. **18**, 159-162 (1988)
101. Guckenheimer, J, Holmes, P: Nonlinear Oscillations, Dynamical Systems, and Bifurcations of Vector Fields. Springer, Berlin (1983)
102. Andronov, AA, Leontovich, EA, Gordan, LL, Maier, AG: Qualitative Theory of Second-Order Dynamic Systems. Wiley, New York (1973)
103. Ciesielski, K: On semicontinuity in impulsive dynamical systems. Bull. Pol. Acad. Sci., Math. **52**, 71-80 (2004)
104. Ciesielski, K: On stability in impulsive dynamical systems. Bull. Pol. Acad. Sci., Math. **52**, 81-91 (2004)
105. Ciesielski, K: On time reparametrizations and isomorphisms of impulsive dynamical systems. Ann. Pol. Math. **84**, 1-25 (2004)
106. Zhang, ZF, Ding, TR, Huang, WZ, Dong, ZX: Qualitative Theory of Differential Equations. Translations of Mathematical Monographs, vol. 101. Am. Math. Soc., Providence (1992)
107. Simeonov, PS, Bainov, DD: Orbital stability of the periodic solutions of autonomous systems with impulse effect. Int. J. Syst. Sci. **19**, 2561-2585 (1988)
108. Iooss, G: Bifurcations of Maps and Applications. North-Holland, New York (1979)